Regulation of secondary metabolites in plant-beneficial microorganisms

Strategies to activate a cryptic biosynthetic gene cluster in *Pseudomonas protegens*

Ácil Maria de Almeida Will

Thesis to obtain the Master of Science Degree in

Biological Engineering

Supervisors: Prof. Lars Jelsbak and Prof. Jorge Humberto Gomes Leitão

Examination Committee

President: Prof. Gabriel António Amaro Monteiro

Supervisor: Prof. Lars Jelsbak

Member of the Committee: Dr. Sílvia Andreia Bento da Silva Sousa Barbosa

November 2021

Declaration

I declare that this document is an original work of my own authorship and that it fulfils all the requirements of the Code of Conduct and Good Practices of the Universidade de Lisboa.

Preface and Acknowledgments

The work presented in this master's thesis was conducted at the Technical University of Denmark (DTU) at the Department of DTU Bioengineering. The project has been performed over 5 months, from May 2021 to October 2021 in the Infection Microbiology Group (IMG), under the supervision of Prof. Lars Jelsbak. The project was co-supervised by Prof. Jorge Leitão in Instituto Superior Técnico (IST). The work of this report corresponds to 30 ECTS credits.

I would like to thank my supervisors Prof. Lars Jelsbak for guiding me throughout this project and sharing his expertise, and Prof. Jorge Leitão for all the help in the several issues and doubts that arose during this period. Being part of the IMG was an incredible experience for the kindness and constructive spirit of all the members. Particularly, I would like to thank the research assistant Joana Queiroz for assisting me with the first steps of this work. The Ph.D. student Morten Hansen for assisting several of the experiments and being always available to share his practical and theoretical knowledge. To Ph.D. student Adele Kaltenyte for her general helpfulness, and the thorough proofreading of this report.

Furthermore, I am grateful to Prof. Ling Ding and Postdoc student Scott Jarmusch provided valuable guidance in LC-MS analysis. Also, I am grateful to Postdoc student Yannick Buijs and Ph.D. student Nathalie Henriksen contributed to the qPCR analysis with technical and analytical inputs.

Abstract

Climate changes and overpopulation present hard challenges for global agriculture, threatening the food security of the world population. Some microbes have plant growth-promoting activities and can increase the yield of crops. Nevertheless, the complex microbial interactions alongside the unknown information hidden in the microbial genome make it harder to regulate plant-beneficial metabolites. This project aims to study strategies for the activation of an unknown cryptic biosynthetic gene cluster (BGC) of the potential plant growth-promoting strain *Pseudomonas protegens* DTU9.1. BGCs encode proteins, here a polyketide synthase (PKS), that synthesise secondary metabolites.

The wild type (WT) and a PKS deletion mutant (ΔPKS) were compared in different media and no significant differences were caused by PKS deletion regarding growth nor fluorescence. Intra- and extracellular metabolites from extracts of both the WT and ΔPKS were analysed by LC-MS and compared. Several metabolites showed different expression levels between the two strains.

Antibiotic rifamycin showed to induce the BGC expression, being influenced by the culture growth phase on which is added. Cultures with D-arabitol as a carbon source resulted in higher expression levels of the BGC than cultures with glucose. With RNA polymerase engineering, selecting a rifamycin-resistant mutant with the mutation D521G in the *rpoB* gene, there was an increase of 4.2-fold in the unknown BGC expression.

This study shows that the use of different carbon sources might be one key factor for the activation of the BGC expression. The moment of supplementation of the inductive antibiotic to the culture should also be considered. RNA polymerase engineering demonstrates to be a promising technique for cryptic BGC expression activation.

Keywords: cryptic biosynthetic gene cluster, polyketide synthase, secondary metabolites, activation, plant-beneficial bacteria, *Pseudomonas protegens*

Resumo

Alterações climáticas e sobrepopulação desafiam a agricultura global, ameaçando a garantia de produtos alimentares para a população. Alguns micoorganismos são benéficos para as plantas, contribuindo para o aumento do rendimento das colheitas. No entanto, as complexas interações microbiais em conjunto com a informação desconhecida escondida no genoma microbiano dificultam a regulação dos metabolitos sintetizados. Este projeto foca-se no estudo de estratégias para a ativação de um *cluster* genético biossintético (BGC) críptico, desconhecido, presente na estirpe *Pseudomonas protegens* DTU9.1. BGCs codificam proteínas, neste caso um policétido sintase (PKS), com capacidade de síntese de metabolitos secundários.

A estirpe selvagem (WT) e o mutante de deleção sem o PKS (ΔPKS) foram comparados em diferentes meios, e nenhuma diferença foi observada entre as estirpes a nível do crescimento nem da fluorescência. Extratos de metabolitos intra e extracelulares de ambas as estirpes foram analisados com LC-MS. Vários metabolitos mostraram níveis diferentes de expressão entre as duas estirpes.

O antibiótico rifamicina induz a expressão do BGC, sendo influenciado pela fase de crescimento da cultura em que é adicionado ao meio. Culturas usando D-arabitol como fonte de carbono resultaram em níveis de expressão mais elevados do que em culturas usando glucose. Engenharia de RNA polymerase, selecionando um mutante resistente a rifamicna, com a mutação D521G no gene *rpo*B, resultou num aumento de expressão do BGC de 4.2 vezes.

Este estudo mostra que diferentes fontes de carbono podem ser um fator chave na ativação da expressão do BGC. O momento de adição do antibiótico indutor à cultura deve também ser considerado. Engenharia de RNA polimerase demonstra ser uma técnica promissora para a ativação do BGC.

Palavras-chave: *cluster* de genes biossintético críptico, policétido sintase, metabolitos secundários, activation, bactérias benéficas para plantas, *Pseudomonas protegens*

Table of Contents

List of Tables

List of Figures

List of abbreviations

ΔPKS	Unknown PKS deletion mutant of *P. protegens* DTU9.1
bp	Base pairs
cDNA	Complementary DNA
CFU	Colony forming unit
Ct	Cycle threshold
EU	European Union
E	Primer efficiency
FP	False positive
GFP	Green fluorescent protein
GOI	Gene of interest
REFs	Reference genes
Geomean	Geometric mean
KB	King's B
LB	Lennox broth
LC-MS	Liquid chromatography–mass spectrometry
MIC	Minimum inhibitory concentration
NRPS	Non-ribosomal peptide synthases
OD_{600}	Optical density measured at a wavelength of 600 nm
PGPM	Plant growth-promoting microorganisms
PIA	Pseudomonas isolation
PKS	Polyketide synthase
Punk-GFP	*P. protegens* DTU9.1 strain with reporter gene GFP
RFU	Relative fluorescence units
Rif^R	Rifamycin resistant *P. protegens* DTU9.1
RT-qPCR	Reverse Transcription Quantitative PCR
SOE	Splicing by overlap extension
$Strep^R$	Streptomycin resistant *P. protegens* DTU9.1
TSB	Tryptic soy broth
WT	Wild type

1. State of the art

1.1. Challenges of global agriculture

The global population is expected to reach approximately 10 billion people by 2050 (an increase of ~2 billion people in the next 30 years)[1]. The intensified demand for food, fibres, and fuel, alongside an increased complexity of meals and consumed calories predicts the expansion of agricultural production to be approximately 70% by 2050[2].

To achieve the required volume of agricultural products, at least two options are available: expanding the cultivated area to increase crop production or improving the yields of the existing crops. The former implies the replacement of natural landscape and might result in increased water pollution, soil erosion, and greenhouse emissions, decreased carbon storage, loss of biodiversity, and damage of important ecosystems[3]. The latter is influenced by four main factors: soil fertility, water availability, climate, and diseases[4]. The use of chemical fertilizers and pesticides is a widely accepted option for crop yield increase. However, the use of agrochemical products is linked to several human diseases, acute and chronic, such as endocrinal and immunity problems, neurotoxicity, and cancer[5]. Regarding the environment, fertilizers and pesticides may result in the accumulation of heavy metals in the soil[6]. Pesticides are common contaminants in soil, air, and water and they can affect non-target organisms including beneficial soil microorganisms, fish, birds, and non-target plants. The consequences for these organisms go from physical malformations to death[7].

To tackle this problem, European Union (EU) regulates the use of chemicals and pesticides to protect human health and the environment. On 1st June 2007, a new legal framework entered into force to regulate the Registration, Evaluation, Authorisation, and Restriction of Chemicals (REACH Regulation). Therefore, authorities can restrict the use of hazardous substances or even ban them if their risks are unmanageable[8].

Fortunately, the awareness about global environmental issues changed the preferences of the consumers and the focus of the companies: global sustainable investment raised by 68% since 2014[9]. The IBM Institute for Business Value conducted a research study in 28 countries and over 7 in 10 consumers considered it at least moderately important that a brand offers products with natural ingredients and considers sustainable and environmental practices[10]. Therefore, more ecological solutions are required urgently, and microorganisms can be part of this change.

1.2. Microorganisms as a solution

In the 1900s, *Bacillus thuringiensis* was discovered as an insect pathogen. In 1938, sporeine, a compound derived from *B. thuringiensis*, was available in France, being the first commercial biopesticide[11]. Plant growth-promoting microorganisms (PGPM) have the potential for several applications in the field of agro-environmental sustainability, from disease suppression in plants to bioremediation of contaminated soils[12]. Beneficial microorganisms include bacteria, mainly from the group *rhizobium*, and fungi. They can be free-living, rhizospheric, or endosymbiotic. According to du

Jardin[13], beneficial microorganisms can be divided into biocontrol agents and biostimulants, with biofertilizers making part of the second group.

1.2.1. Biocontrol agents

Using microorganisms to suppress plant's pathogen populations and control plant diseases[14] has been explored to replace the use of agrochemicals. In 2017, Australia, Brazil, Canada, Europe, Japan, New Zealand, and the United States had registered a total of 101 microbial biological control agents for plant disease control[15].

> *"Biocontrol agents used in plant productions are living organisms protecting plants against their enemies, i.e. reducing the population of pests or diseases to acceptable levels."* – du Jardin (2015)[13]

Modes of action differ and can be primarily divided into indirect or direct, Figure 1.1. Indirectly, microorganisms can act via plant metabolism: plants protect themselves from pathogens through chemical and physical mechanisms activated by stimuli that are recognized by specific recognition receptors. Some of the recognized stimuli have origin in pathogens, but beneficial microbes are also capable of inducing resistance in plants. Bacterial compounds that are plant-resistance inducers include lipopolysaccharides, flagella, iron-regulated compounds, and others [14,16]. This type of induced resistance is only activated in the presence of the stimuli. However, when the effect lasts longer in the absence of the stimuli, the phenomenon is called priming[14]. For example, *Bacillus subtilis* GB03 is a biological fungicide whose volatile organic compounds induce plant resistance on *Arabidopsis* by regulating auxin homeostasis and cell expansion, enhancing photosynthesis by decreasing glucose sensing and abscisic acid levels; conferring salt tolerance by regulating the tissue-specific expression of sodium transporter HKT1; and stimulating iron acquisition [17–21]. Another type of indirect action is competition with the pathogen for nutrients and space. It was successfully applied, for example, in fruit rot prevention, using fast colonizing yeasts to control pathogenic populations, such as fungi[14,22].

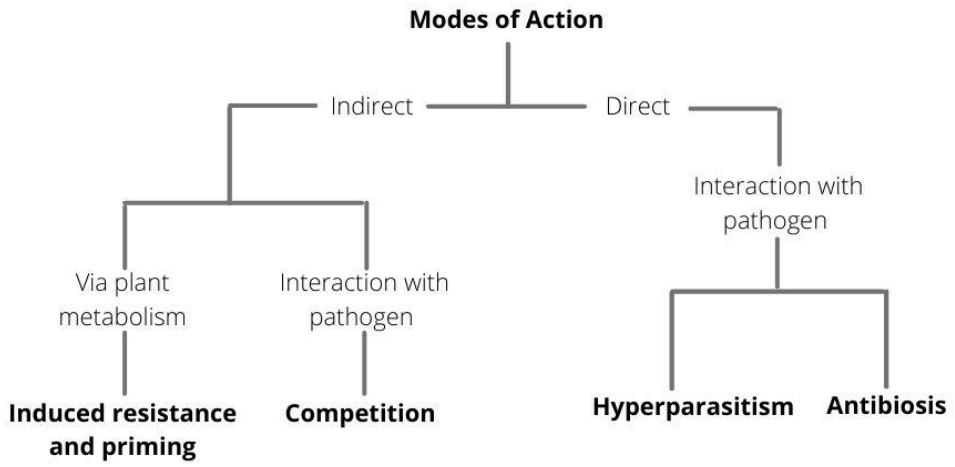

Figure 1.1. Scheme with direct and indirect modes of action of biocontrol agents.

Directly, beneficial microorganisms can interact with pathogens by hyperparasitism, occurring when a parasite infects another parasite, a phenomenon more often observed in fungi; or antibiosis, by producing secondary antimicrobial metabolites with inhibiting effects[14]. Some classes of antibiotic compounds have strong evidence for their function as biocontrol agents, such as phenazines, pyoluteorin, pyrrolnitrin, cyclic lipopeptides, and hydrogen cyanide (HCN).

However, these mechanisms can be combined, as in the case of *Metschnikowia fructicola*, the base yeast of a commercialized biocontrol product (*Shemer*). Its action mechanisms against pathogens in postharvest fruits include iron-binding compounds, induction of defense signaling genes in the fruit, production of enzymes that degrade fungal cell wall, and relatively high amounts of superoxide anions[23].

1.2.2. Biostimulants

Microorganisms can promote plant growth by producing phytohormones (as auxins, gibberellins, and cytokines), modulating the levels of stress-related ethylene, contributing to nitrogen fixation, enhancing phosphorus availability, acting as biostimulants[24].

> *"A plant biostimulant is any substance or microorganism applied to plants with the aim to enhance nutrition efficiency, abiotic stress tolerance and/or crop quality traits, regardless of its nutrients content."* - du Jardin (2015)[13]

An experiment with *Bacillus subtilis* showed that the strain alleviates drought stress in potatoes which maintained a higher photosynthetic process, contents of chlorophyll, soluble proteins, total soluble sugars, and enzymatic activities of CAT, POD, and SOD in the presence of the plant growth promoting bacteria than without it [25]. These results are particularly interesting as drought is one of the most important abiotic stresses in agriculture and has a high risk of increasing due to climate changes[26].

The definition of biostimulants includes the subcategory of biofertilizers.

> *"A biofertilizer is any bacterial or fungal inoculant applied to plants with the aim to increase the availability of nutrients and their utilization by plants, regardless of the nutrient content of the inoculant itself. Biofertilizers may also be defined as microbial biostimulants improving plant nutrition efficiency."* - du Jardin (2015)[13]

Nitrogen is essential for plant growth. Despite the large quantities of nitrogen available in the atmosphere (78%), it is not available for direct uptake by plants, and lack of fixed nitrogen availability in the soil can limit crop productivity. The ability to fix atmospheric nitrogen was found in some species belonging to bacteria and archaea groupsClique ou toque aqui para introduzir texto.. Using the enzyme complex nitrogenase, nitrogen-fixing microorganisms transform nitrogen into ammonia[27,28]. The biological nitrogen fixation process was estimated as the producer of 65% of the nitrogen currently utilized in agriculture[29].

Phosphorus is the second major nutrient required for plant growth and even though it is available in high amounts in the soil (400–1200 mg/kg of soil), most of it is presented in insoluble forms, hence not available for plant uptake. Beneficial bacteria can solubilize phosphorous by acidification, chelation,

exchange reactions, and organic acid production, such as gluconic acid, allowing phosphorus uptake by plants[27].

Other important nutrients such as potassium, zinc, iron, and sulphur can also be bio solubilized. Some of the mechanisms used can be organic acid production, protein extrusion, and production of chelating agents. In the specific case of iron, the chelation is done by the iron-chelating molecules siderophores[27].

1.2.3. Mixed Inoculants

Mixed inoculants technology takes advantage of distinct mechanisms of different microorganisms to promote plant growth by combining them. A successful example of this application is the combination of two ACC deaminase producers, *Rhizobium leguminosarum* RP2 and *Pseudomonas putida* PSE3, nitrogen-fixing and phosphate-solubilizing bacteria, respectively, applied in pea plants[30]. The co-inoculation was found more effective than any single or composite treatments (nitrogenous (urea) or phosphatic (diammonium phosphate) fertilizers) at increasing growth, symbiotic characteristics, nutrient pool, and quantity and quality of pea seeds.

1.2.4. Genetic engineering

Genes linked to plant growth-promoting mechanisms can be overexpressed or integrated into other PGPM by genetic engineering. For example, *Pseudomonas protegens* CHA0-ΔretS-nif strain with introduced nitrogen-fixing ability can promote garlic growth and yields. It was also engineered with bactericidal traits, reducing garlic root rot, as well[31].

1.2.5. PGPM and where to find them

Disease suppressive soils were defined as soils in which the effects of pathogenic agents are less damaging to the culture[32]. The suppressiveness can be attributed to the entire microbiome activity and is often related to competition for resources; or to the activity of specific groups of microorganisms that interfere with the normal development of the pathogen. For this, disease suppressive soils are a potential source of beneficial PGPM. *Fusarium oxysporum* Fo47, isolated from a *Fusarium* suppressive soil, was found to protect pepper plants against *Verticillium dahliae* and *Phytophthora capsici*, and induce plant resistance mechanisms[33].

Organic amendments (composts) can suppress plant diseases, being this ability affected by physicochemical and microbiological composition[34,35]. Therefore, they can be reservoirs for potential PGPM. Several microbes were isolated from the roots of eggplants grown in the compost and tested against *Verticillium dahliae*: two bacterial strains from the *Pseudomonas fluorescens* complex and two fungi strains identified as *Fusarium oxysporum* were selected for further evaluation and proved the ability of microbes to reduce the incidence of the disease [35].

Another strategy to look for PGPM is to identify healthy plants in infested fields. *Bacillus subtilis* HJ5, an antagonistic of *V. dahliae*, was isolated from the roots of healthy cotton plants in a field infested by *Verticillium* wilt[36]. However, PGPM can also be found in places without previous evidence for biological control[37].

1.3. From the lab to the field

Despite the enormous potential of microorganisms for plant growth promotion, there are two main reasons for their low levels of application: (1) the technical difficulties, owing to a lack of fundamental information on them and their ecology, and (2) the costs of product development and regulatory approvals required for each strain, formulation, and use.

1.3.1. Scientific and technical challenges

Despite the existence of several successful cases of microorganisms as biocontrol agents, the application of *in vitro* successful interactions *in vivo* can be very challenging due to the complexity of soil microbiomes. Soil harbours an immense number of microbes (10^{11}–10^{13} microscopic counts/kg) from which only 0.01-0.1% are expected to be cultivable[38]. Together with abiotic factors, the intra- and interspecific interactions of these microbes are responsible for microbiomes modulation, affecting "occurrence, abundance, diversity, distribution, communication, and functions"[39].

The study of PGPM is performed under laboratory, greenhouse, and field conditions, but inconsistent results are often generated on the different conditions. The fault relies mainly on the complexity of microbiome interactions, and the lack of information on them [24]. For example, Bjørnlund and colleagues [40] found that instead of the expected predator-prey relationship between *Pseudomonas* strain DSS73 and the nematode *Caenorhabditis elegans*, these species presented an intricate mutually beneficial system. When feeding on DSS73 strain, nematodes avoided the attack and killing by the flagellate *Cercomonas sp.* (in densities usually mortal to the nematodes); the colonization of soil microcosms by DSS73 increased in the presence of nematodes, which transported the bacteria aggregated in the intestines; the flagellate *Cercomonas* feeding on DSS73 was used as an alternative food source for the nematode *C. elegans*.

An important factor in microbial interaction is the production of secondary metabolites, molecules with a broad range of physiological functions that can also act as signaling molecules and modulate interspecies gene expression (see section 1.4. Secondary metabolism). Moreover, some soil microorganisms have cryptic gene clusters encoding for putative new compounds that are silenced under laboratory growth conditions[41]. In this way, certain organisms might establish more interactions *in vivo* than *in vitro*. Microbiome complexity also creates problems related to when to apply PGPM to the crops, and if the application should be chronic or acute.

Another challenge is related to a successful inoculation whose efficacy relies on assuring a population density active and effective[24]. The difficulties to compete in the new environment are the main reason for failure in soil inoculation, but an efficient immobilization system can protect the microorganisms from biotic and abiotic environmental stresses as well as extend storage periods [42,43]. These preparations can exist in several forms such as powder, pellet, and liquid formulations, and can be applied as a seed coating, directly on the soil, or as sprays[44]. The delivery system of the biocontrol agents into the soil should keep viable $10^{6\text{-}8}$ CFU/g formulation[42], but these levels always decline after some weeks[45,46].

Additionally, microbial biocontrol agents might be incompatible with agrochemicals also present in the soil, such as the pesticides applied on seeds[47]. For this, it is important to opt for compatible

agrochemicals and cell protectors, or different application methods, such as in-furrow inoculation, which showed to alleviate the effects of seed treatment with agrochemicals and micronutrients, when compared to the treatment applied directly on the seeds[48].

1.3.2. Social-economic constraints

The development of highly selective products might lack profit. If on one hand, selectivity reduces environmental and health-related side effects, on the other hand, their effectiveness is limited to some pathogens, in opposition to agrochemicals that impact many kinds of organisms. In this way, the quality and efficacy of biocontrol agents are more dependent on biotic and abiotic factors present in the soil, and these products have a shorter limit number of applications, becoming niche market products[49,50].

It is observed a preference for chemical pesticides among farmers, especially in developing countries. The reluctance in adopting biological crop protection is mainly due to the idea that these products would be mostly counterfeit, the perception that chemical pesticides generate higher yields and efficacy, and that biopesticides are costlier and more time-consuming[51].

Regulatory processes and documentation for biocontrol products registration in the EU can be very complex and time-consuming, resulting in fewer biopesticides available in Europe than, for example, in the U.S., South America, or India. To introduce a pesticide in the European market, first, the pesticidal active substance must be approved for the EU, and then the plant protection product must be approved individually by the member states. Both approvals include several sub-tiers of approval, for which the registration of a biopesticide can take several years[50,52]. Harmonization of registration guidelines would allow data exchange across countries and regulatory agencies, easing the establishment of regulations promoting the registration of low-risk compounds, and consequently increasing the economic viability and application of new biopesticides for crop protection[52].

From July 2022 onwards (Regulation (EU) 2019/1009), it will be possible to follow an EU harmonized marketing process for biostimulants. The marketers will be able to affix the CE mark and the product will have the access to the whole EU market[53].

1.4. Secondary metabolism

Secondary metabolites are small molecules, biologically active, not vital for normal growth, but naturally produced by organisms conferring physiological adaptative tools and improving fitness[54]. Secondary metabolism pathways are associated with low growth rate, stress response, and breakdown of cellular components. As primary metabolism is related to energy production and cellular synthesis, its intermediates are usually substrates or products of enzymes with a high rate of activity and consequently, have fast turnover rates within the cell, being present in low quantities. Contrarily, secondary metabolites are precursors of only a few reactions and have a slower turnover rate when inside the cell. This leads to their intracellular accumulation and, when on adequate concentrations, to their secretion to the extracellular medium[55]. An example of the secondary metabolism's functions is the secretion of the toxic compounds hydrogen cyanide and 2,4-DAPG by *Pseudomonas fluorescens* CHA0 as a mechanism of protection against their major predators, the nematodes [56]. Nevertheless, secondary metabolites can also act as signaling molecules. In antibiotics' case, high concentrations lead to the

inhibition of specific target functions and consequently to inhibition of growth, but low concentrations can modulate gene expression, affecting key biological processes including transcription, metabolite production, motility, and biofilm formation[57–59].

1.4.1. Biosynthetic gene clusters

Figure 1.2 summarily schematizes the tiers required to achieve the final secondary metabolite. The biosynthesis of these compounds is dependent on specific enzymes, in turn, encoded by biosynthetic gene clusters (BGCs).

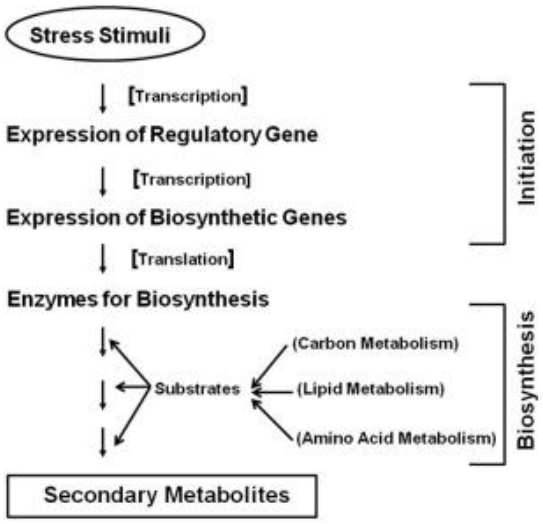

Figure 1.2. Summary of pathways involved in the production of secondary metabolites.

A BGC consists in a group of genes, physically clustered, that together encode a biosynthetic pathway to produce a secondary metabolite, as well as its chemical variants[60]. These clusters usually include a gene encoding a skeleton structure which is one of several key signature enzymes that catalyze the production of compounds. From these key enzymes, polyketide synthases (PKS) and nonribosomal peptide synthetases (NRPS) are usually targeted for natural product discovery due to the broad range of bioactive properties of the synthesized products (polyketides and non-ribosomal peptides, respectively)[61].

A module (operational unit) of a PKS is comprised minimally of a ketosynthase (KS), an acyltransferase (AT), and an acyl-carrier protein (ACP) domain[62]. A module of an NRPS contains three core domains, the condensation (C) domain, the adenylation (A) domain, and the peptidyl carrier (PCP) domain[63]. As KS and C domains of PKS and NRPS, respectively, are highly conserved, they can be used as targets to identify NRPS and PKS within a variety of datasets[64].

PKSs are commonly divided into three types: type I, II, and III. Type I PKSs are modular multifunctional enzymes covalently bonded, whose modules can be used non-iteratively or iteratively. In non-iterative PKSs, each module contains a different active site for the catalysis of one cycle of polyketide chain elongation, e.g., bacterial 6-deoxyerythronolide B synthase (DEBS); in iterative PKSs, at least some of the modules are reused for the successive cycles, e.g., fungal 6-methylsalicylic acid and lovastatin[65]. Type II PKSs are multienzyme complexes, in which each protein carries one iterative enzymatic activity, resulting in multiaromatic compounds, such as the tetracenomyxin PKS that synthesizes aromatic polyketides as tetracenomycin C[65]. Type III PKSs are iterative homodimers that catalyze the condensation of one to several molecules, such as RppA synthase for the biosynthesis of aromatic polyketides, such as flavolin, or PhlD for the biosynthesis of 2,4-DAPG[66].

The remaining genes of the BGC generally encode for tailoring enzymes that modify the secondary metabolite skeleton, such as oxidoreductases, methyltransferases, and acyltransferases. In some

cases, BGCs might include genes for pathway-specific regulators and/or for resistance to the pathway end-product[61,67].

Gene clustering occurs commonly in bacteria where approximately 30–50% of all genes are organized in an operonic structure (groups of genes controlled by a single promoter). BGCs are clusters of operons and genes[68]. The first antibiotic whose whole BGC was cloned was the blue-pigmented aromatic polyketide actinorhodin from *Streptomyces coelicolor*[69]. In eukaryotes, clusters of functionally related but non-homologous genes are similarly organized in terms of physical proximity but are transcribed independently, controlled by different promoters[68].

Advantages of gene clustering can be the coregulation of a set of genes controlling successive steps in a biosynthetic or developmental pathway; and the coinheritance, either by horizontal or vertical gene transfer[67,68].

1.5. Cryptic biosynthetic gene clusters

Cryptic genes are silent/low-level expressed genes under normal laboratory conditions, that can be activated by genetic mechanisms or environmental stimuli [70]. DNA sequencing technologies allowed scientists to informatically identify these genes and classify the putative codified compounds. Analysis of the genomes of the fungi *Aspergillus nidulans*, *A. fumigatus* and *A.oryzae* show that several of them might codify for several key enzymes precursors of secondary metabolites. The number of putative metabolites predicted is higher than the ones already reported to be produced by these species[71]. For this, is essential to activate the silent genes to explore their utility for human activities but also to get more insight into microbiome interactions. The expression of cryptic genes can be achieved through several laboratory techniques either by homologous or heterologous gene expression[72].

1.5.1. Homologous expression of cryptic genes

Culture conditions. Microbial physiology is influenced by culture conditions, including media, temperature, oxygen availability, and many others. Therefore, changes in media composition and culture parameters can change not only the quantity of produced compounds but also the type of molecules synthesized[73]. Paranagama and colleagues identified six new secondary metabolites produced by the plant-associated fungus *Paraphaeosphaeria quadriseptata,* simply by using distilled water for the media preparation instead of tap water[74]. This strategy is also known as “OSMAC”, standing for “one strain many compounds”, as a single strain can produce different compounds just by changing the growing conditions[75].

External chemicals. External chemical compounds can act as signaling molecules triggering the synthesis of other compounds. An example is the already mentioned use of sublethal concentrations of antibiotics[72]. Another is the use of artificial root exudates, a way of mimicking natural cues present in the rhizosphere, that was already proved to induce nitrogen fixation in bacterial communities[76].

Ribosome and RNA polymerase engineering. By screening antibiotic-resistant microbial mutants, spontaneous mutations on their ribosomes or RNA polymerase can be found, leading to an altered expression pattern of secondary metabolites[77]. Mutations in the ribosomal protein S12 are related to

increased stability of the 70S ribosome complex[78] and high levels of ribosome recycling factor[79]. Mutations in the *rpoB* gene, which codifies the RNA polymerase β sub-unit, induced by rifampicin or rifamycin resistance also led to different gene expression patterns. These mutations were responsible for the increased affinity of the RNA polymerase to the promoter regions[80]. In 1996, K. Ochi and his colleagues showed that the strain *Streptomyces lividans* TK24 produced the antibiotic actinorhodin usually not produced by *S. lividans* species. Genetic analyses revealed that a streptomycin-resistant mutation, a point mutation in the *rpsL* gene encoding ribosomal protein S12, was responsible for the induction of the unusual antibiotic synthesis[81]. Since then, ribosome engineering has been used to increase the production of bioactive molecules in several bacterial species and for activating silent or poorly expressed BGCs.

Heterologous promoter insertion. Promoters are regions of DNA where transcription factors bind, and gene transcription is initiated, controlling and regulating gene expression[82]. Replacement of the native promoter by a constitutive or inducible heterologous promoter is used to activate gene expression[73]. These promoters can go under promoter engineering, a way of regulating their strengths and functions[82].

Regulatory gene activation. Genes encoding proteins involved in the biosynthesis of secondary metabolites are often controlled by the expression of an activator gene, Figure 1.2. Activating the expression of these transcriptional regulatory proteins with an activating signal[73] or a heterologous activator gene[83] can lead to the expression of the silent gene cluster.

Co-cultivation. Microorganisms naturally interact with each other either for competition or synergic functions. Thus, the cultivation of two different microbial strains together, to allow direct contact and mimic their natural interactions, might allow the production of new secondary metabolites not observed in the independent culture of the strains. As an example, co-cultures of the fungus *Aspergillus fumigatus* with the soil bacteria *Streptomyces bullii* resulted in the production of ten compounds, not detected in cultures of only *A. fumigatus* [84].

Epigenetics. Epigenetics mechanisms modify the chromosome conformation, controlling gene expression by affecting the ability of the proteins to bind to DNA regulatory regions, without changing the DNA sequence. In eukaryotes, these mechanisms include covalent histone posttranslational modifications (such as acetylation, methylation, and phosphorylation), DNA methylation, chromatin remodeling, and noncoding RNAs[85]. In prokaryotes, the inexistence of histones and nucleosomes that modify chromosome structure makes DNA methylation the most important epigenetic regulator[86].

Metabolic engineering. Metabolic precursors are required for biosynthetic and assimilatory reactions[87]. For example, acyl-CoA precursors have a role in the production of a plethora of secondary metabolites; acetyl-CoA, malonyl-CoA, and methylmalonyl-CoA are used as building blocks for polyketide synthesis. The availability of precursors molecules affects the production yield of secondary metabolites, and it can be modified by manipulating the biochemical pathways that generate or consume them[54]. For example, the level of FK506 production (a polyketide macrolide with immunosuppressant activity) was increased by engineering the level of methylmalonyl-CoA in *Streptomyces clavuligerus* through a combination of

chemical supplementation and genetic approaches (methyl oleate supplementation in the medium and methyl-malonyl-CoA mutase pathway introduction, respectively).

1.5.2. Heterologous expression of silent genes

Expression of the cryptic BGC in a host microorganism has some advantages: the heterologous host can have higher growth rates and yields of production; the information regarding the host can be broader and clearer, allowing more understanding of genetic manipulation tools and background information[88]. One example of application is the cloning of an NRPS BGC from the marine actinomycete *Saccharomonospora sp.* on the model expression host *Streptomyces coelicolor* to produce the antibiotic taromycin A[89]. However, cloning techniques might be laborious and time-consuming. Host incompatibilities due to the complexity of the regulatory network can present some challenges and require gene substitution, enzyme evolution, promoter replacement, and transcriptional repressor knock-out[88]. The BGCs encoding putative bioactive compounds are usually large (10–100 kb) and constituted by many genes, making the cloning and expression of these BGC's more challenging[72]. A suitable expression host should contain several essential features, such as a variety of natural product precursors required to construct abundant complex molecules; a simplified secondary metabolite background; and a known regulatory network[88].

1.6. Pseudomonas protegens

Pseudomonas genus is composed of rod-shaped, aerobic Gram-negative bacteria. They have motility ability, owing to one or several polar flagella, and a high genomic G+C content (59–68%). This *genus* inhabits diverse terrestrial and aquatic environments, due to its versality related to metabolic and physiologic characteristics. Although some *Pseudomonas* species have pathogenic traits, such as the opportunistic parasite *P. aeruginosa*, or the plant pathogen *P. syringae*, some others have beneficial activities, such as the bioremediation agent *P. putida* [90–92], or the plant aide *P. protegens*.

P. protegens are soil inhabitants and belong to the group of rhizobacteria, having the ability to colonize roots. The name "*protegens*", which stands for protecting, was attributed due to the species power to protect plants from soil-born phytopathogens[93,94]. They are characterized as a fluorescent *Pseudomonas* strain able to produce the secondary metabolites 2,4-diacetylphloroglucinol and pyoluteorin, two biocontrol agents[93]. *P. protegens* also have biofertilizer properties, such as phosphate solubilization, nitrogen-fixing, and zinc solubilization ability[95,96], and can produce biofilms[97].

2. Background and aim of the study

Several soil *Pseudomonas* strains were isolated in a previous study conducted at Infection Microbiology Group (DTU) [98]. The genome sequences were submitted into *antiSMASH*[99] to predict biosynthetic gene clusters (BGCs). *Pseudomonas protegens* DTU9.1 stood out for harbouring in its genome several biocontrol genes, including orfamide, pyoluteorin, pyrrolnitrin and 2,4-DAPG genes. Moreover, the presence of genes encoding for phytotoxins was not detected. Finally, the strain showed a highly effective biocontrol activity against plant pathogens, including bacteria and fungi. *antiSMASH* predicted a BGC encoding for a type I polyketide synthase (PKS) not identified in the data base. Posteriorly, the BGC was identified as cryptic, and a high throughput study was conducted in a *Biolog* plate to find out possible environmental cues that could activate the expression of the BGC. The antibiotic rifamycin and the carbon source D-arabitol were selected as good candidates.

The compound resultant from this PKS might have relevant functions. Metabolites with biocontrol activities are desired for biocontrol agents. However, it is also important to confirm the absence of prejudicial effects caused by these microorganisms. Hence, the aim of this study is to find out ways of activating the expression of the unknown BGC in *P. protegens* DTU9.1, contributing to a further identification of the secondary metabolite synthesized by the PKS.

3. Materials and Methods

3.1. Chemicals and reagents

Chemical products used were acquired from *Sigma-Aldrich*®, *Milipore*® and *ACROS ORGANICS* and PCR reagents were obtained from Thermo-Fisher SCIENTIFIC (with indicated exceptions). Plasmids were ordered from IDT®.

3.2. Bacterial strains and plasmids

This study focused on *Pseudomonas protegens* DTU9.1 and included the use of *Escherichia coli* strains for the steps of transformation and mating, Table 3.1. The list of plasmids used in this study is presented in Table 3.1. *P. protegens* DTU9.1 will be referred as wild type (WT) and the variants will be referred to with an indicative of the variation.

Table 3.1. Bacterial strains, and relevant characteristics, used in this project.

Strain	Description	Source
Pseudomonas protegens		
DTU9.1	Wild type	Technical University of Denmark – DTU, Kongens Lyngby, Denmark
DTU9.1 ΔPKS	Unknown polyketide synthase (PKS) gene knockout mutant	Technical University of Denmark – DTU, Kongens Lyngby, Denmark
DTU9.1 Rif^R	Spontaneously resistant to rifamycin mutant	This project
DTU9.1 Strep^R	Spontaneously resistant to streptomycin mutant	This project
Escherichia coli		
CC118λspir	Δ(ara-leu) araD ΔlacX74 galE galK phoA20 thi-1 rpsE rpoB argE(Am) recA1, lysogenized with λpir phage	Kvitko et al [100]
HB101	F$^-$mcrB mrr hsdS20($r_B^-m_B^-$) recA13 leuB6 ara-14 proA2 lacY1 galK2 xyl-5 mtl-1 rpsL20(Sm^R) gln V44 λ$^-$	Boyer and Roulland-Dussoix [101]

Table 3.2. Plasmids, and relevant characteristics, used in this project.

Plasmid	Description	Source
pSEVA237::P_{unk}-GFP	Km^R, ori pBBR1, cargo GFP with the promoter region upstream the unk PKS gene inserted for transcription analysis	Technical University of Denmark – DTU, Kongens Lyngby, Denmark Vector developer: de Lorenzo´s lab [102]
pSEVA237::P_{phlA}-GFP	Km^R, ori pBBR1, cargo GFP with the promoter region upstream the *phlA* gene inserted for transcription analysis	Technical University of Denmark – DTU, Kongens Lyngby, Denmark Vector developer: de Lorenzo´s lab [102]
pNJ1	Tc^R sacB+ R6K ori, mobRP4, allelic replacement vector derived from pDS132	Yang et al [103]
pRK600	Cm^R , ori ColE1 RK2-Mob+ RK2-Tra+ helper plasmid in triparental matings	Kessler et al [104]
pBG42	Km^R Gm^R, ori R6K, pBG-derived	Zobel et al

3.3. Cultivation and storage conditions

3.3.1. Culture media

All the media used in this project are described in Table 3.3.

Table 3.3. Media used in this project.

	Composition	
Medium	**Liquid**	**Solid**
ABT	Composed by A-10 medium mixed with BT-medium in a proportion of 1:9, respectively. **A-10 medium** 1000 ml of A-10 medium were prepared adding 20 g of $(NH_4)_2SO_4$, 60 g of Na_2HPO_4, 30 g of KH_2PO_4, 30 g of NaCl, and 1000 ml of H_2O. pH was 6,4. **BT medium** 900 ml of BT medium were prepared adding 1 ml of 1 M MgCl, 1 ml of 0.1 M $CaCL_2$, 1 ml of $FeCl_3$, 2.5 ml of 1 mg/ml Thiamin and 900 ml of H_2O.	-
ABTG	ABT medium with 4% of glucose.	Composition of the respective liquid medium with addition of 1.5 % agar.
LB (Lennox broth)	Standard medium *(Carl Broth).*	
King's B (KB)	100 ml were prepared adding 2 g of proteose peptone (No. 3) and 861 µl of K_2HPO_4 (1M) to distilled water. The pH was adjusted to 7.2 +/- 0.2. After autoclaving, 1.25 ml of $MgSO_4$ and 2 ml of glycerol (50%), preheated to 50 celsius, were added.	
10% Tryptic soy broth (TSB)	Prepared by diluting tryptic soy broth (*Sigma-Aldrich*®) 10 times.	

Pseudomonas isolation agar (PIA)	-	Standard medium (*Milipore®*).

Overnight bacterial cultures were obtained by inoculating single bacterial colony in LB medium, at 30°C with gyratory agitation at 200 rpm (*New Brunswick Scientific Edison, N.J. U.S.A. – Gio Gyratory Shaker*).

Long-term storage was prepared by centrifugation of 1 ml of overnight bacterial culture and resuspension of the pellets in 1 ml of LB medium. The resuspension was mixed with an aqueous solution of glycerol 50% in 1:1 (v:v) proportion. The cultures were stored at -80ºC.

3.4. Unknown BGC expression and phenotype comparison in different media

3.4.1. Expression and growth comparison assay

Growth (optical density at a wavelength of 600 nm (OD600)) and fluorescence (relative units of fluorescence (RFU)) differences between bacterial cultures of WT and the PKS deletion mutant (ΔPKS) were analysed. Fluorescence difference between cultures of WT and the WT with the reporter gene (Punk-GFP) were used to evaluate the relative expression of the unknown biosynthetic gene cluster (BGC). The assay was carried out in a 96-well microtiter plate, analysing three biological replicates of each strain in four different media, ABTG, TSB, LB, and KB (the first two are poor media and the last two are rich media). at 30 °C and 282 rpm for 24h. The initial OD600 was set to 0.01 (*Amersham Biosciences – Ultrospec 10*) and each well contained a volume of 200 µl. A negative control with only media was included, to be used as blank and contamination assessment. The plates were incubated in a multimode microplate reader (*Biotek Synergy H1 Hybrid Reader),* at 30 °C and 282 rpm for 24h (with initial double agitation of 282 rpm for 10 secs). Excitation and emission wavelength for fluorescence reading were 485 and 513 nm, respectively.

3.4.2. Spots comparison

To analyse possible phenotype variations of the unknown PKS deletion mutant, 5 µl of WT and ΔPKS cultures washed in NaCl 0.9% (OD600 = 1.0) were spotted on ABTG, TS, LB, and KB agar plates, with three biological replicates for each condition. The cultures were grown at 30 °C. Differences were observed after two days of growth on the plates and the diameter of the spots was measured.

3.4.3. WT comparison with ΔPKS on ABTG medium

In a 96-well microtiter plate, the growth and natural fluorescence of WT and ΔPKS while exposed to rifamycin (0.177 – 60.0 µg/ml) were compared (2-fold serial dilution). Two negative controls were included: a row containing inoculated ABTG medium (0 µg/ml of antibiotic), to observe the bacteria behaviour without the effect of rifamycin; a row containing only ABTG medium to be used as blank and contamination assessment. At the end of the setup, each well contained a total volume of 200 µl and an OD600 of 0.01. The plates were incubated in a multimode microplate reader, at 30 °C and 282 rpm for 24h (with initial double agitation of 282 rpm for 10 secs).

3.5. MIC assays

Minimum inhibitory concentrations (MICs) of the antibiotics rifamycin and streptomycin were estimated in a 96-well plate using four biological replicates of WT. The strain was exposed to a range of antibiotic concentrations (2-fold serial dilution) (Table 3.4). Two negative controls were included: a row containing inoculated LB medium (0 µg/ml of antibiotic), to observe the bacteria behaviour without the effect of rifamycin; a row containing only LB medium to be used as blank and contamination assessment. At the end of the setup, each well contained a total volume of 200 µl and an OD600 of 0.01. The plates were incubated in a shaker at 30°C with orbital agitation at 300 rpm (*Heidolph - Titramax 100*).

Table 3.4. Antibiotics used in the MIC assays.

Compound	Concentration range (µg/ml)	Notes
Rifamycin	0.250 – 128	As a control, it was ensured that dimethyl sulfoxide (rifamycin's stock solution solvent) was not toxic to the strain
Streptomycin	1.06 - 540	

3.6. BGC expression assays

Growth and the promoter activity through the fluorescence emission of GFP were analysed, under the influence of the compounds rifamycin, rifampicin, and D-Arabitol (with and without glucose), Table 3.5. Two negative controls were included: a row containing inoculated medium, to observe the bacterial behaviour without the effect of the compound; a row containing only medium to be used as blank and contamination assessment. Each well of the 96-well microtiter plate contained a total volume of 200 µl and an OD600 of 0.01. The plates were incubated in a multimode microplate reader, at 30 °C and 282 rpm for 24h (with initial double agitation of 282 rpm for 10 secs).

Table 3.5. Antibiotics and carbon source tested in the expression and antibiotic assays.

Compound	Concentration (µg/ml)	Media	Strain
Rifamycin	0.177 – 60.0	ABTG	Punk-GFP (DTU9.1 + pSEVA237::P_{unk}-GFP)
			DTU9.1 + pSEVA237::P_{phla}-GFP
Rifampicin	0.177 – 60.0		Punk-GFP
D-Arabitol	9.76 - 5.00×10^3	ABT	Punk-GFP
		ABTG	

3.6.1. Shake flasks assay

Three biological replicates of Punk-GFP were tested in 100 ml Erlenmeyer flasks containing a total volume of 25 ml at 30 ºC and 200 rpm (*Infors HT Labotron*). The conditions included different concentrations of rifamycin: 0 µg/ml, 3.75 µg/ml, 25 µg/ml, and 3.75 µg/ml and 25 µg/ml added after 15 h and 30 mins of growth. The initial OD600 was 0.01. The volume of samples analysed each time was 150 µl, and the samples were incubated in a multimode microplate reader, at 282 rpm for 6 min (with initial double agitation of 282 rpm for 10 secs), reading OD600 and fluorescence values 4 times.

3.7. LC-MS

Extracts of cellular metabolites were physically separated by liquid chromatography (LC) and had their mass analysed by mass spectrometry (MS). The resultant data was analysed by *MS-Dial*[105] software and *MetaboAnalyst 5.0*[106] online tool. The chromatograms were constructed with *Agilent MassHunter*[107] software. The metabolites extraction procedures are described below.

3.7.1. Extracellular metabolites extraction

Three biological replicates of WT and ΔPKS strains, grown in ABTG, were analysed. 100 ml cultures were cultivated in 250 ml Erlenmayer flasks at 30 °C and 200 rpm and samples of 20 ml of each bacterial culture were taken after 30h. The samples were then centrifuged (*Heraeus – Multifuge X3R Centrifuge*) for 5 min at 8000 rpm and the supernatant was filter sterilized (pore diameter of 0.25 µm). For a two-phase extraction, 20 ml of the extraction solvent ethyl acetate, were added to the 20 ml of filtered supernatant. The mixture was vortexed for 5 min and centrifuged for 5 min at 8000 rpm, resulting in two distinct phases: an upper organic phase and the lower aqueous phase. 14 ml of the upper phase were collected, dried with a nitrogen pump, and dissolved in 200 µl of methanol. The final solution was transferred to an LC-MS vial and sent to the Natural Products Chemistry group (DTU Bioengineering) for LC-MS analysis.

3.7.2. Intracellular metabolites extraction

Three biological replicates of WT and ΔPKS strains, grown in ABTG, were analysed. 100 ml cultures were cultivated in 250 ml Erlenmeyer flasks at 30 °C and 200 rpm and after 35h. The entire volume of cultures was centrifuged (for 5 min at 8000 rpm), washed with 25 ml of 0.9% NaCl, and centrifuged again. The supernatant was completely removed, and the pellets were resuspended in 10 ml ethyl acetate. The suspension was sonicated for 20 mins and then centrifuged. 8 ml of the ethyl acetate layer was transferred to a falcon tube, dried with a nitrogen pump, and reconstituted with 200 µl of methanol. The solution was transferred to an LC-MS vial and sent to the Natural Products Chemistry group for LC--MS analysis.

3.8. Ribosome and RNA polymerase Engineering

3.8.1. Mutant colonies selection

100 µl of three biological replicates of WT cultures (OD600 = 3,0) were spread on LB agar, LB agar supplemented with rifamycin (65 µg/ml), and LB agar supplemented with streptomycin (135 µg/ml) in dilutions of 10^{-11}, $10^{0,}$ and 10^{-2}, respectively for each media. The value of antibiotics concentration was chosen by doubling the MIC value (section 3.5. MIC assays). Colony-forming units (CFU's) were counted two days after plating to assess the mutation rate. One colony of each plate supplemented with an antibiotic (resistant colonies) was stocked with glycerol at -80 ºC for further analyses.

3.8.2. Detection of mutations in antibiotic-resistant strains

Two colonies (biological replicates) of WT, rifamycin resistant (Rif^R) and streptomycin resistant ($Strep^R$) mutant strains were placed in microcentrifuge tubes containing 30 µl of H_2O, boiled at 99 ºC for 10 min

to lyse the cells, and centrifuged at 12 000 x g for 3 min. The supernatant, containing genomic DNA, was used as a template for PCR reaction (DreamTaq™ DNA Polymerase kit). The list of primers used in the PCR reactions can be found in Table 3.6.

Table 3.6. Primers used to check *rpsL* and *rpoB* genes mutations.

Target gene	Primer name	Sequence (5'- 3')
rpsL	rpsL_fw_DTU_9.1	actgcaaaacgaccgattac
	rpsL_rev_DTU_9.1	acagtggagctagtagatggc
	rpsL_mut_check_fw	taagccctcaaacggtcttcagg
	rpsL_mut_check_rev	ttgactgggggcaagatcc
rpoB	1_rpoB_mc_fw	tcacgtgttattcggtttcc
	1_rpoB_mc_rev	agaagatcaatcgcatggtcg
	2_rpoB_mc_fw	aggttgttcgccagatccagg
	2_rpoB_mc_rev	agatccgcgtatcgttgaagg
	3_rpoB_mc_fw	aagaccgtcgagaacttcatcg
	3_rpoB_mc_rev	accagaacacctgcatcaacc
	4_rpoB_mc_fw	atttccacgccatgaacgcg
	4_rpoB_mc_rev	taccgtgtggtgaaagacgc
	5_rpoB_mc_fw	aactggcctttgtcgttcatcg
	5_rpoB_mc_rev	ttgccgtactgaagactctgg
	6_rpoB_mc_fw	aacacgacggttacccagg
	6_rpoB_mc_rev	acaagggcaaggttattgtcg
	7_rpoB_mc_fw	tttgataccggctttttccagc
	7_rpoB_mc_rev	aaagaatcgtcgaacaaagcg
	8_rpoB_mc_fw	aaggtaccgttctcagtcatcagg
	8_rpoB_mc_rev	aacgctgatggcttactcatatactg

Samples (20 µl) were loaded in an agarose (0.8%) gel containing ethidium bromide. The buffer Gene Ruler Express DNA Ladder was used to determine the size of the PCR bands. The DNA was purified with NucleoSpin® Gel and PCR Clean-up kit (*Macherey-Nagel*). The fragments of DNA were sequenced, to check the similarity with WT gene sequences, by *Eurofins Scientifics*. DNA sequences were compared using the online tool *Benchling*.

3.8.3. Sample collection for RNA extraction

Three biological replicates of WT, Rif^R, and $Strep^R$ were incubated in 100 ml Erlenmeyer flasks containing 50 ml of ABTG medium (OD600 = 0.01) at 30 ºC with orbital agitation at 200 rpm (*Infors HT Ecootron – Buch & Holm*) for 30h. Samples were collected at 14h, 24h, and 30h, to analyse the unknown BGC expression at different growth phases. The samples were centrifuged, the supernatant was discarded, and the pallets were stored at -23 ºC.

3.8.4. Transcriptional analysis by RT-qPCR

Reverse transcription-quantitative PCR technique was used to analyse the relative expression of the unknown BGC in the WT and the antibiotic-resistant mutants. For that, RNA was extracted from the pellets obtained in the previous step with RNeasy® Mini kit (*QUIAGEN*) according to the protocol supplied by the manufacturer. 1 µg of the obtained sample was converted into complementary DNA

(cDNA) using the iScript™ Reverse Transcription Supermix for RT-qPCR (*Bio-Rad*) kit, according to the protocol supplied by the manufacturer. RNA and cDNA concentrations were measured by spectrophotometry with DS-11+Spectrophotometer (*DeNovix®*). Quantitative PCR (qPCR) samples were prepared with PowerUp™ SYBR™ Green Master Mix (*Thermo Fisher Scientific*) following manufacturer instructions to a final volume of 10 µl per sample. The samples were analysed in technical and biological triplicates and a no-template control was included, using water instead of cDNA. The reactions were performed and analyzed by the instrument *Stratagene Mx3005P qPCR*. First, a 1:10 dilution series of one sample of cDNA, ranging from 10^{-1} to 10^{-5}, was used to obtain the standard curve for each primer pair, listed in Table 3.7, by representing the average cycle threshold (Ct) value in function of logarithmic quantity range. With the resultant slopes (Annex A), the respective efficiency was calculated through Equations 3.1 and 3.2 (based on the study of Hellemans and colleagues[108]).

Table 3.7. Primers used for qPCR analysis.

Target gene	Primer	Sequence
***gyrB* (reference gene)**	qPCR_gyrB_F_1	cggtaagttcgacgataactcc
	qPCR_gyrB_R_1	ggacataggtctgttcccagat
***rpoD* (reference gene)**	qPCR_rpoD_F_3	gaagtcgaaacaggcttgaaga
	qPCR_rpoD_R_3	tacttcttggcgatggagatca
CLA18_06265 (Unknown PKS)	qPCR_unk_F_3	cttgttgaagctgttctcgact
	qPCR_unk_R_3	gatgacatcttgtactccgctg

$$E\ (\%) = \left(10^{\frac{-1}{slope}} - 1\right) \times 100 \quad \textbf{(3.1)}$$

With *E* standing for primer efficiency.

$$Converted\ primer\ efficiency = \left(\frac{E\ (\%)}{100}\right) + 1 \quad \textbf{(3.2)}$$

To ensure reproducible data, primer efficiency is recommended to be within 90%-110%[109]. The comparative transcriptional assays were normalized to the transcriptional levels of the housekeeping genes *gyrB* and *rpoD*. Relative gene expression values were obtained with Equation 3.3 to 3.5.

$$\Delta Ct = Control\ average\ Ct - Sample\ Ct \quad \textbf{(3.3)}$$

$$RQ = E^{\Delta Ct} \quad \textbf{(3.4)}$$

In which *RQ* means relative quantity.

$$Relative\ gene\ expression = \frac{RQ_{GOI}}{Geomean[RQ_{REFs}]} \quad \textbf{(3.5)}$$

With *GOI* standing for the gene of interest, *REFs* for the reference genes and *Geomean* to the geometric mean. All reactions were performed under the conditions described in Table 3.8.

Table 3.8. Thermal cycling program applied in qPCR using primers with melting temperatures under 60 °C[110].

Step	Temperature (°C)	Duration	Cycles
UDG activation	50	2 min	-
Dual-Lock™ DNA polymerase	95	2 min	-
Denaturation	95	15 sec	40
Annealing	55	15 sec	
Extension	72	1 min	
Dissociation Step	95	15 sec	-
	60	1 min	-
	95	15 sec	-

3.8.5. Triparental mating

The plasmid pSEVA237::P_{unk}-GFP was inserted into the Rif^R and $Strep^R$ strains by triparental mating. For that, the donor strain, the helper strain, and the recipient strains were cultured overnight. The cells were washed in 0.9% NaCl (OD600=1.0). Control conjugation mixes were prepared, including an antibiotic selection control (water:water:recipient proportion), and pseudomonas selection control (donor:helper:water proportion) to ensure that only pseudomonas with the desired plasmid would be selected. A conjugation mix with the three strains was prepared (donor:helper:recipient proportion). The final volumes of the conjugation mixes were equal to approximately 1 ml. The cells were centrifuged at 10 000 rpm for 1 min and the supernatant was discarded by decanting. The pellets were resuspended in the remaining liquid. 20 µl of the conjugation mix were spotted on a LB plate and incubated at 30°C overnight. The conjugation spot was scraped off the LB plate and resuspended in 1 ml 0.9% NaCl. 100 µl of diluted cultures (10^3 to 10^5 times) were spread on PIA plates with 50 µg/ml kanamycin and incubated at 30°C for two days. Positive conjugant strains were selected and stored.

3.8.6. BGC expression assay

Growth and fluorescence differences between cultures of WT, Rif^R, and $Strep^R$, and the same three strains containing the reporter gene GFP for the Punk promoter were analysed. Fluorescence differences between cultures of WT and the WT with the reporter gene (Punk-GFP) were used to evaluate the relative expression of the unknown biosynthetic gene cluster. The assay was carried out in a 96-well microtiter plate, analysing three biological replicates of each strain in ABTG at 30 °C and 282 rpm for 24h. The initial OD600 was set to 0.01 (*Amersham Biosciences – Ultrospec 10*) and each well contained a volume of 200 µl. A negative control with only media was included, to be used as blank and contamination assessment.

3.9. Allelic replacement

The allelic replacement technique replaces a specific region of DNA with homologous recombination. Here, the method was initiated with the purpose of switching the promoter region upstream of the unknown BGC by a stronger one.

3.9.1. SOE PCR

A fragment DNA insert was constructed by Splicing by Overlap Extension (SOE) PCR, containing the promoter 14g to be inserted in the target genomic region of the genome surrounded by elements homologous upstream and downstream (HR1 and HR2, respectively) of the target genomic region. HR1 and HR2 were amplified from the WT genome and the promoter (p14g) was amplified from plasmid pBG42. The primers used for each region can be found in Table 3.9. The construction of the fragment started by fusing HR2 to the promoter region (primers 364/363), which was then fused to HR1 in a second PCR reaction (primers 366/363).

Table 3.9. Primers used for SOE PCR. Small letters represent overhangs. Bold letters represent enzymatic restriction sites.

Target fragment	Primer	Sequence	Description
HR2 FW	Pr362	ATGAGAAAGATCGCCA TCGTAG	Annealing immediately downstream of the promoter sequence to be altered
HR2 R	Pr363	atccgg**gagctc**GACCAAAT ATCGTTGCAGGC	Annealing further downstream with an overhang including the restriction enzyme site (SacI) and extra nucleotides to increase restriction efficiency
Promoter FW	Pr364	TGCTCCATAACATCAAA CATCG	Annealing directly to the beginning of the promoter region
Promoter R	Pr365	acgatggcgatctttctcatTAGA AAACCTCCTTAGCATGA TTAAG	Annealing directly to the end of the promoter region with an overhang including a complementarity region to the HR2 fragment
HR1 FW	Pr366	atcccg**tctaga**AATGTGTT CTCGGTGGTCG	Annealing further upstream with an overhang including the restriction enzyme site (XbaI) and extra nucleotides to increase restriction efficiency
HR1 R	Pr367	gtcgatgtttgatgttatggagcaC GTGGTTTTTGTCGTCTC AG	Annealing directly upstream the promoter sequence to be altered with an overhang including a complementarity region to the promoter fragment

3.9.2. Plasmid purification

Plasmid pNJ1 was purified from 12ml of *E. coli* CC118 λspir + pNJ1 overnight culture using NucleoSpin® Plasmid kit (*Macherey-Nagel*) following the protocol supplied by the manufacturer.

3.9.3. Restriction digestion

Both SOE PCR product and the plasmid went through restriction digestion using the enzymes SacI and XbaI, and 10X FastDigest Green Buffer (*ThermoFisher Scientific*). In one trial of plasmid digestion, Fast AP (thermosensitive alkaline phosphatase) was also added to dephosphorylate DNA ends. The thermal conditions used are shown in Table 3.10.

Table 3.10. Thermal conditions for restriction digest.

	Plasmid reaction	**SOE product reaction**
Temperature	**Time**	**Time**
37°C	20min	60min
65°C	20min	20min
4°C	Hold	

The plasmid and the SOE PCR product digested were purified by gel and PCR purification, respectively (NucleoSpin® Gel and PCR Clean up).

3.9.4. Ligation

The concentrations used for vector/insert ligation were such to obtain a base pair ratio (insert/plasmid) of approximately 1:5 (plasmid: 6692 bp; insert: 1489 bp). A false positive control was obtained by not adding the SOE PCR insert to the ligation mix. Ligation reaction was performed using a thermocycler program with ligation (22 °C, 2h) and protein degradation (65 °C, 10 min) steps.

3.9.5. Transformation

After ligation, the DNA was transformed into *E. coli* CC118 λpir by heat shock transformation. The cells were mixed with 2.5 µl DNA and placed in ice for 30 mins, incubated at 42°C for 1 min, and placed again in ice for 2 mins. 450 µl of LB were added to each tube and the mixed sample was incubated at 37°C for 1 hour for recovery. The cells were spread on selective LB agar plates. After one day, the transformant cells were verified by colony PCR using the primers presented in Table 3.11 and some were also analysed by sequencing. A third and fourth controls were added: an antibiotic selection control, in which water was added to the competent cells instead of DNA, and a transformation control, in which 1µl of approximately 100 ng purified plasmid vector was added. The experiment was halted after transformation as no positive transformant was obtained.

Table 3.11. Primers used for insertion evaluation on plasmid pNJ1.

Primer	Sequence
pNJ1_fw (120)	AACAAACCCGCGCGATTTAC
pNJ1_rev (121)	GTAACGCACTGAGAAGCCCT

3.10. Statistical Analysis

In MetaboAnalyst 5.0, data filtering was based on interquartile range, samples were normalized by sum and the data scaling chosen was Pareto scaling. Differences were considered statistically significant for p-values lower than 0.05.

4. Results

4.1. The unknown BGC has low expression levels

To seek changes in the expression of the unknown biosynthetic gene cluster (BGC) within different culture conditions, the *P. protegens* DTU9.1 wild type (WT), the unknown PKS knockout mutant (ΔPKS), and the WT with a transcription reporter gene for the promoter upstream the BGC region (Punk-GFP) were cultured in four different media: LB, KB, ABTG, and TSB.

Figure 4.1.A shows the growth rates of the three strains (WT, ΔPKS and Punk-GFP) cultured in different media (LB, KB, ABTG and TSB). The variance between WT and ΔPKS growth rates was not considered statistically significant, meaning that the deletion of the gene did not influence the growth rate under the assayed conditions.

The fluorescence levels (relative fluorescence units (RFU)) of the cultures after 24h of growth are displayed in Figure 4.1.B, as well as the negative control (only media). For all the media, the addition of the fluorescent reporter gene leads to an increase of the fluorescent signal of 988, 1097, 1320, and 1358 RFU, for ABTG, KB, TSB, and LB media, respectively. This means that the promoter is active in all the studied conditions. LB and KB media intrinsic levels of fluorescence are very high, making it difficult to analyse bacterial levels of fluorescence. The lower levels of fluorescence of the cultures in comparison to the media after 24h can be due to the consumption of the fluorescent compounds in the media.

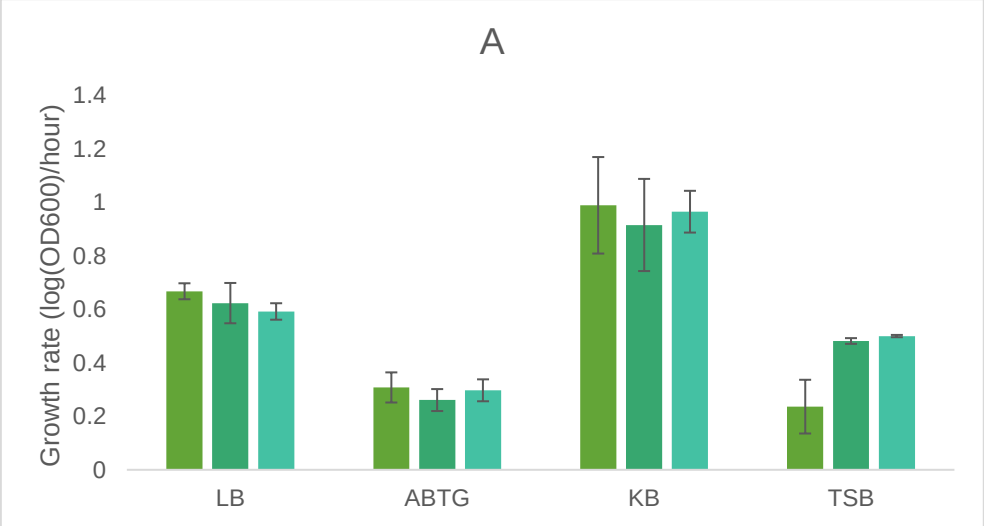

Figure 4.1. Bar chart – Growth rates and fluorescence of WT, ΔPKS, and Punk-GFP strains in LB, KB, ABTG and TSB media. The three strains, WT (■), ΔPKS (■), and Punk-GFP (■), were cultured in KB, LB, TSB, and ABTG media on a microtiter plate at 30°C and 282 rpm. **(A)** Growth rate. **(B)** Fluorescence levels measured after 24h of culture (not normalized to the medium fluorescence (■)). Standard deviation bars are displayed.

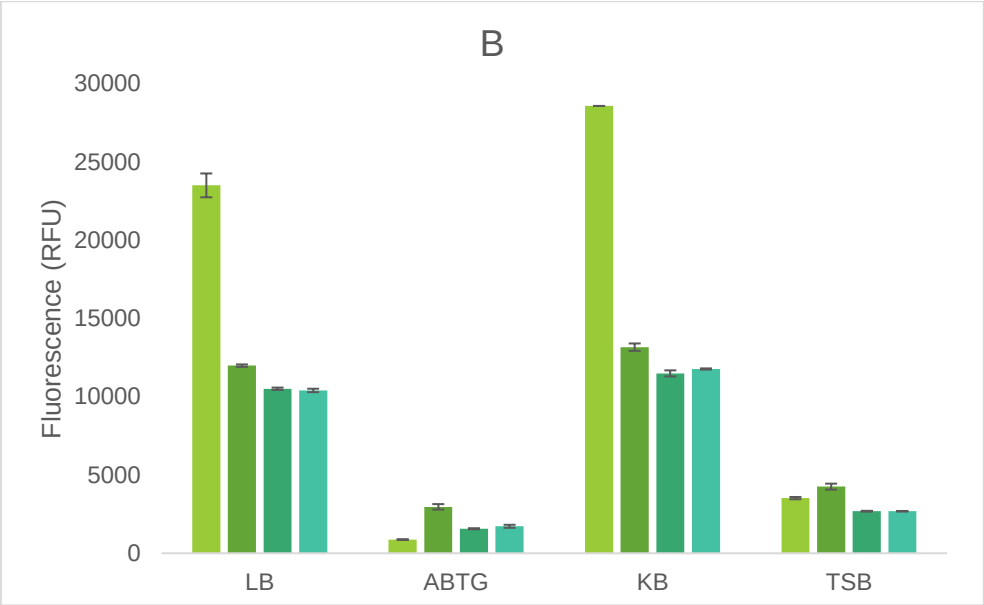

Figure 4.1. (cont.) Bar chart – Growth rates and fluorescence of WT, ΔPKS, and Punk-GFP strains in LB, KB, ABTG and TSB media. The three strains, WT (■), ΔPKS (■), and Punk-GFP (■), were cultured in KB, LB, TSB, and ABTG media on a microtiter plate at 30ºC and 282 rpm. **(A)** Growth rate. **(B)** Fluorescence levels measured after 24h of culture (not normalized to the medium fluorescence (■)). Standard deviation bars are displayed.

WT and ΔPKS were plated in four solid media (LB, KB, ABTG and TSB) and again, no significant difference was observed in the growth between each strain, evaluating the diameter of the spots, Figure 4.2, and Table 4.1.

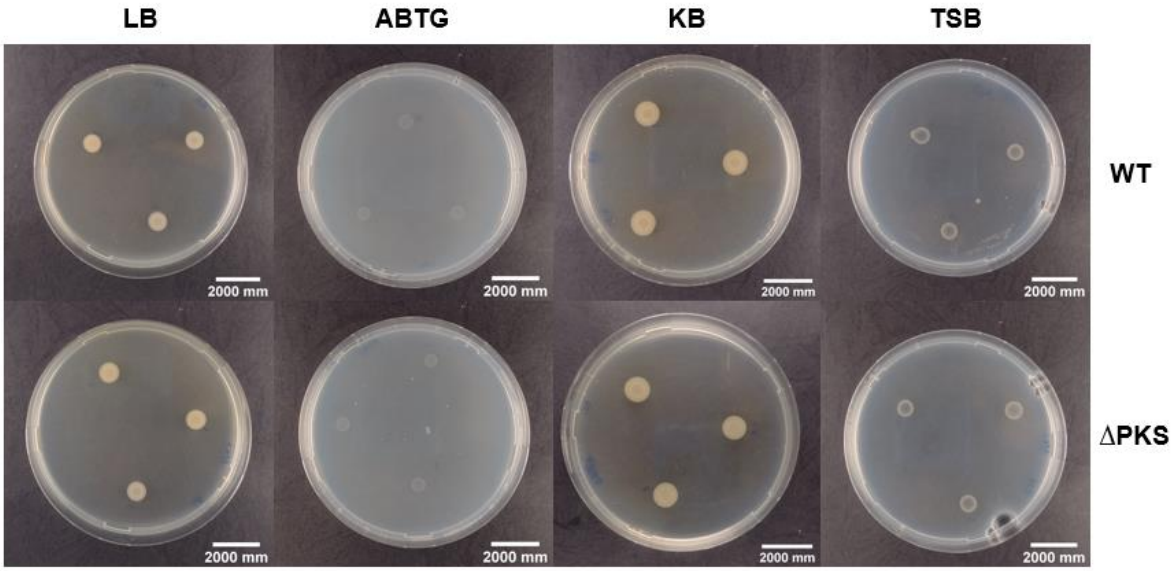

Figure 4.2. WT and ΔPKS spots in LB, KB, ABTG and TSB media after 2 days. The sizes of the colonies are presented in Table 4.1.

Table 4.1. Diameter of WT and ΔPKS spots after 2 days of growth on four different solid media. Three biological replicates were tested.

Media	Strain	Diameter (µm)
LB	WT	(8.59±0.2) x10^2
	ΔPKS	(8.34±0.2) x10^2
ABTG	WT	(5.63±0.2) x10^2
	ΔPKS	(5.67±0.2) x10^2
KB	WT	(9.78±0.2) x10^2
	ΔPKS	(1.03±0.03) x10^3
TSB	WT	(7.43±0.3) x10^2
	ΔPKS	(7.36±0.03) x10^2

Together, the information leads to the conclusion that the unknown BGC is expressed, but in low levels, not impacting the cellular growth.

4.2. WT and ΔPKS present different expression of intracellular metabolites

After confirmation of unknown BGC expression, intra- and extracellular metabolites of the WT and ΔPKS in the late stationary phase were compared by LC-MS. The fold change of metabolites up/downregulated in ΔPKS extracts in comparison to WT extracts was analysed with *MetaboAnalyst 5.0*, Figure 4.3.A and 4.3.B, based on peak areas.

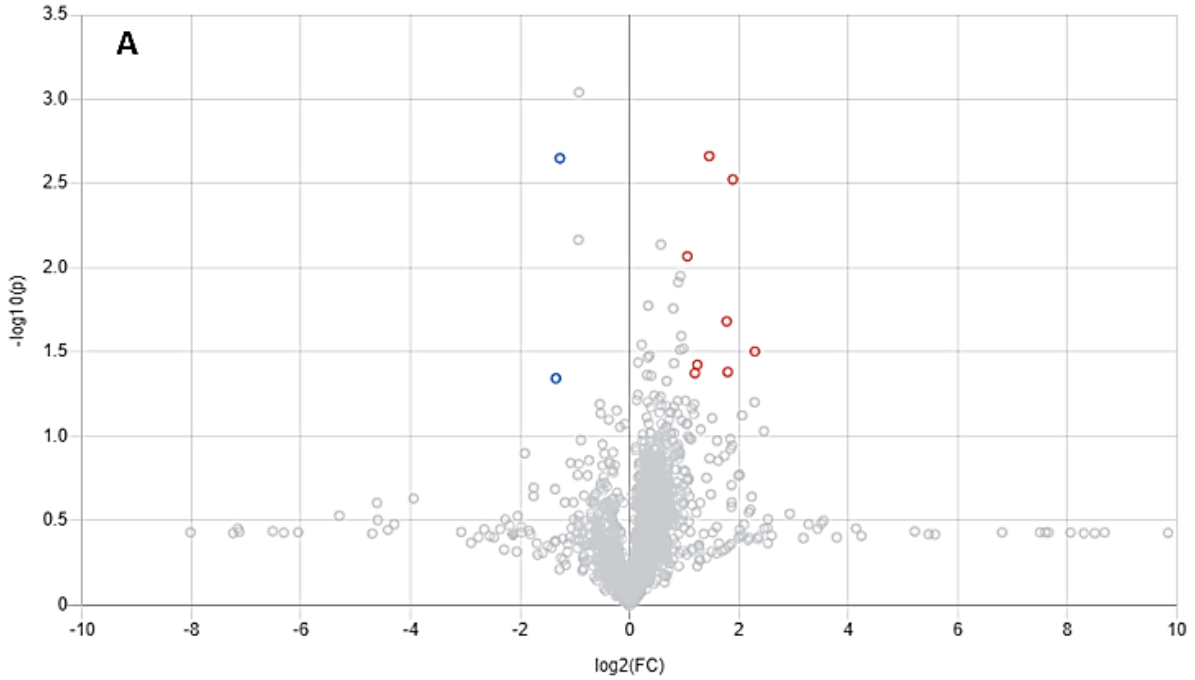

Figure 4.3. Volcano plots – Metabolite comparison of WT and ΔPKS in late exponential phase - A) Comparison of extracellular metabolites (Downregulated – 1, Upregulated – 7, Unsigned - 1524), **B)** Comparison of intracellular metabolites (Downregulated – 88, Upregulated – 30, Unsigned - 1770). Fold change threshold = 2.0, p<0.05. ● – Upregulated, ● - Downregulated, ● – Unsigned.

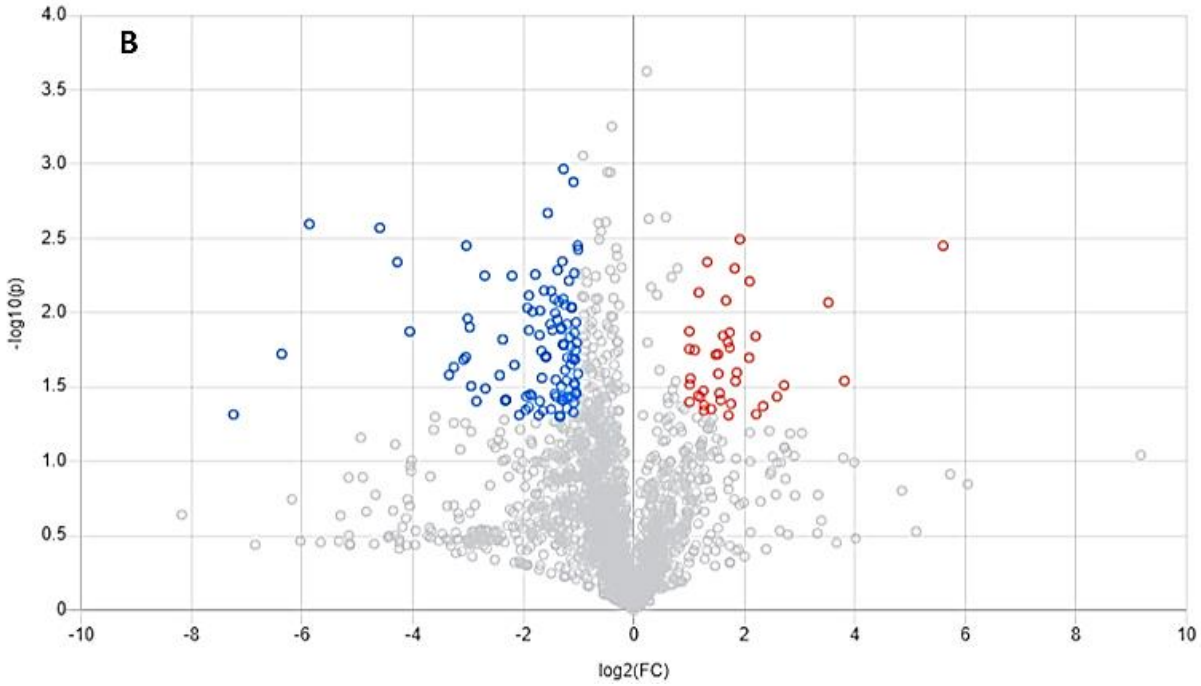

Figure 4.3. (cont.) Volcano plots – Metabolite comparison of WT and ΔPKS in late exponential phase - A) Comparison of extracellular metabolites (Downregulated – 1, Upregulated – 7, Unsigned - 1524), **B)** Comparison of intracellular metabolites (Downregulated – 88, Upregulated – 30, Unsigned - 1770). Fold change threshold = 2.0, p<0.05. ● – Upregulated, ● - Downregulated, ● – Unsigned.

In the extracellular extract, LC-MS showed that only 8 metabolites were considered differently expressed comparing fold change between WT and ΔPKS strains, Figure 4.3.A, and none of them was completely absent in the ΔPKS extract. In the intracellular extract, 118 metabolites were considered differently expressed (Annex B), Figure 4.3.B, with 2 of them having base peak areas close to zero in the ΔPKS extract (Annex C), Table 4.2.

Table 4.2. List of the metabolites with lowest fold change in ΔPKS in comparison with WT.

Average m/z	Average retention time (min)	Fold change
270.09402	2.226	0.011892
248.11168	2.240	0.016812

Analysing the chromatograms, Figure 4.4.A and 4.4.B, no evidence of a missing peak in ΔPKS extract in this retention times is visible.

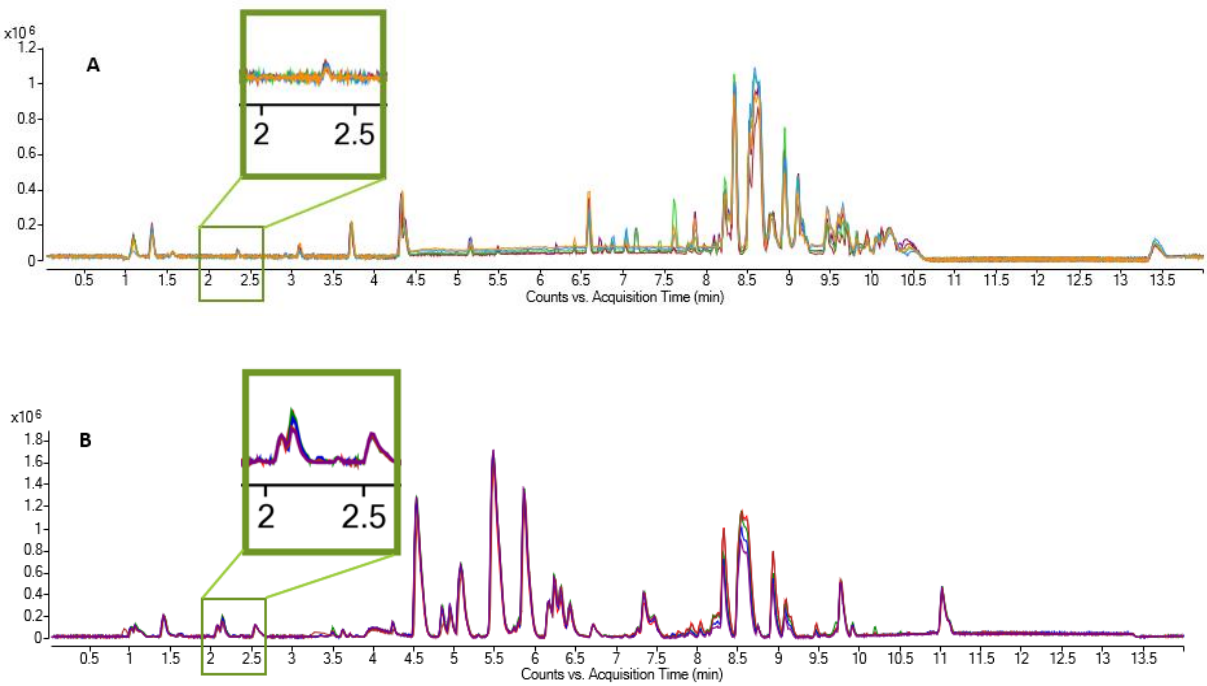

Figure 4.4. Base peak chromatogram – Results of LC-MS analysis to WT and ΔPKS extracts – (A) Extracellular extract chromatogram; **(B)** Intracellular extract chromatogram. Isolated peaks for each sample are shown in Annex D. The green box surrounds the area where a different peak between the extracts of the strains was expected.

Although 8 and 118 metabolites were differently expressed by the WT and the ΔPKS, respectively, the low expression level might not be enough to generate a product detectable by LC-MS. Hence, the identification of the produced compound is dependent on the overexpression of the unknown BGC.

4.3. Do antibiotics rifamycin and rifampicin activate the promoter?

The antibiotics rifamycin and its derivative rifampicin were tested on Punk-GFP strain to assess their effect in the activation of Punk expression by measuring the fluorescence intensity. The presence of rifamycin and rifampicin increased the fluorescence signal, Figure 4.5.B and 4.6.B, with an exception for the concentration of 3.75 µg/ml of rifampicin, which strongly inhibited culture growth, Figure 4.5.A and 4.6.A. However, the normalized fluorescence/OD600 plot, Figures 4.5.C and 4.6.C, show higher values for higher concentrations (below MIC) in both cases (with the exception for 3.75 µg/ml of rifampicin).

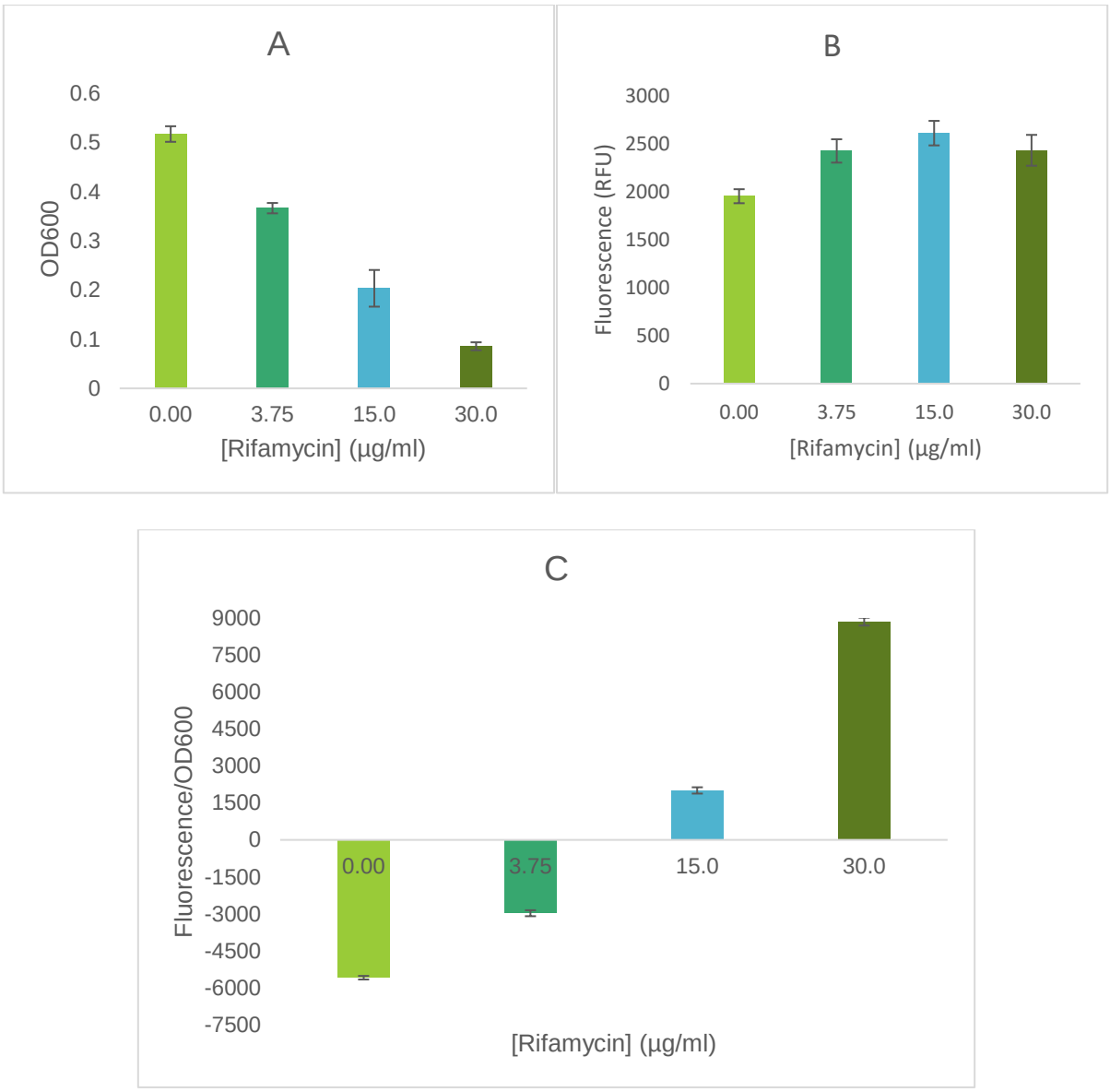

Figure 4.5. Bar graph - Rifamycin effect on promoter Punk activation in Punk-GFP after 24h of growth. Results of exposure to rifamycin concentrations of 0.00 µg/ml, 3.75 µg/ml, 15.0 µg/ml and 30.0 µg/ml. **(A)** growth (OD600), **(B)** fluorescence (RFU), **(C)** fluorescence normalised per OD600. Four biological replicates were tested two times each in a microtiter plate. Cells were grown in ABTG at 30 ºC and 282 rpm for 24h. Standard deviation bars are displayed.

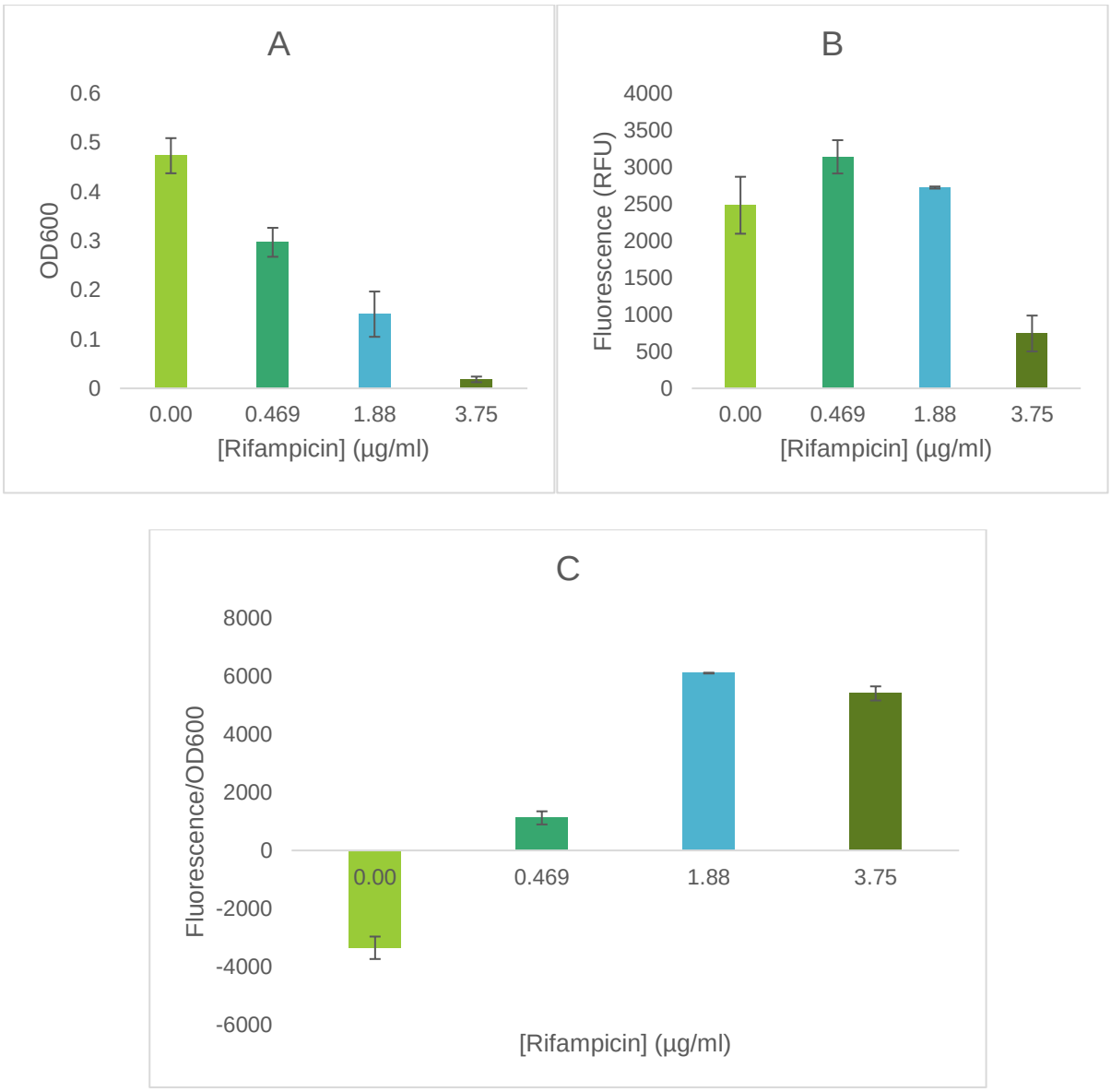

Figure 4.6. Bar graph – Rifampicin effect on promoter Punk activation in Punk-GFP after 24h of growth. Results of exposure to rifamycin concentrations of 0.00 µg/ml, 0.469 µg/ml, 1.88 µg/ml and 3.75 µg/ml. **(A)** growth (OD600), **(B)** fluorescence (RFU), **(C)** fluorescence normalised per OD600. Four biological replicates were tested two times each in a microtiter plate. Cells were grown in ABTG at 30 ºC and 282 rpm for 24h. Standard deviation bars are displayed.

The inductive effect of rifamycin was confirmed by culturing Punk-GFP in shake flasks in two different modes: with antibiotic supplementation 1) from the beginning of the culture and 2) at the middle of the growth phase. Although both cultures with 3.75 µg/ml rifamycin had the same OD600 after 40h of growth, Figure 4.7.A, the culture with the late addition of 3.75 µg/ml rifamycin showed the highest fluorescence, Figure 4.7.B. This means that the addition of the compound in a later growth phase induced the promoter Punk differently. On the opposite, the late addition of 25 µg/ml of rifamycin had a stronger inhibitory effect, Figure 4.7.A, significantly reducing the fluorescence, Figure 4.7.B. As seen before, the concentration closer to the MIC value added at the beginning of growth resulted in higher fluorescence/OD600, Figure 4.7.C.

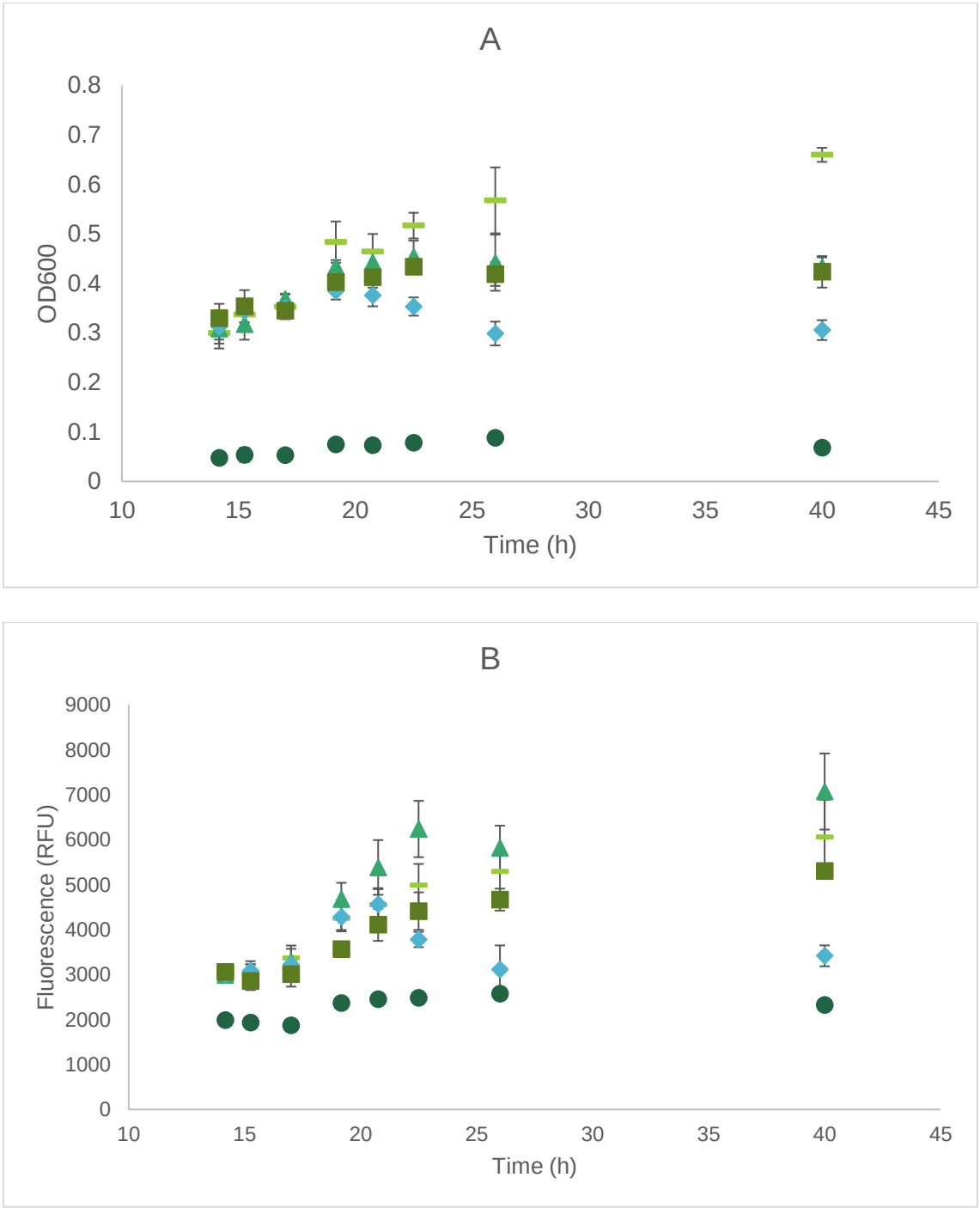

Figure 4.7 Scattering plot - Rifamycin effect on promoter Punk activation of Punk-GFP (shake flasks). Results of exposure to rifamycin concentrations of 0.00 µg/ml (-), 3.75 µg/ml (■),25.0 µg/ml (●), and 3.75 µg/ml (▲), and 25.0 µg/ml (♦), added only after 15h 30 min of growth. **(A)** growth (OD600), **(B)** fluorescence (RFU), **(C)** fluorescence normalised per OD600. Three biological replicates were tested for each condition and cultured in shake flasks with ABTG at 30 ºC and 200 rpm. Standard deviation bars are displayed.

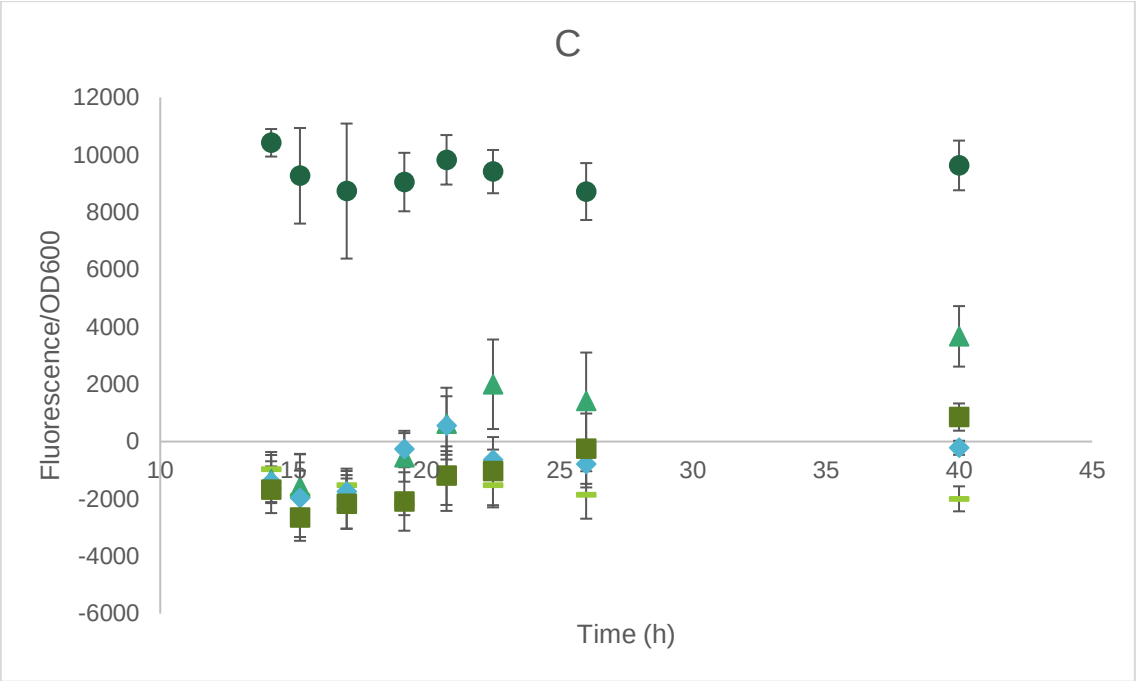

Figure 4.7. (cont.) Scattering plot - Rifamycin effect on promoter Punk activation of *Punk-GFP* (shake flasks). Results of exposure to rifamycin concentrations of 0.00 µg/ml (-), 3.75 µg/ml (■), 25.0 µg/ml (●), and 3.75 µg/ml (▲), and 25.0 µg/ml (♦), added only after 15h 30 min of growth. **(A)** growth (OD600), **(B)** fluorescence (RFU), **(C)** fluorescence normalised per OD600. Three biological replicates were tested for each condition and cultured in shake flasks with ABTG at 30 ºC and 200 rpm. Standard deviation bars are displayed.

Again, the fluorescence/OD600 increased with the increase of antibiotic concentration. Additionally, this assay shows that the addition of rifamycin at the exponential phase can change this tendency: with a lower concentration of rifamycin, the fluorescence of the culture increased without reduction of the growth; with a higher concentration of rifamycin, the fluorescence of the culture decreased with reduction of the growth.

4.4. Intrinsic fluorescence levels of *P. protegens* must be considered for GFP reporter gene analysis

To evaluate the inhibitory effect caused by the antibiotic rifamycin, one control was selected. The promoter upstream of *phlA* gene (PphlA), the first gene of the 2,4-DAPG biosynthetic operon, was used as a control as it is already known not to be induced by antibiotic rifamycin. Figure 4.8.A indicates the final OD600 values obtained after 24h of growth. Although Figure 4.8.B shows that the presence of the antibiotic led to a decrease in the fluorescence intensity, Figure 4.8.C demonstrates that the fluorescence/OD600 values increased with the increase in antibiotic concentration.

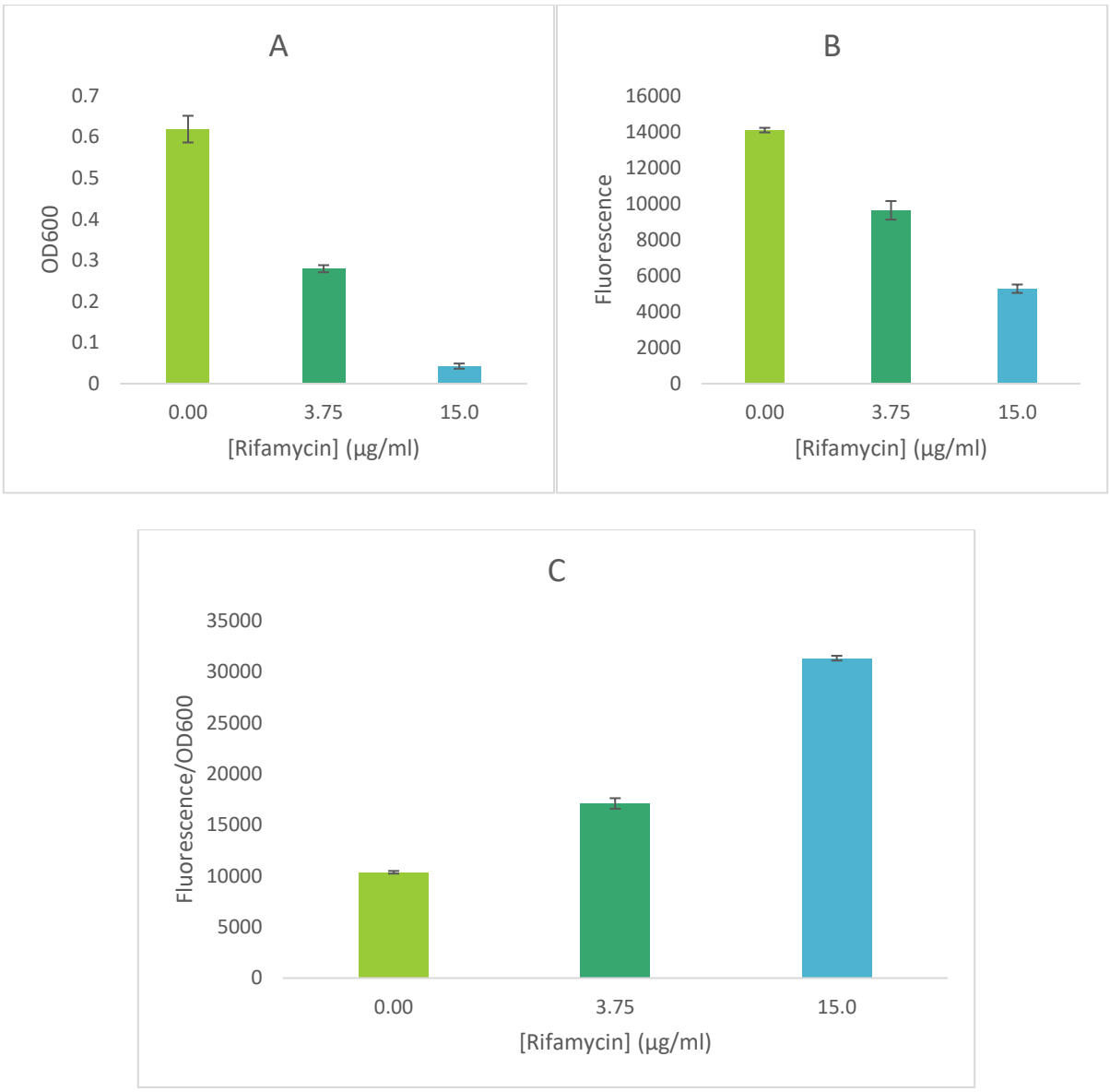

Figure 4.8. Bar graph - Rifamycin effect on promoter Pphla activation of P. protegens pSEVA237::P_{phlA}-GFP after 24h. Results of exposure to rifamycin concentrations of 0.00 µg/ml, 3.75 µg/ml, and 15.0 µg/ml. **(A)** growth (OD600), **(B)** fluorescence (RFU), **(C)** fluorescence normalised per OD600. Four biological replicates were tested in a microtiter plate at 30 ºC and 282 rpm in ABTG. Standard deviation bars are displayed.

The increased levels of fluorescence/OD600 with the increase of antibiotic concentration were also observed when the WT and ΔPKS were cultured with different concentrations of rifamycin, Fig. 4.9.C. Here, despite the inhibitory effect, Figure 4.9.A, the intrinsic fluorescence levels were higher when in presence of rifamycin, Figure 4.9.B.

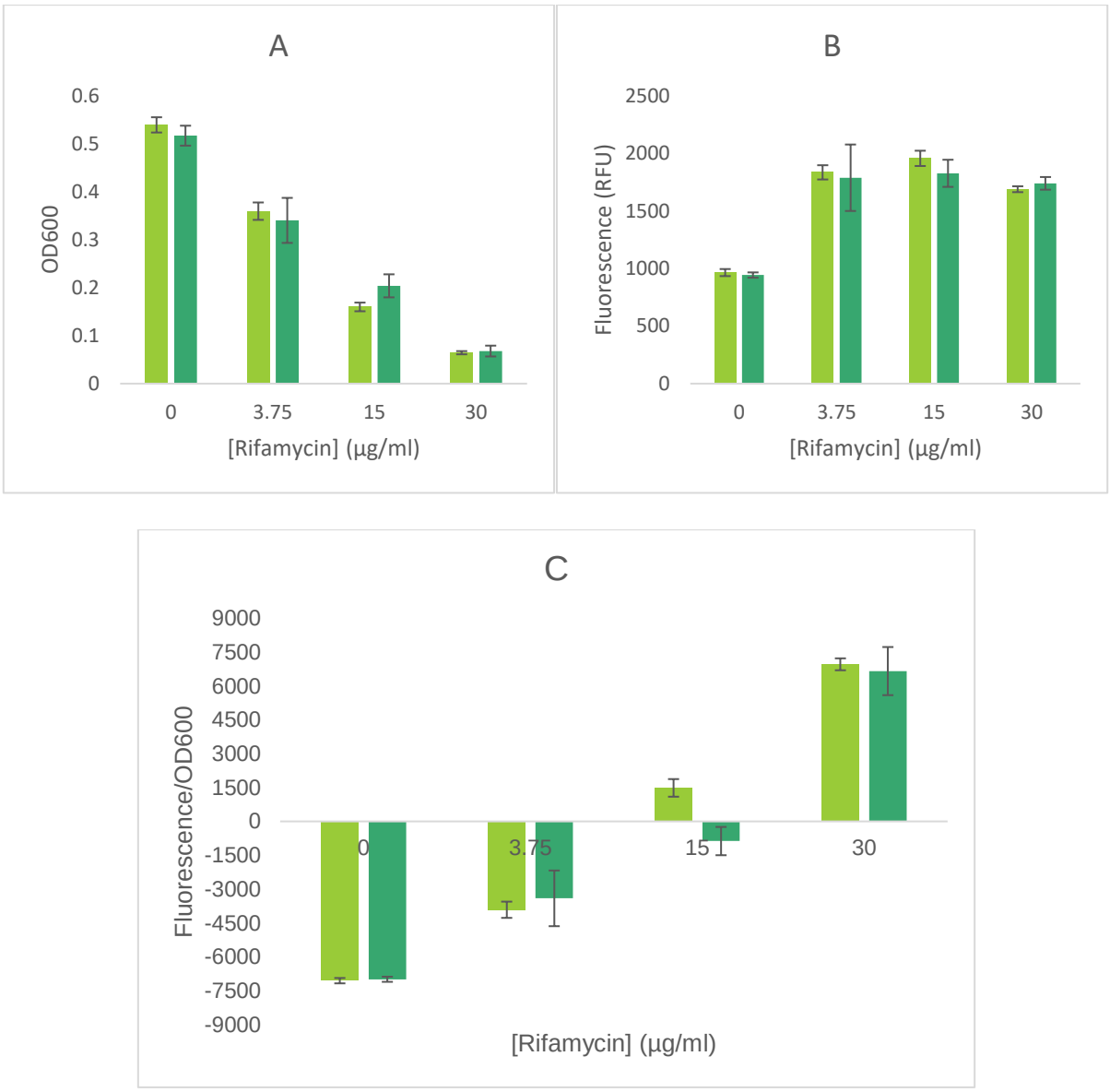

Figure 4.9. Bar graph – Rifamycin effect on WT (■) and ΔPKS (■) growth and intrinsic fluorescence curves after 24h of culture. Results of exposure to rifamycin concentrations of 0.00 µg/ml, 3.75 µg/ml, 15.0 µg/ml, and 30 µg/ml. (A) growth (OD600), (B) fluorescence (RFU), (C) fluorescence normalised per OD600. Four WT and ΔPKS biological replicates were tested in a microtiter plate at 30 ºC and 200 rpm in ABTG. Standard deviation bars are displayed.

However, the final OD600 is significantly different ($p<0.05$) between WT and ΔPKS when cultured with 15.0 µg/ml of rifamycin, meaning that the absence of the unknown BGC made the cell react differently. Together with the information obtained from the shake flasks, it is possible to argue that rifamycin induces promoter activation.

4.5. Carbon source D-arabitol induces unknown BGC expression

To test a condition that did not inhibit culture growth, the effect of carbon source D-arabitol on the unknown BGC promoter was observed. WT and Punk-GFP were cultured with ABTG medium supplemented with D-arabitol (data not shown), but also with ABT medium (without glucose) supplemented with D-arabitol.

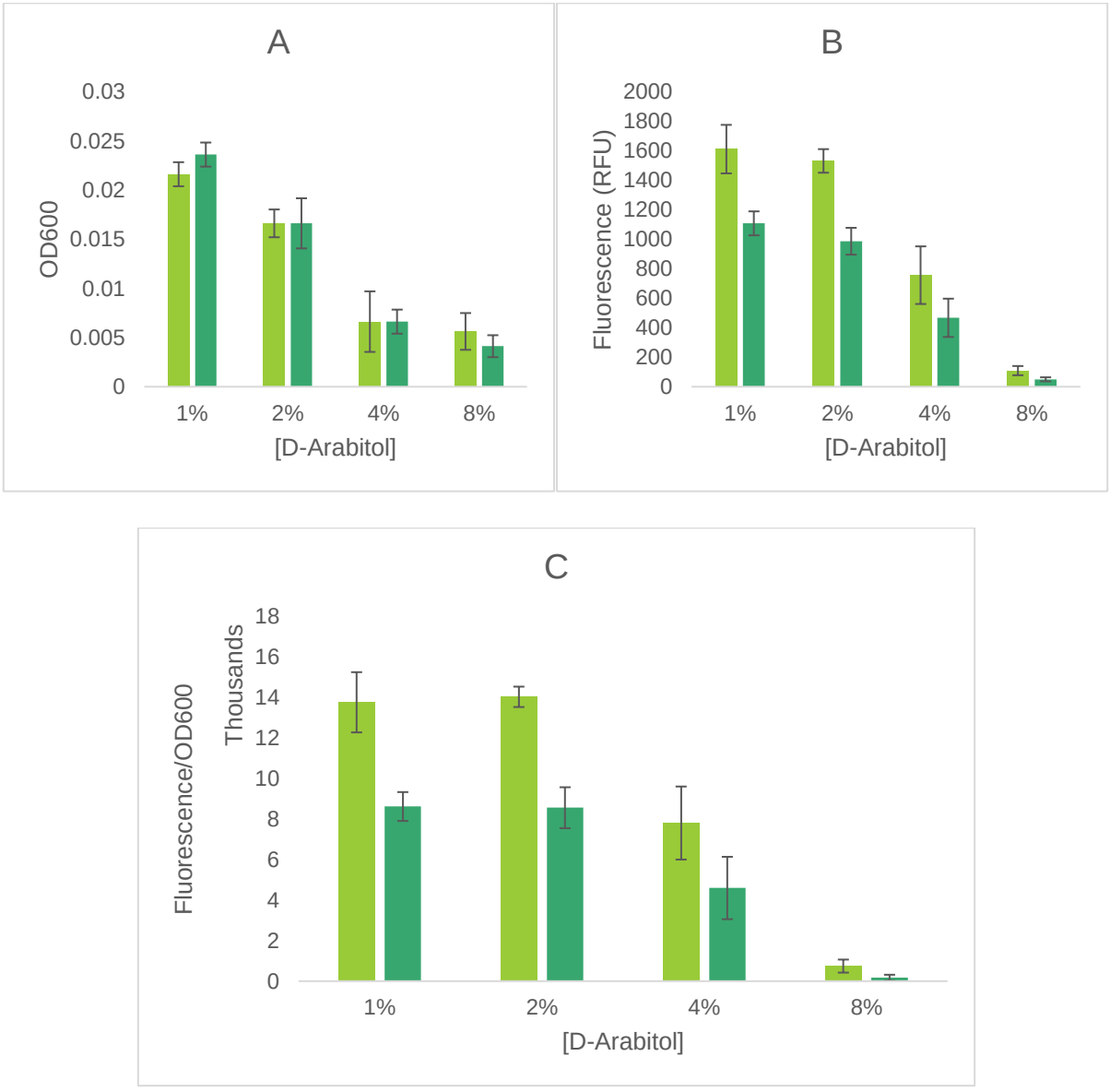

Figure 4.10. Bar graph – D-Arabitol effect on promoter Punk activation (Punk-GFP (■) compared to WT (■)) after 30h of growth. Results of cultivation with D-arabitol concentrations of 1%, 2%, 4% and 8%. **(A)** growth (OD600), **(B)** fluorescence (RFU), **(C)** fluorescence normalised per OD600. Four biological replicates were tested in a microtiter plate at 30 ºC and 282 rpm in ABT. Standard deviation bars are displayed.

Supplementation of D-arabitol to ABTG medium did not change growth nor fluorescence levels. Cultures grown in ABT with D-arabitol led to low final values of OD600, being the maximum value of 0.02 when cultured in 1% D-arabitol, Figure 4.10.A. However, there was a significant increase of fluorescence compared to the control (WT without reporter gene), being this difference larger when the cultures were

grown with 1% and 2% D-arabitol, meaning that the promoter was more active in these two conditions, Figure 4.10.B and 4.10.C. Moreover, the difference in normalised fluorescence (5474 RFU/OD600 for 2% D-arabitol), Figure 4.10.C, is larger than the calculated for the conditions in Figure 4.1 (the highest value, 2971 RFU/OD600, was obtained for TSB media).

The increased fluorescence levels in the Punk-GFP strain in comparison to the WT indicate that the use of D-arabitol as a carbon source might lead to a higher expression of the unknown BGC in comparison to cultures with ABTG.

4.6. Rif^R mutant overexpresses the unknown BGC

An attempt of RNA polymerase and ribosome engineering was performed by selecting rifamycin (Rif^R) and streptomycin (Strep^R) spontaneous resistant mutants, expecting point mutations in *rpoB*, and *rpsL* genes, respectively. The antibiotic resistance mutation rates were 8.54×10^{-13} and 6.53×10^{-11}, respectively. The expression of the unknown BGC in the mutants and the WT were analysed by qPCR and the results are shown in Figure 4.11.

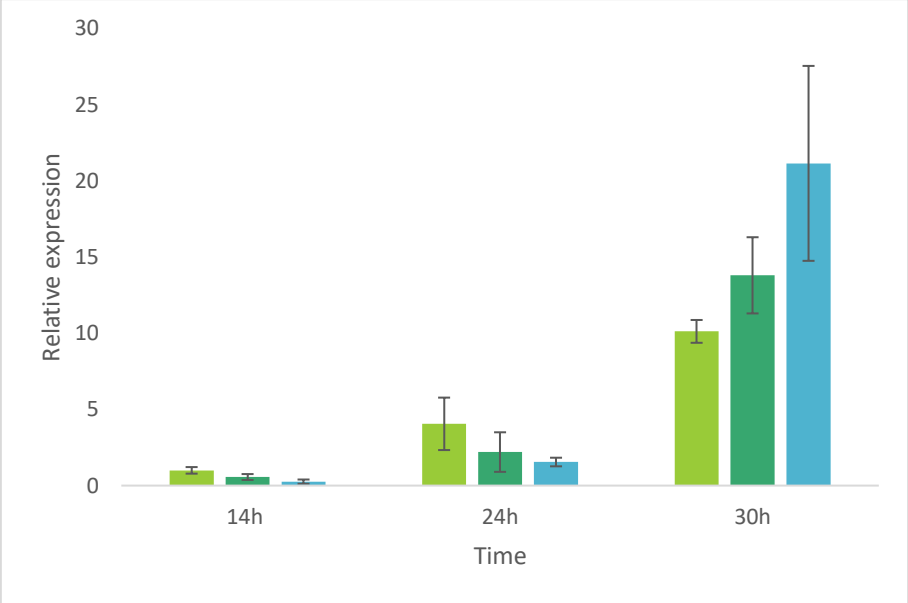

Figure 4.11. Bar graph – Relative expression of unknown BGC in the ■ - WT, and ■ - Strep^R and ■ - Rif^R mutants obtained by qPCR. The samples were obtained after 14h, 24h, and 30h of culture at 30 ºC and 200 rpm in ABTG, and normalised to WT expression at 14h. Three biological replicates were tested. Standard deviation bars are displayed.

Statistical analysis indicates that the difference between the values obtained for each hour is not significant. However, the qPCR still suggests that the production is higher in the late stationary phase. The qPCR thermal cycle setup included the steps required for the formation of a melting curve: all the components were denatured at 95°C, completely annealed at 60°C, and subjected to a gradual increase in temperature up to 95°C. Fluorescence intensity was monitored during the final temperature increase and the negative first derivative of the fluorescence curve in the function of time (-Rn'(T)) was returned by the analytical software. This curve allows to analyse amplicons melting temperature (T_m), as an indication of their size, and the peak height as an indication of the DNA template amount.

The melting curve of reference gene *rpoD* amplicons for the 14h samples shows a good profile, as the curves peak in one single T_m (no extra amplicons were produced) with the same height (similar quantity of amplified product), Figure 4.12.

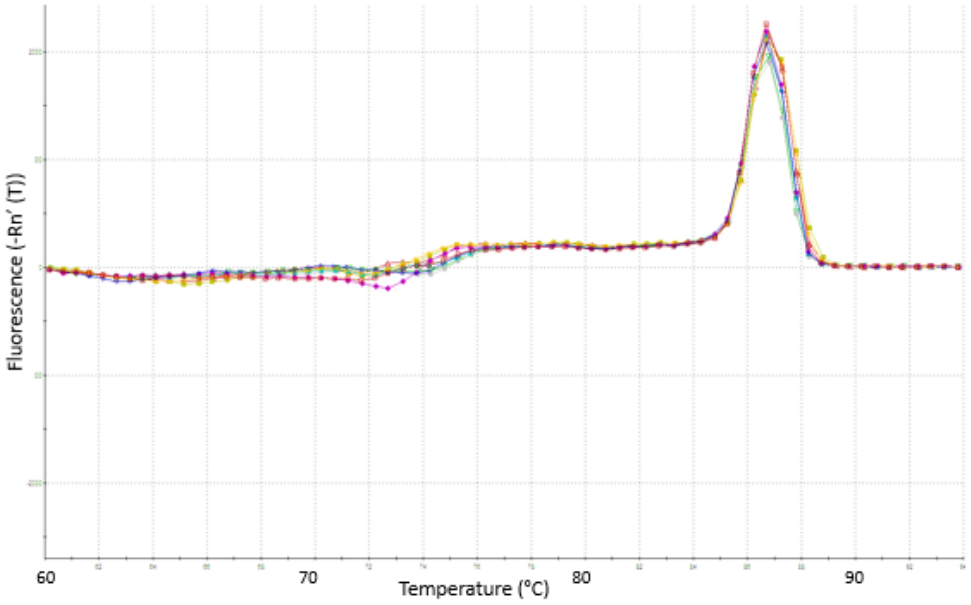

Figure 4.12. Melting curves – Analysis of reference gene *rpoD* amplicons for the 14h samples.

Contrarily, the plot of reference gene *gyrB* amplicons for the 30h samples, Figure 4.13, shows curves peaking at slightly different temperatures and different heights, meaning that this set of samples includes several outliers.

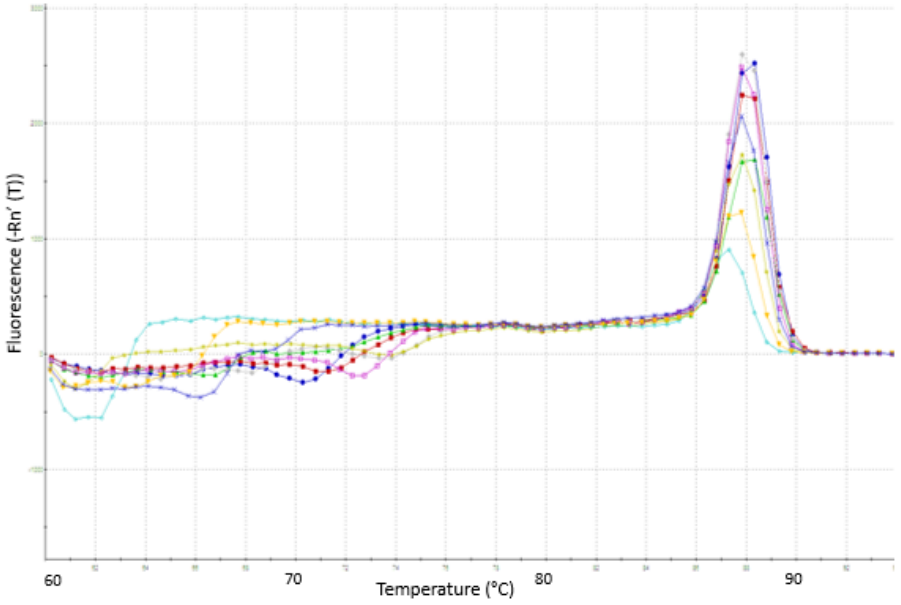

Figure 4.13. Melting curves – Analysis of reference gene *gyrB* amplicons for the 30h samples.

The analysis of the no template control showed that only one of the curves had a peak of small height at similar T_m in comparison to the curves of the experimental samples, Figure 4.14. This suggests that

this well was contaminated with one of the samples. The additional melting curves are included in the Annex E and show evidence of other outlier samples.

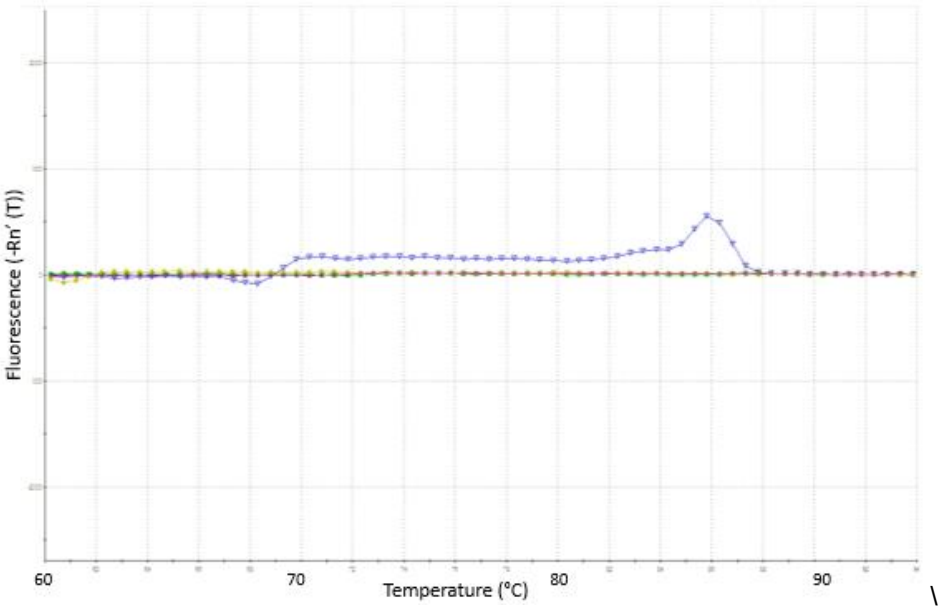

Figure 4.14. Melting curves – Analysis of the no template controls of the 14h samples. Image obtained from *MxPro qPCR*.

These melting curves explain why the assay lacked in statistical confidence. The analysis of the ribosome and RNA polymerase engineering was pursued with a GFP expression assay. The plasmid pSEVA237::P_{unk}-GFP was inserted in the mutants by triparental conjugation.

There is a clear difference in growth between the Rif^R mutant and the rest of the strains, Figure 4.15.A. The difference in normalised fluorescence with the reporter gene compared to the fluorescence without the reporter gene is higher for Rif^R strain. The ratio between the differences of normalised fluorescence of Rif^R strains and normalised fluorescence of WT strains, Figure 4.15.C estimates an increase in expression of the unknown BGC of approximately 4.2-fold with RNA polymerase engineering.

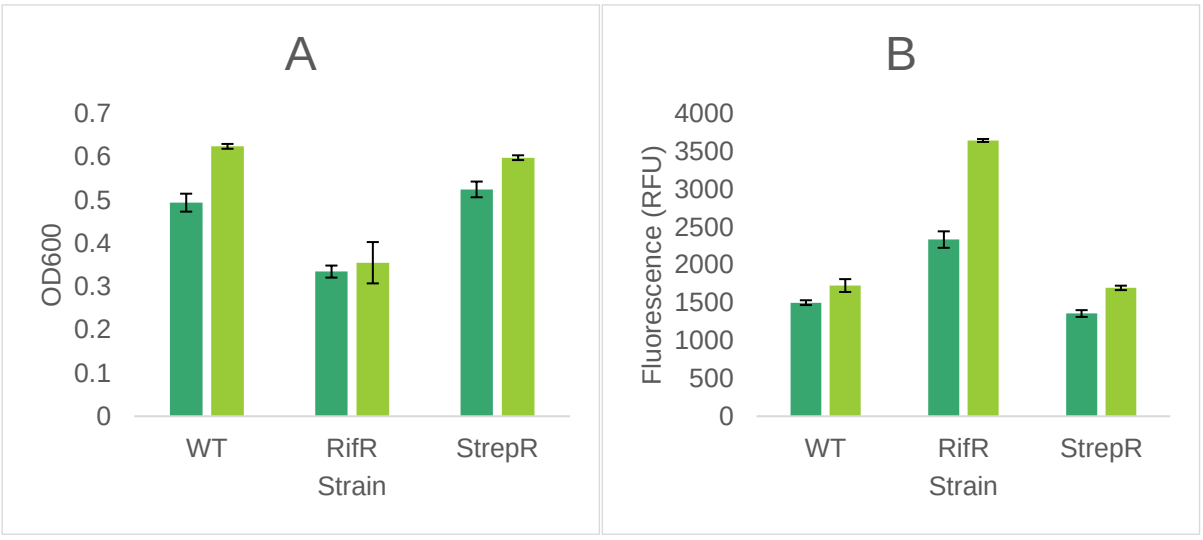

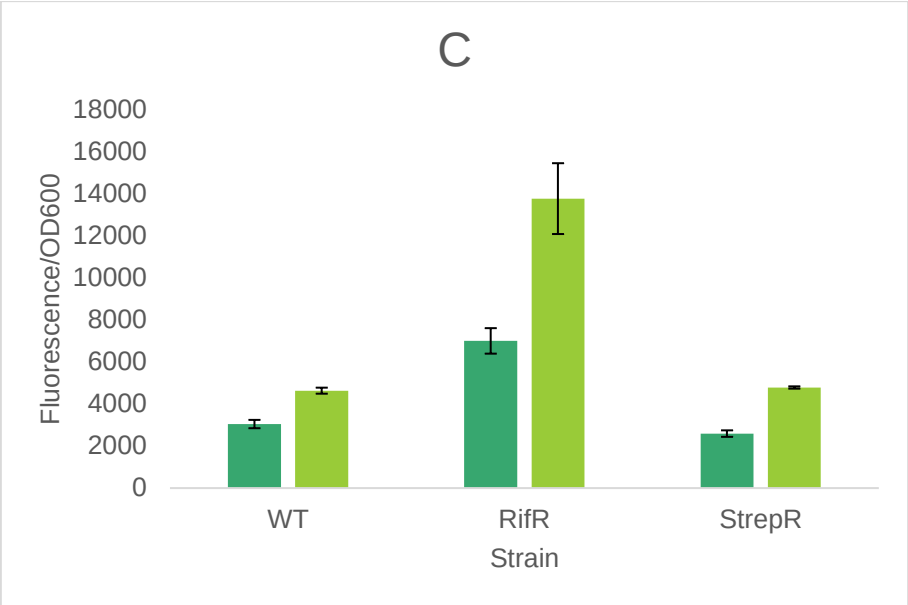

Figure 4.15. Bar graph – Promoter Punk expression in WT, Rif^{R,} and Strep^{R} strains after 30h. ■ - without GFP reporter gene, ■ - with GFP reporter gene. **(A)** growth (OD600), **(B)** fluorescence (RFU), **(C)** fluorescence normalised per OD600 was calculated. Three biological replicates of each strain were tested in a microtiter plate 30 ºC and 282 rpm in ABTG. Standard deviation bars are displayed.

Surprisingly, there was no significant difference between WT and Strep^{R} growth and fluorescence, Figures 4.15.A and 4.15.B. Sequencing results for *rpsL* mutation check were revisited and the analysis was repeated with different primers, evaluating a broader region of the genome. The first results indicated an insertion that the second results contradicted, explaining why the ribosome engineering failed.

The point mutation in the *rpoB* gene resulted from the replacement of a thymine to a cytosine, leading to aspartate-521 to glycine substitution, Figure 4.16.

Figure 4.16. Rif^{R} strain carries a single point mutation in the rpoB gene. The thymine in position 2513 of the gene was replaced by a cytosine, generating aspartate-521 substitution by a glycine.

Although a more exact determination of relative expression was not obtained by qPCR, the expression assay clearly shows that RNA polymerase engineering led to an overexpression of the unknown BGC.

4.7. Insertion of a stronger promoter by allelic replacement – troubleshooting

To increase the gene expression and compound production for possible chemical identification of the compound and phenotype studies in the WT, the process of replacing the original promoter for a stronger one was initiated. A DNA fragment, containing the promoter and homology regions to the place of insertion, was constructed with splicing by overlap extension (SOE) PCR (1489 bp). The DNA fragment was inserted in pNJ1 plasmid, and the recombinant plasmid was transformed into the competent cells (*E. coli* CC118λspir) by heat shock transformation. After the transformation of the competent cells, antibiotic selection and transformation controls showed positive results: no colonies grew in the former, and several grew in the latter (in the order of 10^2 CFU).

However, the false positive (FP) control, where very few or no colonies were expected, showed a similar number in comparison to the transformation plate (T) (FP – 16 CFU, T – 18 CFU). Several attempts to solve the problem were performed: by retrying the digestion steps for both fragments (including one trial with the addition of Fast AP and another with freshly bought enzymes), using a sample of digested plasmid previously used. The difference in the number of FP and transformant colonies increased, but when the transformants were analysed by colony PCR, by amplifying the region where the promoter should have been inserted, the resultant bands had several different sizes, as exemplified in Figure 4.17 (1-8). The eight colony PCR fragments had different sizes ranging from 500 base pairs (bp) to 1100 bp when the expected size for a succeed transformation was approximately 2000 bp, when using the primers 120/121. This primer pair results in fragments with 500 bp when applied in plasmid pNJ1.

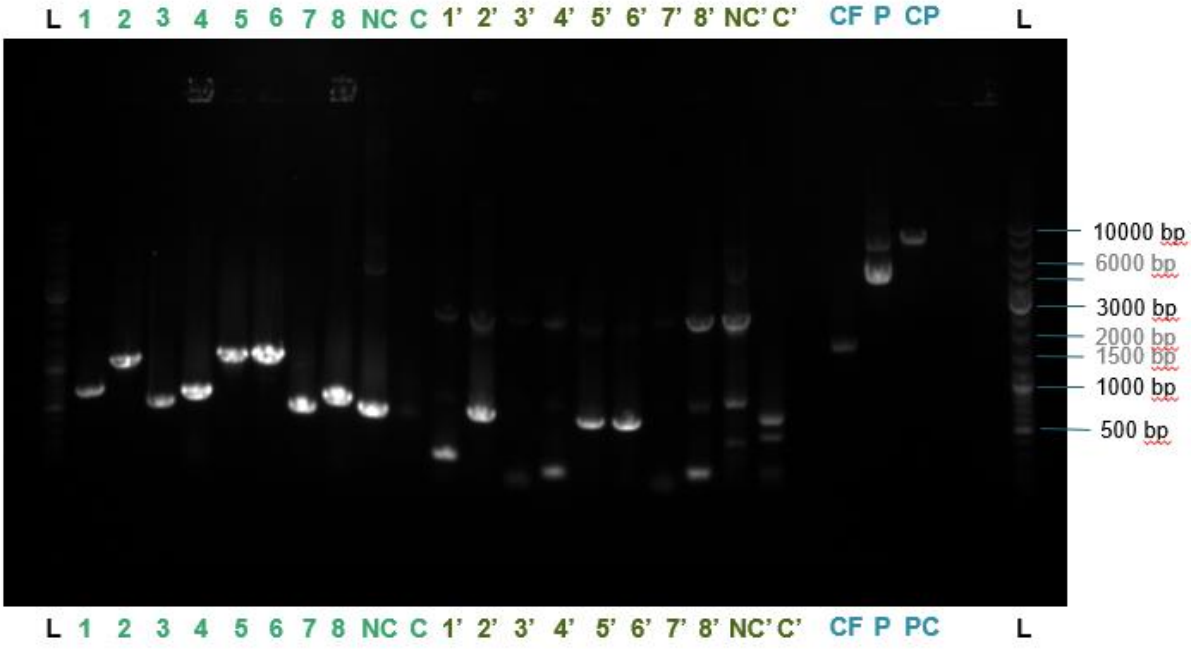

Figure 4.17 Agarose gel electrophoresis of colony PCR products of transformed *E. coli* CC118 λspir. Two sets of primers were used: 120/121 and 363/366. **Legend**: L – GeneRuler™ DNA ladder mix, 1-8 – PCR products resultant from primers' 120/121 application in eight different transformant

colonies, NC – control with the original plasmid pNJ1, C - control with the non-digested plasmid pNJ1, 1'-8' – PCR products resultant from primers 363/366 application in eight different transformant colonies; CF – digested SOE fragment, P – original plasmid pNJ1, PC – digested plasmid pNJ1 loaded with DNA Gel Loading Dye (6X).

The colonies showing bands with sizes closer to what was expected were selected for plasmid purification and posterior sequencing of the local of insertion (primers 120/121). The sequencing results showed that the plasmid seemed to have been torn apart and fused again, as the different parts were aligning with different regions of the original plasmid, Figure 4.18.

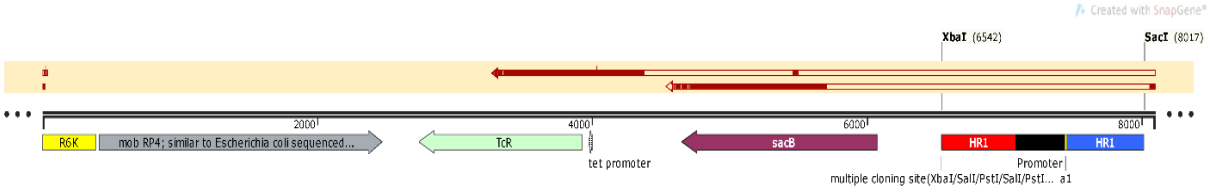

Figure 4.18. ***pNJ1-p14g (Unk_PKS) insertion aligned to colony PCR sequencing results –*** *An example of the sequencing results of the transformant colony PCR is in the top yellow rectangle. The red crosses show the aligned regions.*

A new sample of plasmid was purified from an overnight culture of *E. coli* and the fragment resultant from the enzymatic digestion step showed a single band with the expected size, Figure 4.17 (PC). The integrity of the gene fragment created with SOE PCR was evaluated in an agarose gel, confirming the right size, Figure 4.17 (CF).

In the PCR products generated with primers 120/121, the control with the original plasmid (NC) shows the correct band size (~500 bp). The control with the cut plasmid (C) does not show a strongly visible band. In the PCR products generated with primers 363/366, both the plasmid controls (NC' and C') show several bands, which means that the pair of primers was binding to multiple regions of the plasmid. All the PCR products include a band with approximately 2000 bp (1' to NC'), with an exception for the digested plasmid product (C'). The other bands have sizes inferior to 1000 bp, meaning that none of the transformants evaluated included the SOE fragment (~1500 bp).

Due to the mentioned technical difficulties, no colonies with the desired plasmid were obtained. For this, the process of insertion of a stronger promoter upstream of the unknown BGC was halted.

5. Discussion

The regulation of secondary metabolites in plant-beneficial strains can contribute to an increased number of available agricultural solutions based on microorganisms. This project was focused on the study of a cryptic biosynthetic gene cluster (BGC) of *P. protegens* DTU9.1, whose expression might be relevant for the selection of this strain as a biocontrol agent.

Growth phenotypic analyses were performed on *P. protegens* wild type (WT) and the polyketide synthase (PKS) deletion mutant (ΔPKS) in four different media, and growth rate, fluorescence, and spot size were not impacted by the deletion of the unknown PKS. Fluorescence levels of the reporter strain Punk-GFP were higher than the levels of the other strains, meaning that unknown BGC expression was active at a low level. Intra- and extracellular metabolomes of both strains were analysed by LC-MS and compared. While only 8 extracellular metabolites were up/downregulated, 118 intracellular metabolites were differently expressed between the two strains. The two metabolites with lower levels of fold-change were selected as possibly representing the compound produced by the unknown BGC. However, no absent peak in ΔPKS intracellular metabolome chromatogram was observed in comparison with the WT, meaning that the expression of the unknown BGC is so low that the produced compound is not observable by LC-MS. This metabolite might take part in metabolic pathways or interact with regulatory molecules, explaining the observed fold-change. Nevertheless, this assay consisted of a first exploratory MS analysis, and the information provided is not enough to hypothesize about the compound structure nor function. Expression activation of the cryptic BGC is important for compound identification.

The inductive effect of different concentrations of rifamycin and rifampicin to the promoter upstream of the unknown PKS (Punk) was evaluated in a GFP reporter assay. In the stationary phase, after 24h of culture, the values of normalised fluorescence per OD600 were higher for sub-minimum inhibitory concentration (MIC) concentrations. Goh and colleagues proved that several antibiotics, including rifamycin, were shown to influence bacterial transcription modulation at sub-MIC concentrations[57]. Yim and colleagues showed that some promoters of *Salmonella enterica* were affected by the antibiotic rifampin (rifampicin) concentration and that their expression generally peaked at a concentration close to the MIC value[111]. The results also support a previous experiment performed in the working group in a *Biolog* plate (not published), in which the highest levels of normalised fluorescence per OD600 in *P. protegens* DTU9.1 were obtained at sub-MIC concentrations of rifamycin. For this, it would be of interest to narrow the interval of values tested for concentrations closer to the MIC value.

A shake flask assay was performed including cultures treated with the antibiotic since the moment of inoculation and the middle of the growth phase. Again, the highest value of fluorescence/OD600 was obtained for the concentration closest to the MIC. However, with the late supplementation of the lowest antibiotic concentration, the cells ended up with the same OD600, but the fluorescence was higher in the cultures with delayed exposure. With the late supplementation of the highest antibiotic concentration, the growth was impaired and the values of fluorescence/OD600 decreased with time, in contrast with what was observed in the other curves. The results for the lowest concentration show that the addition of a more tolerable concentration of the antibiotic in the exponential phase might induce the promoter

without affecting the growth. A GFP expression assay with rifamycin supplementation was performed with WT and ΔPKS strains. A relevant difference in OD600 was observed between WT and ΔPKS when cultured with 15 µg/ml of antibiotic, as the final OD600 of the WT was lower than the final OD600 of ΔPKS. If this concentration of rifamycin induced the expression of the unknown BGC more significantly, the metabolic burden might have diminished the growth of the WT strain.

Additionally, the increase in antibiotic concentration increased the intrinsic fluorescence/OD600 values of both WT and ΔPKS strains. Fluorescent pseudomonas species produce pyoverdine, a yellow-green, fluorescent pigment, responsible for the fluorescent phenotype and identified as a key factor of P. aeruginosa virulence[112]. The study of Goh[57] and Yim[111] revealed that antibiotic presence activated the expression of genes linked to a variety of functions, including virulence and iron metabolism. In this way, rifamycin and rifampicin may have altered the expression of pyoverdine as well. However, the bacterial intrinsic fluorescence creates background noise for the transcriptional analysis with the fluorescent reporter gene GFP making it difficult to identify the overexpression if it is low. In this way, when using GFP reporter gene in *P. protegens*, it is relevant to use a control with the WT to compare the increase of fluorescence and evaluate whether the effect is due to the target gene overexpression.

Alternatively, background fluorescence could be lowered by using another reporter gene, exploring fluorescence with other emission wavelengths, such as red fluorescent protein, which lowers the auto-fluorescent background. However, systems with GFP have been intensively optimized for several years, while the other alternatives are relatively recent and less developed. Other mechanisms include luciferase, which uses a bioluminescence reaction for gene expression quantification. Although luciferase assays are more sensitive than GFP assays, they can be more time-consuming and laborious.

The inductive effect of D-arabitol on the promoter Punk was also analysed by a GFP assay, either by supplementing D-arabitol to ABTG media or ABT media. With the former set-up, no difference in growth nor fluorescence was observed, meaning that D-arabitol does not work as a signalling molecule for Punk activation. With the latter, using D-arabitol as a carbon source, low values of growth were achieved. The already mentioned *Biolog* plate assay also tested D-arabitol and the results were concordant. However, for concentrations of D-arabitol equal to 1% and 2%, the increase in normalised fluorescence generated by the insertion of the plasmid were very in comparison to what had been observed with other media. For this, it can be said that carbon source composition and/or growth speed affected the expression of the unknown BGC. It is known that carbon and energy sources can affect the production of secondary metabolites. The catabolic process of breaking down these molecules generates end-products that are reassembled to form primary intermediates, which in turn will be part of the structure of more complex compounds, the primary metabolites. The metabolic pathways of primary metabolism can supply the precursors of secondary metabolism, hence being affected by the carbon source composition and its abundance[113]. Moreover, secondary metabolism is associated with low levels of growth, and rapidly used substrates, like glucose, represses the synthesis and activity of some enzymes[113,114]. Duffy and Défago[115] observed that antibiotic and siderophore biosynthesis is strongly affected by the available carbon source in *P. fluorescens* strains. For the observed repression of pyoluteorin production by glucose, they pointed out that glucose might block antibiotic production through repression of

dehydrogenases that catalyse glucose oxidation (catabolite repression). Acidification of the media during bacterial growth can affect secondary metabolism, such as biocontrol activity[116]. For this, the evaluation of the final pH of the cultures when grown with glucose or D-arabitol can give further details to explain the different expression levels observed.

Ribosome and RNA polymerase engineering were applied as a strategy to increase the unknown BGC expression, by selecting streptomycin ($Strep^R$) and rifamycin (Rif^R) resistant mutants, respectively, with *rpsL* and *rpoB* gene mutations, respectively. Unknown BGC expression analysis was done by RT-qPCR. At the end, the analysis lacked statistical confidence. A dissociation step is usually performed when working with DNA-binding dyes, such as SYBR Green I. The resultant melting curves give indications of the uniqueness (observing peak T_m) and quantity (observing peak heights) of the fragments amplified. Here, some of the plots showed slightly different T_m's. To verify if more than one product was amplified, an ethidium bromide-stained agarose gel could have been used. If multiple bands had appeared, an optimum annealing temperature should be determined by gradient PCR or new primers should be designed. If a single band had appeared, the problem could be related to localized AT or GC-rich regions or short repeats in PCR product causing imperfect reannealing of amplicon resulting in different melting profiles, which is a possible motive, due to the nucleotide content of the DNA sequences of the desired amplicons. For this last case, no alterations are required[117].

The melting curves also show that several of the peaks had different heights, meaning that the amplicons were present in different concentrations, hence, being outliers. In the case of the unknown BGC amplicons, groups with different heights would be acceptable, as this would mean that the BGC was differently expressed in the different strains. However, several peaks do not align with any other. In this way, it is important to consider the optimization of some of the several steps performed. For example, RNA and DNA quantification was performed using a spectrophotometric method. Fluorometric techniques or molecular probes, although more expensive, would have achieved more sensitive and accurate measurements.

qPCR internal error control by normalization with reference genes also presents some challenges. Reference genes are expected to be expressed constitutively with low levels of variability. In this project, *gyrB* and *rpoD* classic reference genes[118] were used as control. However, some authors refer to the importance of validating the reference genes by comparing expression variability in the different conditions in the study. The use of multiple reference genes is also suggested to increase the robustness of the study, but this is not always possible due to limited sample availability and high cost. It is important to refer that for publication effects the MIQE Guidelines (Minimum Information for Publication of Quantitative Real-Time PCR Experiments) should be followed[119].

The unknown BGC expression was evaluated by a GFP assay, and the results showed that the Rif^R mutant overexpressed the unknown BGC, with an estimation of 4.2-fold compared to the WT. In actinomycetes, different mutations of *rpoB* were evaluated for activation of cryptic BGCs, obtaining an increase up to 70-fold expression, but also lower levels of overexpression, such as 3-fold[120]. The final OD600 of Rif^R was lower in comparison to the final OD600 of the WT and $Strip^R$ strains and the expression of the fluorescent siderophore increased. These changes can be justified by the high

demand for RNA polymerase occurring in the strain, increasing the metabolic cost and changing the expression pattern. This effect was described[121] in rifampicin-resistant mutants with RNA polymerase mutations, and the metabolic cost was proved to be driven by demand for RNA polymerase. This adverse effect can be lowered by reducing the demand for polymerase with antagonistic epistasis, which can be achieved through inhibition of ribosomal activity, indirectly controlling the transcription rate. Mutations in the *rpsL* gene or some antibiotics addition are possible strategies.

The obtained mutation on the *rpoB* gene, D521G, was reported as highly common in *P. aeruginosa* and *P. putida*. It is associated with approximately 70% of mild resistance cases to rifampicin (cultivated at 30°C), and 49% of strong resistance cases of *P. aeruginosa* (cultivated at 37°C)[122]. As several different rifamycin-resistant mutations can occur in *rpoB*, leading to different phenotypes, other mutations should be analysed to find the most suitable for overproduction of the desired product[120,123].

The mutant selected for streptomycin resistance did not contain a mutation in the *rpsL* gene and no inductive effect was observed. Also, the growth phenotype did not change in comparison to the WT. Besides alterations of the ribosomal target site, bacterial streptomycin resistance mechanisms include the production of streptomycin-modifying enzymes and permeability barriers, not affecting ribosomal translational ability[124]. Paulander and colleagues[125] showed that different mutations in the *rpsL* gene do not have the same fitness cost, with some of the mutants showing no different growth rate compared to the WT. In this way, other types of mutation may have arisen, not affecting the fitness cost of the mutant.

Troubleshooting was performed in the steps preceding plasmid pNJ1-p14g transformation, as the expected results were not achieved. The plasmid and the SOE PCR fragment, run in agarose gel, had the correct size. However, transformant colony PCR sequencing to the region with the insert showed that the fragments aligned to non-expected regions of the plasmid. The agarose gel shows that most of the negative transformant colonies were due to undesired inserts, indicating that the cut plasmid was damaged. The UV light used in the process of excision of the band containing the cut plasmid from the gel can have damaged the DNA. However, this does not explain why the experiment failed when a cut plasmid previously used was applied. The motive might be behind the storage time that the plasmid had undergone. In this way, it can be concluded that some of the colonies could have the desired plasmid, but it would have been a matter of probabilities to find them.

Another reason for the failed transformation results might be the fact that restriction enzymes can be inhibited in reactions with complex DNA, in which sequences similar to the target restriction site function as enzyme inhibitors or alternative substrates if in high concentrations. For this, the solution could pass by the optimization of the concentration of reagents added. The success of ligation reactions is also affected by the concentration of reagents, enzymes, and other extra agents and, to a lesser extent, time and temperature[126]. For difficult cloning, Lund and collegues[127] proposed a procedure in which high enzyme activity and DNA annealing are balanced by constant temperature cycling for 12-16h. This method increased the efficiency of cloning approximately from 4 to 8-fold. If a colony with the correct plasmid had been found, the plasmid should be transferred to *P. protegens* WT strain by triparental mating. The colonies where the first gene crossover had occurred would have been selected with the antibiotic tetracyclin. Then, a second selection in media with sucrose would have been carried out. The

presence of the *sacB* gene present in the plasmid generates a toxic compound for the cells. In this way, only cells without the *sacB* gene, meaning a complete second crossover, would be selected. As the second crossover can lead to the restoration of the wild-type allele, the cells would have been analysed by DNA sequencing of the target region.

6. Conclusion and future remarks

This project aimed to identify successful strategies to the activation of a cryptic biosynthetic gene cluster (BGC) in *Pseudomonas protegens* DTU9.1, a plant-beneficial bacteria. The identification of the resultant secondary metabolites of cryptic BGCs can unravel mechanisms relevant for the use of microorganisms as plant growth-promoting agents.

Expression assays indicate that the unknown BGC is being expressed. The deletion of the unknown polyketide synthase (PKS), analysed by LC-MS analysis, showed to interfere with the concentration of several metabolites, mainly the intracellular metabolites. However, the low expression levels were not enough to analyse the structure and function of the putative produced compound. Hence, the expression activation is required to progress in this study.

Based on the expression assays performed with antibiotic media supplementation, it can be concluded that rifamycin is a strong candidate for the activation of the unknown BGC. The assay with delayed addition of the antibiotic indicates that the best moment for an elicitor addition to the media should also be a case of study. The cultivation of the strain with D-arabitol as an alternative carbon source led to lower growth levels but higher fluorescence/OD600 values, adding that the expression of the BGC might be carbon source composition and/or low growth dependent. In both cases, and as expression assays were subject to fluorescence background effects, the fold change in expression levels should be evaluated with qPCR, a more precise method. Based on these results, studies with other carbon sources should be addressed. The use of artificial root exudates containing different concentrations of organic (including carbon sources) and inorganic molecules could be particularly relevant. Another alternative is to use a *fed-batch* culture maintaining glucose at a very low concentration, reducing the effect of catabolite repression. This method would also facilitate the expression evaluation by addition of antibiotics in a later growth phase.

RNA polymerase engineering, by selecting a spontaneously rifamycin-resistant colony with a *rpoB* gene mutation, resulted in the highest expression increase observed in this project. The study of other mutations in the *rpoB* gene and ribosome-related genes might result in a more expressive BGC activation. The conjugation of some of these mutations can even result in more stable phenotypes, improving the growth rate usually impaired by these mutations.

Switching the endogenous promoter with a stronger promoter was a technique attempted in this report. Although technical limitations hampered the conclusion of the process, successful results could have opened the doors to the metabolite identification, by a retrial in LC-MS, or using nuclear magnetic resonance (NMR) which has more analytical precision, for the metabolite identification.

Different approaches for cryptic BGC activation have already been described in Section 1. Introduction, and could be considered for extra analysis of this unknown BGC. Additionally, the biofilm production capacity of *P. protegens* strains could be used to assess if the unknown BGC is activated by phenomena related to the populational density (quorum sensing).

After successful overexpression of the BGC, bioactivity assays should be conducted. For example, bactericidal and fungicidal activity, assessed by co-cultivation the strain with other microorganisms. The plant growth-promoting effect could be analysed by the cultivation of plants in presence of the strain in the roots space. The effect on stress toleration could be observed by culturing the cells under different stresses, like UV-light, oxidative stress, or osmotic stress.

7. References

1. Nations U. Population | United Nations. Accessed April 29, 2021. https://www.un.org/en/global-issues/population

2. The World Bank. Water in Agriculture. Global Issues in Water Policy. Published 2019. Accessed April 29, 2021. file:///E:/my major/article 2/references/Water in Agriculture-the world bank b 2017.pdf

3. Portilla LM, Alving B. *Reaping the Benefits of Biomedical Research: Partnerships Required*. Vol 2.; 2010. doi:10.1126/scitranslmed.3001137

4. Factors that influence crop yield - Omnia Nutriology®. Accessed August 23, 2021. http://www.fertilizer.co.za/public-relations/news/2017/259-factors-that-influence-crop-yield

5. Sharma N, Singhvi R. Effects of Chemical Fertilizers and Pesticides on Human Health and Environment: A Review. *International Journal of Agriculture, Environment and Biotechnology*. 2017;10(6):675. doi:10.5958/2230-732x.2017.00083.3

6. Atafar Z, Mesdaghinia A, Nouri J, et al. Effect of fertilizer application on soil heavy metal concentration. *Environmental Monitoring and Assessment*. 2010;160(1-4):83-89. doi:10.1007/s10661-008-0659-x

7. Aktar W, Sengupta D, Chowdhury A. Impact of pesticides use in agriculture: Their benefits and hazards. *Interdisciplinary Toxicology*. 2009;2(1):1-12. doi:10.2478/v10102-009-0001-7

8. Parlament E. Chemicals and pesticides | Fact Sheets on the European Union | European Parliament. Published 2021. Accessed May 7, 2021. https://www.europarl.europa.eu/factsheets/en/sheet/78/chemicals-and-pesticides

9. Henisz W, Koller T, Nuttall R. Five ways that ESG creates value. McKinsey Quarterly. Published 2019. Accessed May 3, 2021. https://www.mckinsey.com/business-functions/strategy-and-corporate-finance/our-insights/five-ways-that-esg-creates-value

10. Haller Karl, Lee Jim, Cheung Jane. *Meet the 2020 Consumers Driving Change*.; 2020. Accessed May 3, 2021. https://www.ibm.com/downloads/cas/EXK4XKX8

11. Watkins PR, Huesing JE, Margam V, Murdock LL, Higgins TJV. Insects, nematodes, and other pests. *Plant Biotechnology and Agriculture*. Published online January 1, 2012:353-370. doi:10.1016/B978-0-12-381466-1.00023-7

12. Syed S, Prasad Tollamadugu NVKV. Role of plant growth-promoting microorganisms as a tool for environmental sustainability. *Recent Developments in Applied Microbiology and Biochemistry*. Published online January 1, 2018:209-222. doi:10.1016/B978-0-12-816328-3.00016-7

13. du Jardin P. Plant biostimulants: Definition, concept, main categories and regulation. *Scientia Horticulturae*. 2015;196:3-14. doi:10.1016/j.scienta.2015.09.021

14. Köhl J, Kolnaar R, Ravensberg WJ. Mode of action of microbial biological control agents against plant diseases: Relevance beyond efficacy. *Frontiers in Plant Science*. 2019;10. doi:10.3389/fpls.2019.00845

15. van Lenteren JC, Bolckmans K, Köhl J, Ravensberg WJ, Urbaneja A. Biological control using invertebrates and microorganisms: plenty of new opportunities. *BioControl*. 2018;63(1):39-59. doi:10.1007/s10526-017-9801-4

16. Winkelmann G, Drechsel H. Microbial Siderophores. In: Varma A, Chincholkar S, eds. *Biotechnology: Second, Completely Revised Edition*. Vol 7-12. Springer; 2008:199-246. doi:10.1002/9783527620999.ch5g

17. Zhang H, Sun Y, Xie X, Kim MS, Dowd SE, Paré PW. A soil bacterium regulates plant acquisition of iron via deficiency-inducible mechanisms. *Plant Journal*. 2009;58(4):568-577. doi:10.1111/j.1365-313X.2009.03803.x

18. Zhang H, Kim MS, Sun Y, Dowd SE, Shi H, Paré PW. Soil bacteria confer plant salt tolerance by tissue-specific regulation of the sodium transporter HKT1. *Molecular Plant-Microbe Interactions*. 2008;21(6):737-744. doi:10.1094/MPMI-21-6-0737

19. Zhang H, Xie X, Kim MS, Kornyeyev DA, Holaday S, Paré PW. Soil bacteria augment Arabidopsis photosynthesis by decreasing glucose sensing and abscisic acid levels in planta. *Plant Journal*. 2008;56(2):264-273. doi:10.1111/j.1365-313X.2008.03593.x

20. Zhang H, Kim MS, Krishnamachari V, et al. Rhizobacterial volatile emissions regulate auxin homeostasis and cell expansion in Arabidopsis. *Planta*. 2007;226(4):839-851. doi:10.1007/s00425-007-0530-2

21. Ryu CM, Farag MA, Hu CH, Reddy MS, Kloepper JW, Paré PW. Bacterial volatiles induce systemic resistance in Arabidopsis. *Plant Physiology*. 2004;134(3):1017-1026. doi:10.1104/pp.103.026583

22. Lewis KA, Tzilivakis J, Warner DJ, Green A. An international database for pesticide risk assessments and management. *Human and Ecological Risk Assessment*. 2016;22(4):1050-1064. doi:10.1080/10807039.2015.1133242

23. Piombo E, Sela N, Wisniewski M, et al. Genome sequence, assembly and characterization of two Metschnikowia fructicola strains used as biocontrol agents of postharvest diseases. *Frontiers in Microbiology*. 2018;9(APR):9:593. doi:10.3389/fmicb.2018.00593

24. Martínez-Viveros O, Jorquera MA, Crowley DE, Gajardo G, Mora ML. Mechanisms and practical considerations involved in plant growth promotion by Rhizobacteria. *Journal of Soil Science and Plant Nutrition*. 2010;10(3):293-319. doi:10.4067/S0718-95162010000100006

25. Batool T, Ali S, Seleiman MF, et al. Plant growth promoting rhizobacteria alleviates drought stress in potato in response to suppressive oxidative stress and antioxidant enzymes activities. *Scientific Reports*. 2020;10(1):1-19. doi:10.1038/s41598-020-73489-z

26. Transitions M holocene. Climate Change and. Quaternary International. Published August 18, 2011. Accessed October 14, 2021. http://www.ncbi.nlm.nih.gov/pubmed/21796962

27. Verma M, Mishra J, Arora NK. Plant Growth-Promoting Rhizobacteria: Diversity and Applications. In: *Environmental Biotechnology: For Sustainable Future*. 1st ed. Springer, Singapore; 2019:129-173. doi:10.1007/978-981-10-7284-0_6

28. Dixon R, Kahn D. Genetic regulation of biological nitrogen fixation. *Nature Reviews Microbiology*. 2004;2(8):621-631. doi:10.1038/nrmicro954

29. Matiru VN, Dakora FD. Potential use of rhizobial bacteria as promoters of plant growth for increased yield in landraces of African cereal crops. *African Journal of Biotechnology*. 2004;3(1):1-7. doi:10.5897/ajb2004.000-2002

30. Ahmad E, Khan MS, Zaidi A. ACC deaminase producing Pseudomonas putida strain PSE3 and Rhizobium leguminosarum strain RP2 in synergism improves growth, nodulation and yield of pea grown in alluvial soils. *Symbiosis*. 2013;61(2):93-104. doi:10.1007/s13199-013-0259-6

31. Wang M, Bian Z, Shi J, et al. Effect of the nitrogen-fixing bacterium Pseudomonas protegens CHA0-ΔretS-nif on garlic growth under different field conditions. *Industrial Crops and Products*. 2020;145:111982. doi:10.1016/j.indcrop.2019.111982

32. Weller DM, Raaijmakers JM, McSpadden Gardener BB, Thomashow LS. Microbial populations responsible for specific soil suppressiveness to plant pathogens. *Annual Review of Phytopathology*. 2002;40:309-348. doi:10.1146/annurev.phyto.40.030402.110010

33. Veloso J, Díaz J. Fusarium oxysporum Fo47 confers protection to pepper plants against Verticillium dahliae and Phytophthora capsici, and induces the expression of defence genes. *Plant Pathology*. 2012;61(2):281-288. doi:10.1111/j.1365-3059.2011.02516.x

34. Termorshuizen AJ, van Rijn E, van der Gaag DJ, et al. Suppressiveness of 18 composts against 7 pathosystems: Variability in pathogen response. *Soil Biology and Biochemistry*. 2006;38(8):2461-2477. doi:10.1016/j.soilbio.2006.03.002

35. Malandraki I, Tjamos SE, Pantelides IS, Paplomatas EJ. Thermal inactivation of compost suppressiveness implicates possible biological factors in disease management. *Biological Control*. 2008;44(2):180-187. doi:10.1016/j.biocontrol.2007.10.006

36. Li S, Zhang N, Zhang Z, et al. Antagonist Bacillus subtilis HJ5 controls Verticillium wilt of cotton by root colonization and biofilm formation. *Biology and Fertility of Soils*. 2013;49(3):295-303. doi:10.1007/s00374-012-0718-x

37. Deketelaere S, Tyvaert L, França SC, Hofte M. Desirable traits of a good biocontrol agent against Verticillium wilt. *Frontiers in Microbiology*. 2017;8:1186. doi:10.3389/fmicb.2017.01186

38. Yim G, Wang HH, Davies J. Antibiotics as signalling molecules. *Philosophical Transactions of the Royal Society B: Biological Sciences*. 2007;362(1483):1195-1200. doi:10.1098/rstb.2007.2044

39. Islam W, Noman A, Naveed H, Huang Z, Chen HYH. Role of environmental factors in shaping the soil microbiome. *Environmental Science and Pollution Research*. 2020;27(33):41225-41247. doi:10.1007/s11356-020-10471-2

40. Bjørnlund L, Rønn R, Péchy-Tarr M, Maurhofer M, Keel C, Nybroe O. Functional gacS in pseudomonas DSS73 prevents digestion by caenorhabditis elegans and protects the nematode from killer flagellates. *ISME Journal*. 2009;3(7):770-779. doi:10.1038/ismej.2009.28

41. Tyc O, van den Berg M, Gerards S, et al. Impact of interspecific interactions on antimicrobial activity among soil bacteria. *Frontiers in Microbiology*. 2014;5(OCT). doi:10.3389/fmicb.2014.00567

42. Khan MR, Majid S, Mohidin FA, Khan N. A new bioprocess to produce low cost powder formulations of biocontrol bacteria and fungi to control fusarial wilt and root-knot nematode of pulses. *Biological Control*. 2011;59(2):130-140. doi:10.1016/j.biocontrol.2011.04.007

43. Cassidy MB, Lee H, Trevors JT. Environmental applications of immobilized microbial cells: A review. *Journal of Industrial Microbiology*. 1996;16(2):79-101. doi:10.1007/BF01570068

44. Sandikar BM, Awasthi RS. Preparation and Shelf-life Study of Pseudomonas and Bacillus Bioformulations Against Phytopathogenic Pythium and Fusarium species. *International Journal of Plant Protection*. 2010;2(2):251-254.

45. Bahme JB. Spatial-Temporal Colonization Patterns of a Rhizobacterium on Underground Organs of Potato. *Phytopathology*. 1987;77(6):1093. doi:10.1094/phyto-77-1093

46. Weller DM. Colonization of Wheat Roots by a Fluorescent Pseudomonad Suppressive to Take-All. *Phytopathology*. 1983;73(11):1548. doi:10.1094/phyto-73-1548

47. Campo RJ, Araujo RS, Hungria M. Nitrogen fixation with the soybean crop in Brazil: Compatibility between seed treatment with fungicides and bradyrhizobial inoculants. *Symbiosis*. 2009;48(1-3):154-163. doi:10.1007/BF03179994

48. Campo RJ, Araujo RS, Mostasso FL, Hungria M. In-furrow inoculation of soybean as alternative to fungicide and micronutrient seed treatment. *Revista Brasileira de Ciencia do Solo*. 2010;34(4):1103-1112. doi:10.1590/s0100-06832010000400010

49. Chandler D, Bailey AS, Mark Tatchell G, Davidson G, Greaves J, Grant WP. The development, regulation and use of biopesticides for integrated pest management. *Philosophical*

Transactions of the Royal Society B: Biological Sciences. 2011;366(1573):1987-1998. doi:10.1098/rstb.2010.0390

50. Timmusk S, Behers L, Muthoni J, Muraya A, Aronsson AC. Perspectives and challenges of microbial application for crop improvement. *Frontiers in Plant Science*. 2017;8:49. doi:10.3389/fpls.2017.00049

51. Santos MS, Nogueira MA, Hungria M. Microbial inoculants: reviewing the past, discussing the present and previewing an outstanding future for the use of beneficial bacteria in agriculture. *AMB Express*. 2019;9(1):1-22. doi:10.1186/s13568-019-0932-0

52. Teicher H. Biopesticide Regulation: A Comparison of EU and U.S. Approval Processes. AgriBusiness Global. Published February 28, 2018. Accessed October 13, 2021. https://www.agribusinessglobal.com/biopesticides/biopesticide-regulation-a-comparison-of-eu-and-u-s-approval-processes/

53. Placing a biostimulant on the European market. Eurofins Scientific. Accessed October 13, 2021. https://www.eurofins.com/agroscience-services/services/regulatory-consultancy/biostimulants-fertilizers/placing-a-biostimulant-on-the-european-market/

54. Craney A, Ahmed S, Nodwell J. Towards a new science of secondary metabolism. *Journal of Antibiotics*. 2013;66(7):387-400. doi:10.1038/ja.2013.25

55. Pinu FR, Villas-Boas SG, Aggio R. Analysis of intracellular metabolites from microorganisms: Quenching and extraction protocols. *Metabolites*. 2017;7(4):53. doi:10.3390/metabo7040053

56. Neidig N, Paul RJ, Scheu S, Jousset A. Secondary Metabolites of Pseudomonas fluorescens CHA0 Drive Complex Non-Trophic Interactions with Bacterivorous Nematodes. *Microbial Ecology*. 2011;61(4):853-859. doi:10.1007/s00248-011-9821-z

57. Goh EB, Yim G, Tsui W, McClure JA, Surette MG, Davies J. Transcriptional modulation of bacterial gene expression by subinhibitory concentrations of antibiotics. *Proceedings of the National Academy of Sciences of the United States of America*. 2002;99(26):17025-17030. doi:10.1073/pnas.252607699

58. Townsley L, Shank EA. Natural-Product Antibiotics: Cues for Modulating Bacterial Biofilm Formation. *Trends in Microbiology*. 2017;25(12):1016-1026. doi:10.1016/j.tim.2017.06.003

59. Romero D, Traxler MF, López D, Kolter R. Antibiotics as signal molecules. *Chemical Reviews*. 2011;111(9):5492-5505. doi:10.1021/cr2000509

60. Medema MH, Kottmann R, Yilmaz P, et al. Minimum Information about a Biosynthetic Gene cluster. *Nature Chemical Biology*. 2015;11(9):625-631. doi:10.1038/nchembio.1890

61. Wang H, Fewer DP, Holm L, Rouhiainen L, Sivonen K. Atlas of nonribosomal peptide and polyketide biosynthetic pathways reveals common occurrence of nonmodular enzymes.

Proceedings of the National Academy of Sciences of the United States of America. 2014;111(25):9259-9264. doi:10.1073/pnas.1401734111

62. Robbins T, Liu YC, Cane DE, Khosla C. Structure and mechanism of assembly line polyketide synthases. *Current Opinion in Structural Biology*. 2016;41:10-18. doi:10.1016/j.sbi.2016.05.009

63. Challis GL, Naismith JH. Structural aspects of non-ribosomal peptide biosynthesis. *Current Opinion in Structural Biology*. 2004;14(6):748-756. doi:10.1016/j.sbi.2004.10.005

64. Ziemert N, Podell S, Penn K, Badger JH, Allen E, Jensen PR. The natural product domain seeker NaPDoS: A phylogeny based bioinformatic tool to classify secondary metabolite gene diversity. *PLoS ONE*. 2012;7(3):34064. doi:10.1371/journal.pone.0034064

65. Staunton J, Weissman KJ. Polyketide biosynthesis: A millennium review. *Natural Product Reports*. 2001;18(4):380-416. doi:10.1039/a909079g

66. Katsuyama Y, Ohnishi Y. Type III polyketide synthases in microorganisms. *Methods in Enzymology*. 2012;515:359-377. doi:10.1016/B978-0-12-394290-6.00017-3

67. Osbourn A. Secondary metabolic gene clusters: Evolutionary toolkits for chemical innovation. *Trends in Genetics*. 2010;26(10):449-457. doi:10.1016/j.tig.2010.07.001

68. Chu HY, Wegel E, Osbourn A. From hormones to secondary metabolism: The emergence of metabolic gene clusters in plants. *Plant Journal*. 2011;66(1):66-79. doi:10.1111/j.1365-313X.2011.04503.x

69. Malpartida F, Hopwood DA. Molecular cloning of the whole biosynthetic pathway of a Streptomyces antibiotic and its expression in a heterologous host. *Nature*. 1984;309(5967):462-464. doi:10.1038/309462a0

70. Tamburini E, Mastromei G. Do bacterial cryptic genes really exist? *Research in Microbiology*. 2000;151(3):179-182. doi:10.1016/S0923-2508(00)00137-6

71. Brakhage AA, Schuemann J, Bergmann S, Scherlach K, Schroeckh V, Hertweck C. Activation of fungal silent gene clusters: A new avenue to drug discovery. *Progress in Drug Research*. 2008;66(1):1-12. doi:10.1007/978-3-7643-8595-8_1

72. Ochi K. Insights into microbial cryptic gene activation and strain improvement: Principle, application and technical aspects. *Journal of Antibiotics*. 2017;70(1):25-40. doi:10.1038/ja.2016.82

73. Reen FJ, Romano S, Dobson ADW, O'Gara F. The sound of silence: Activating silent biosynthetic gene clusters in marine microorganisms. *Marine Drugs*. 2015;13(8):4754-4783. doi:10.3390/md13084754

74. Paranagama PA, Wijeratne EMK, Gunatilaka AAL. Uncovering biosynthetic potential of plant-associated fungi: Effect of culture conditions on metabolite production by Paraphaeosphaeria

quadriseptata and Chaetomium chiversii. *Journal of Natural Products*. 2007;70(12):1939-1945. doi:10.1021/np070504b

75. Bode HB, Bethe B, Höfs R, Zeeck A. Big effects from small changes: Possible ways to explore nature's chemical diversity. *ChemBioChem*. 2002;3(7):619-627. doi:10.1002/1439-7633(20020703)3:7<619::AID-CBIC619>3.0.CO;2-9

76. Li Y, Yuan L, Xue S, Liu B, Jin G. Artificial root exudates excite bacterial nitrogen fixation in the subsurface of mine soils. *Applied Soil Ecology*. 2021;157:103774. doi:10.1016/j.apsoil.2020.103774

77. Zhu S, Duan Y, Huang Y. The application of ribosome engineering to natural product discovery and yield improvement in streptomyces. *Antibiotics*. 2019;8(3). doi:10.3390/antibiotics8030133

78. Hosaka T, Tamehiro N, Chumpolkulwong N, et al. The novel mutation K87E in ribosomal protein S12 enhances protein synthesis activity during the late growth phase in Escherichia coli. *Molecular Genetics and Genomics*. 2004;271(3):317-324. doi:10.1007/s00438-004-0982-z

79. Hosaka T, Xu J, Ochi K. Increased expression of ribosome recycling factor is responsible for the enhanced protein synthesis during the late growth phase in an antibiotic-overproducing Streptomyces coelicolor ribosomal rpsL mutant. *Molecular Microbiology*. 2006;61(4):883-897. doi:10.1111/j.1365-2958.2006.05285.x

80. Hosaka T, Ohnishi-Kameyama M, Muramatsu H, et al. Antibacterial discovery in actinomycetes strains with mutations in RNA polymerase or ribosomal protein S12. *Nature Biotechnology*. 2009;27(5):462-464. doi:10.1038/nbt.1538

81. Shima J, Hesketh A, Okamoto S, Kawamoto S, Ochi K. Induction of actinorhodin production by rpsL (encoding ribosomal protein S12) mutations that confer streptomycin resistance in Streptomyces lividans and Streptomyces coelicolor A3(2). *Journal of Bacteriology*. 1996;178(24):7276-7284. doi:10.1128/jb.178.24.7276-7284.1996

82. Blazeck J, Alper HS. Promoter engineering: Recent advances in controlling transcription at the most fundamental level. *Biotechnology Journal*. 2013;8(1):46-58. doi:10.1002/biot.201200120

83. Jiang L, Wang L, Zhang J, et al. Identification of novel mureidomycin analogues via rational activation of a cryptic gene cluster in Streptomyces roseosporus NRRL 15998. *Scientific Reports*. 2015;5(1):1-13. doi:10.1038/srep14111

84. Rateb ME, Hallyburton I, Houssen WE, et al. Induction of diverse secondary metabolites in Aspergillus fumigatus by microbial co-culture. *RSC Advances*. 2013;3(34):14444-14450. doi:10.1039/c3ra42378f

85. Albini S, Zakharova V, Ait-Si-Ali S. Histone Modifications. In: *Epigenetics and Regeneration*. 1st ed. Academic Press; 2019:47-72. doi:10.1016/b978-0-12-814879-2.00003-0

86. Casadesús J, Low D. Epigenetic Gene Regulation in the Bacterial World. *Microbiology and Molecular Biology Reviews*. 2006;70(3):830-856. doi:10.1128/mmbr.00016-06

87. Gunsalus IC. Bacterial metabolism. *Annual review of biochemistry*. 1948;17:627-656. doi:10.1146/annurev.bi.17.070148.003211

88. Liu Z, Zhao Y, Huang C, Luo Y. Recent Advances in Silent Gene Cluster Activation in Streptomyces. *Frontiers in Bioengineering and Biotechnology*. 2021;9(632230). doi:10.3389/fbioe.2021.632230

89. Yamanaka K, Reynolds KA, Kersten RD, et al. Direct cloning and refactoring of a silent lipopeptide biosynthetic gene cluster yields the antibiotic taromycin A. *Proceedings of the National Academy of Sciences of the United States of America*. 2014;111(5):1957-1962. doi:10.1073/pnas.1319584111

90. Silby MW, Winstanley C, Godfrey SAC, Levy SB, Jackson RW. Pseudomonas genomes: Diverse and adaptable. *FEMS Microbiology Reviews*. 2011;35(4):652-680. doi:10.1111/j.1574-6976.2011.00269.x

91. Yong YC, Wu XY, Sun JZ, Cao YX, Song H. Engineering quorum sensing signaling of Pseudomonas for enhanced wastewater treatment and electricity harvest: A review. *Chemosphere*. 2014;140:18-25. doi:10.1016/j.chemosphere.2014.10.020

92. Haas D, Défago G. Biological control of soil-borne pathogens by fluorescent pseudomonads. *Nature Reviews Microbiology*. 2005;3(4):307-319. doi:10.1038/nrmicro1129

93. Ramette A, Frapolli M, Saux MF le, et al. Pseudomonas protegens sp. nov., widespread plant-protecting bacteria producing the biocontrol compounds 2,4-diacetylphloroglucinol and pyoluteorin. *Systematic and Applied Microbiology*. 2011;34(3):180-188. doi:10.1016/j.syapm.2010.10.005

94. Wang X, Mavrodi D v., Ke L, et al. Biocontrol and plant growth-promoting activity of rhizobacteria from Chinese fields with contaminated soils. *Microbial Biotechnology*. 2015;8(3):404-418. doi:10.1111/1751-7915.12158

95. Yasmin R, Hussain S, Rasool MH, Siddique MH, Muzammil S. Isolation, Characterization of Zn Solubilizing Bacterium (Pseudomonas protegens RY2) and its Contribution in Growth of Chickpea (Cicer arietinum L) as Deciphered by Improved Growth Parameters and Zn Content. *Dose-Response*. 2021;19(3):1-12. doi:10.1177/15593258211036791

96. Andreolli M, Zapparoli G, Angelini E, Lucchetta G, Lampis S, Vallini G. Pseudomonas protegens MP12: A plant growth-promoting endophytic bacterium with broad-spectrum antifungal activity against grapevine phytopathogens. *Microbiological Research*. 2019;219:123-131. doi:10.1016/j.micres.2018.11.003

97. Ueda A, Saneoka H. Characterization of the Ability to Form Biofilms by Plant-Associated Pseudomonas Species. *Current Microbiology*. 2015;70(4):506-513. doi:10.1007/s00284-014-0749-7

98. Aune MI. Isolation and Characterisation of Bioactive Pseudomonas from Soil. *(Unpublished) Bachelor Thesis at DTU Department of Biotechnology and Biomedicine*. 2017.

99. Blin K, Shaw S, Kloosterman AM, et al. AntiSMASH 6.0: Improving cluster detection and comparison capabilities. *Nucleic Acids Research*. 2021;49(W1):W29-W35. doi:10.1093/nar/gkab335

100. Herrero M, de Lorenzo V, Timmis KN. Transposon vectors containing non-antibiotic resistance selection markers for cloning and stable chromosomal insertion of foreign genes in gram-negative bacteria. *Journal of Bacteriology*. 1990;172(11):6557-6567. doi:10.1128/jb.172.11.6557-6567.1990

101. Boyer HW, Roulland-dussoix D. A complementation analysis of the restriction and modification of DNA in Escherichia coli. *Journal of Molecular Biology*. 1969;41(3):459-472. doi:10.1016/0022-2836(69)90288-5

102. Environmental Synthetic Biology Laboratory - Victor de Lorenzo. Accessed October 21, 2021. https://vdl-lab.com/

103. Yang L, Hengzhuang W, Wu H, et al. Polysaccharides serve as scaffold of biofilms formed by mucoid Pseudomonas aeruginosa. *FEMS Immunology and Medical Microbiology*. 2012;65(2):366-376. doi:10.1111/j.1574-695X.2012.00936.x

104. Kessler B, de Lorenzo V, Timmis KN. A general system to integrate lacZ fusions into the chromosomes of gram-negative eubacteria: regulation of the Pm promoter of the TOL plasmid studied with all controlling elements in monocopy. *MGG Molecular & General Genetics*. 1992;233(1-2):293-301. doi:10.1007/BF00587591

105. Tsugawa H et al. CompMS | MS-DIAL. Accessed November 27, 2021. http://prime.psc.riken.jp/compms/msdial/main.html

106. MetaboAnalyst. Accessed November 27, 2021. https://www.metaboanalyst.ca/home.xhtml

107. Antognoni P, Cerizza L, Vavassori V, et al. Postoperative radiation therapy for adult soft tissue sarcomas: A retrospective study. Annals of Oncology. doi:10.1093/annonc/3.suppl_2.s103

108. Hellemans J, Mortier G, de Paepe A, Speleman F, Vandesompele J. qBase relative quantification framework and software for management and automated analysis of real-time quantitative PCR data. *Genome Biology*. 2008;8(2):R19. doi:10.1186/gb-2007-8-2-r19

109. Troutman M. Optimize qPCR Using SYBR Green Assays - Ask TaqMan #38 - Behind the Bench. Thermo Fisher Scientific. Published July 27, 2016. Accessed August 18, 2021.

https://www.thermofisher.com/blog/behindthebench/optimize-qpcr-using-sybr-green-assays-ask-taqman-38/

110. Scientific TF. PowerUp ™ SYBR ™ Green Master Mix Universal 2X master mix for real-time PCR workflows. Published 2021. Accessed August 18, 2021. https://www.thermofisher.com/order/catalog/product/A25741

111. Yim G, de La Cruz F, Spiegelman GB, Davies J. Transcription modulation of Salmonella enterica serovar typhimurium promoters by sub-MIC levels of rifampin. *Journal of Bacteriology*. 2006;188(22):7988-7991. doi:10.1128/JB.00791-06

112. Kang D, Kirienko N v. An in vitro cell culture model for pyoverdine-mediated virulence. *Pathogens*. 2021;10(1):1-14. doi:10.3390/pathogens10010009

113. Drew SW, Demain AL. Effect of primary metabolites on secondary metabolism. *Annual review of microbiology*. 1977;31:343-356. doi:10.1146/annurev.mi.31.100177.002015

114. Sánchez S, Chávez A, Forero A, et al. Carbon source regulation of antibiotic production. *Journal of Antibiotics*. 2010;63(8):442-459. doi:10.1038/ja.2010.78

115. Duffy BK, Défago G. Environmental factors modulating antibiotic and siderophore biosynthesis by Pseudomonas fluorescens biocontrol strains. *Applied and Environmental Microbiology*. 1999;65(6):2429-2438. doi:10.1128/aem.65.6.2429-2438.1999

116. Ownley BH, Weller DM, Thomashow LS. Influence of In Situ and In Vitro pH on Suppression of Gaeumannomyces graminis var. tritici by Pseudomonas fluorescens 2-79. *Phytopathology*. 1992;82:178-184. doi:10.1094/phyto-82-178

117. Merck. RT-PCR / RT-qPCR Troubleshooting. Merck. Published 2021. Accessed October 27, 2021. https://www.sigmaaldrich.com/NL/en/technical-documents/technical-article/genomics/pcr/troubleshooting

118. Krzyżanowska DM, Supernat A, Maciąg T, Matuszewska M, Jafra S. Selection of reference genes for measuring the expression of aiiO in Ochrobactrum quorumnocens A44 using RT-qPCR. *Scientific Reports*. 2019;9(1):1-11. doi:10.1038/s41598-019-49474-6

119. Huggett J, Dheda K, Bustin S, Zumla A. Real-time RT-PCR normalisation; strategies and considerations. *Genes and Immunity*. 2005;6(4):279-284. doi:10.1038/sj.gene.6364190

120. Tanaka Y, Kasahara K, Hirose Y, Murakami K, Kugimiya R, Ochi K. Activation and products of the cryptic secondary metabolite biosynthetic gene clusters by rifampin resistance (rpoB) mutations in actinomycetes. *Journal of Bacteriology*. 2013;195(13):2959-2970. doi:10.1128/JB.00147-13

121. Hall AR, Iles JC, MacLean RC. The fitness cost of rifampicin resistance in Pseudomonas aeruginosa depends on demand for RNA polymerase. *Genetics*. 2011;187(3):817-822. doi:10.1534/genetics.110.124628

122. Jatsenko T, Tover A, Tegova R, Kivisaar M. Molecular characterization of Rifr mutations in Pseudomonas aeruginosa and Pseudomonas putida. *Mutation Research - Fundamental and Molecular Mechanisms of Mutagenesis*. 2010;683(1-2):106-114. doi:10.1016/j.mrfmmm.2009.10.015

123. Cai XC, Xi H, Liang L, et al. Rifampicin-resistance mutations in the rpoB gene in Bacillus Velezensis CC09 have pleiotropic effects. *Frontiers in Microbiology*. 2017;8:178. doi:10.3389/fmicb.2017.00178

124. Han HS, Nam HY, Koh YJ, Hur JS, Jung JS. Molecular bases of high-level streptomycin resistance in Pseudomonas marginalis and Pseudomonas syringae pv. actinidiae. *Journal of Microbiology*. 2003;41(1):16-21. Accessed November 3, 2021. https://www.koreascience.or.kr/article/JAKO200311921570794.page

125. Paulander W, Maisnier-Patin S, Andersson DI. The fitness cost of streptomycin resistance depends on rpsL mutation, carbon source and RpoS (σS). *Genetics*. 2009;183(2):539-546. doi:10.1534/genetics.109.106104

126. Matsumura I. Why Johnny can't clone: Common pitfalls and not so common solutions. *BioTechniques*. 2015;59(3):4-13. doi:10.2144/000114324

127. Lund AH, Duch M, Pedersen FS. Increased cloning efficiency by temperature-cycle ligation. *Nucleic Acids Research*. 1996;24(4):800-801. doi:10.1093/nar/24.4.800

8. Annexes A - E

8.1. Annex A

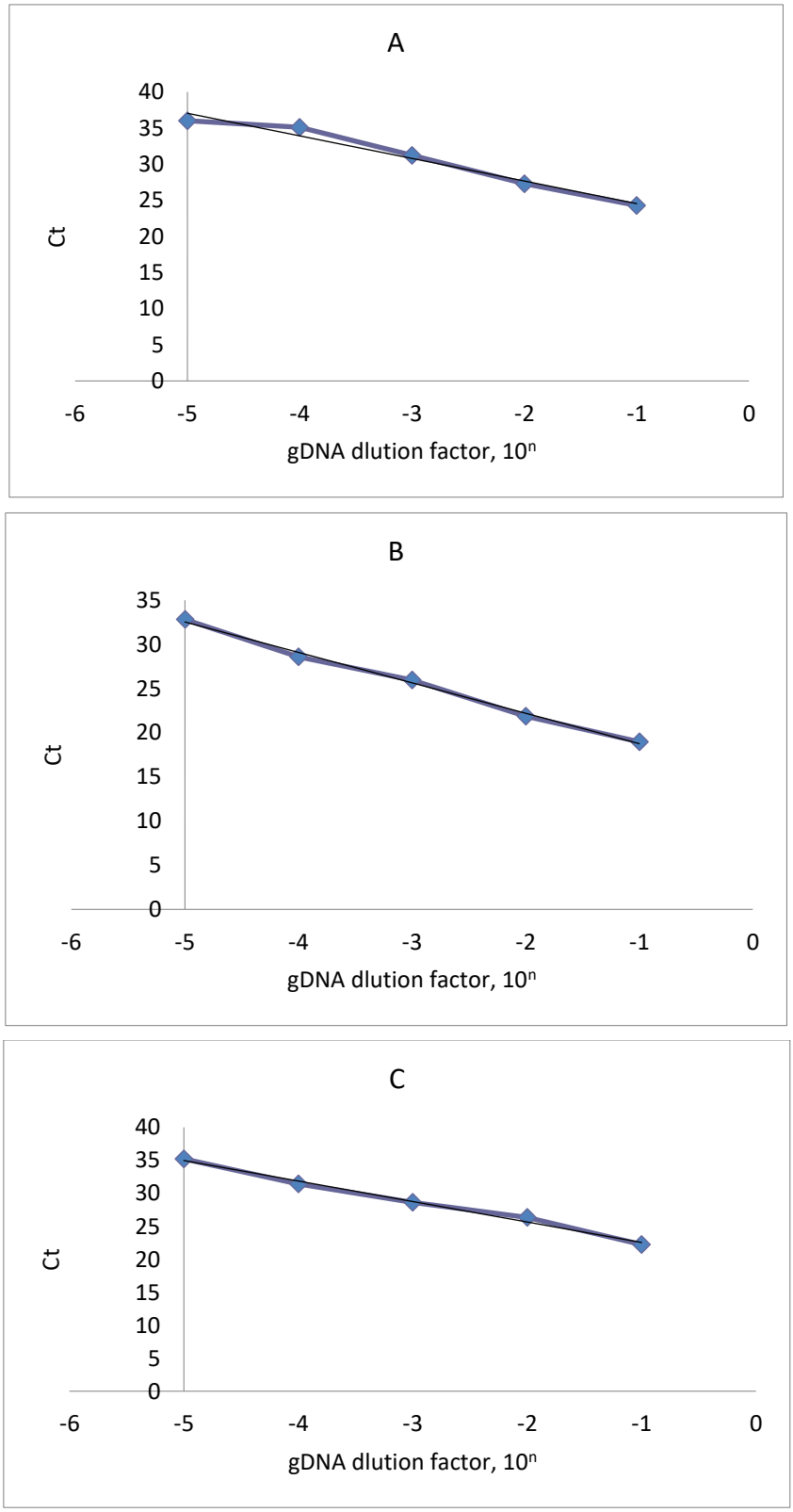

Figure 8.1. Standard curves for primer efficiency calculation. Target gene: (A) gyrB (R^2 = 0.9715, Slope = -3.125); (B) rpoD (R^2 = 0.9951, Slope = -3.445); (C) unknown BGC (R^2 = 0.9915, Slope = -3.104). Ct - average cycle threshold.

8.2. Annex B

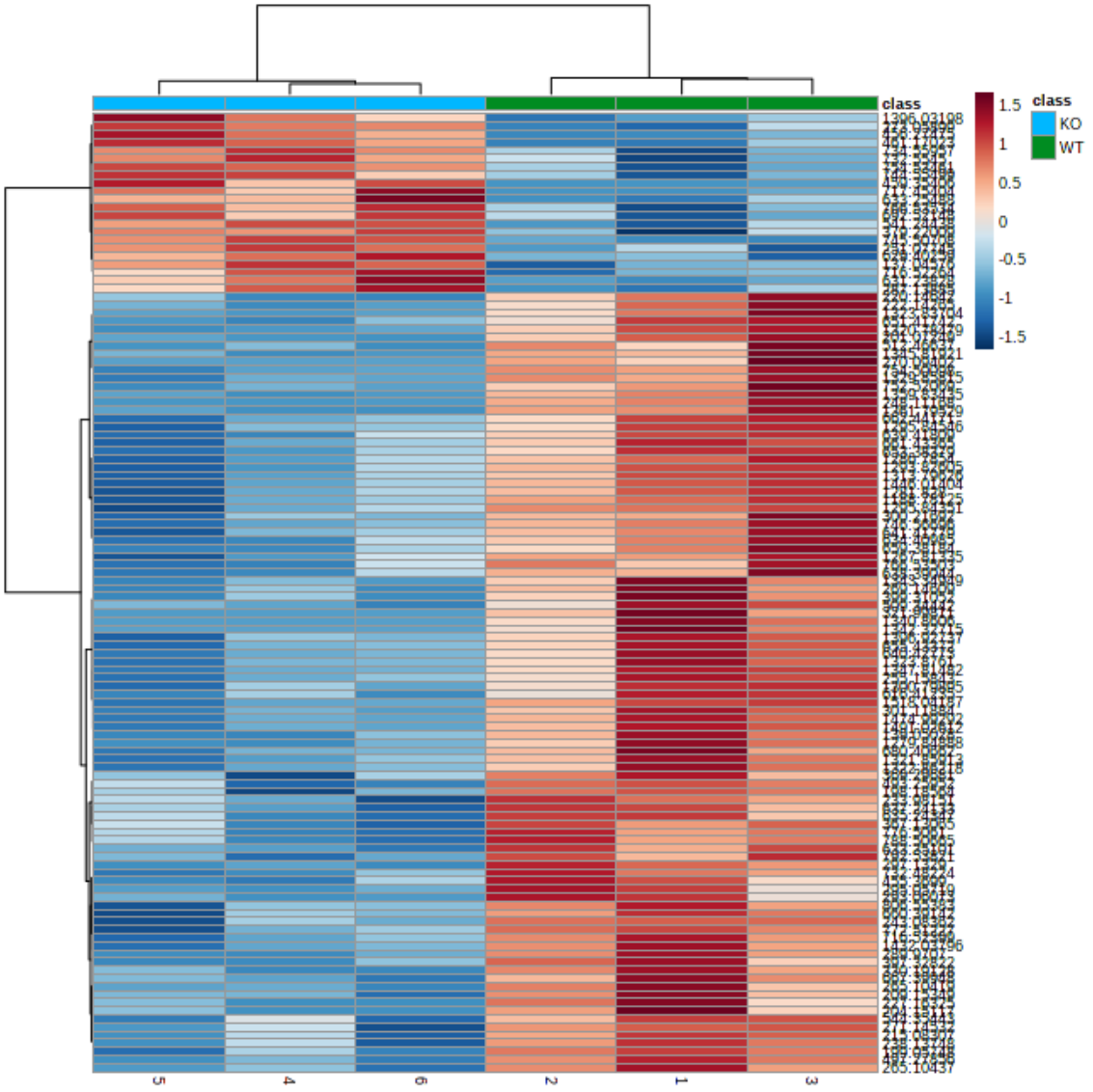

Figure 8.2. Heat map – Comparison of intracellular metabolites between the WT vs ΔPKS.

8.3. Annex C

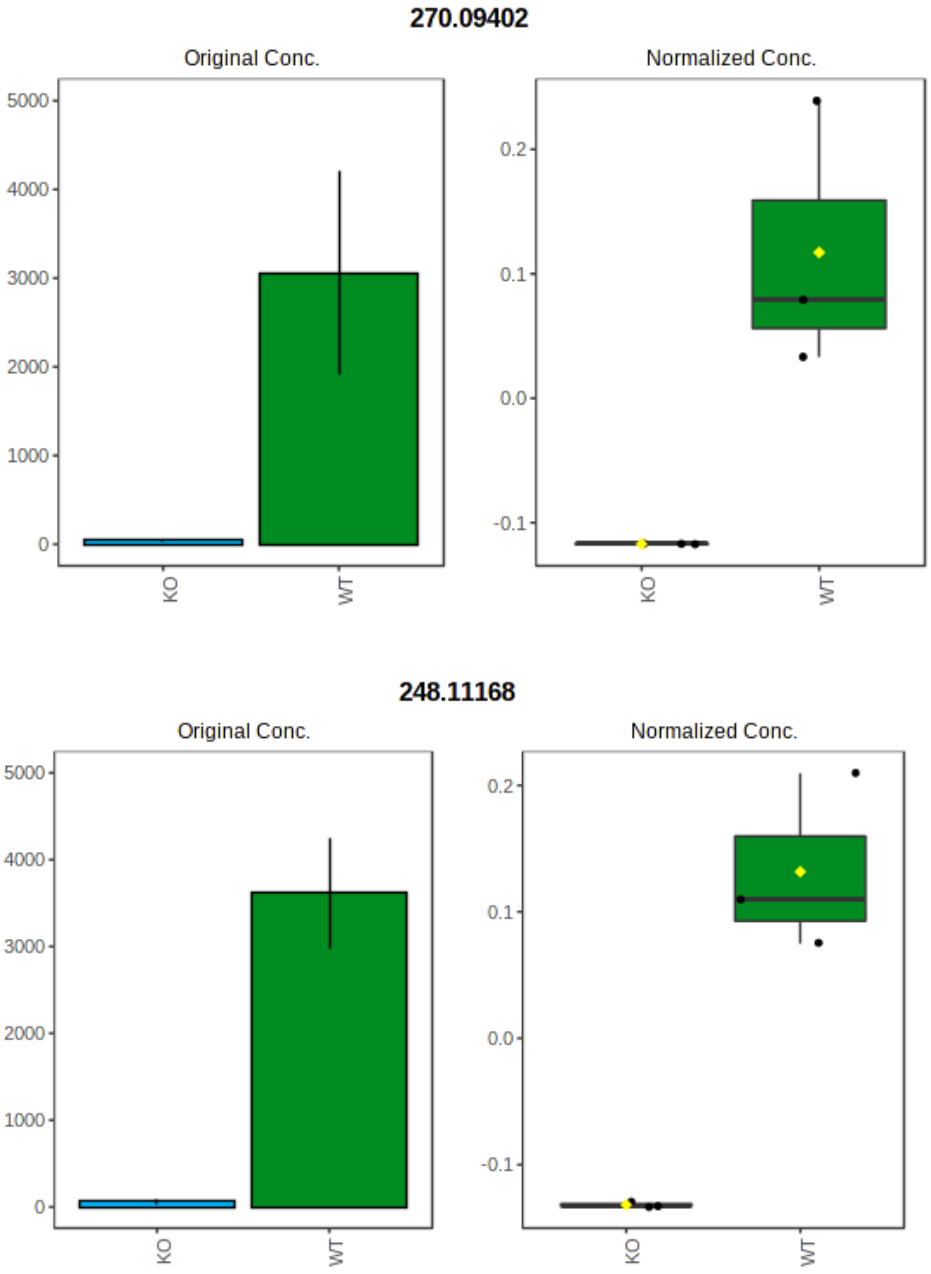

Figure 8.3. Bar and box graph – Intracellular metabolites with the lowest folder change between ΔPKS and WT

8.4. Annex D

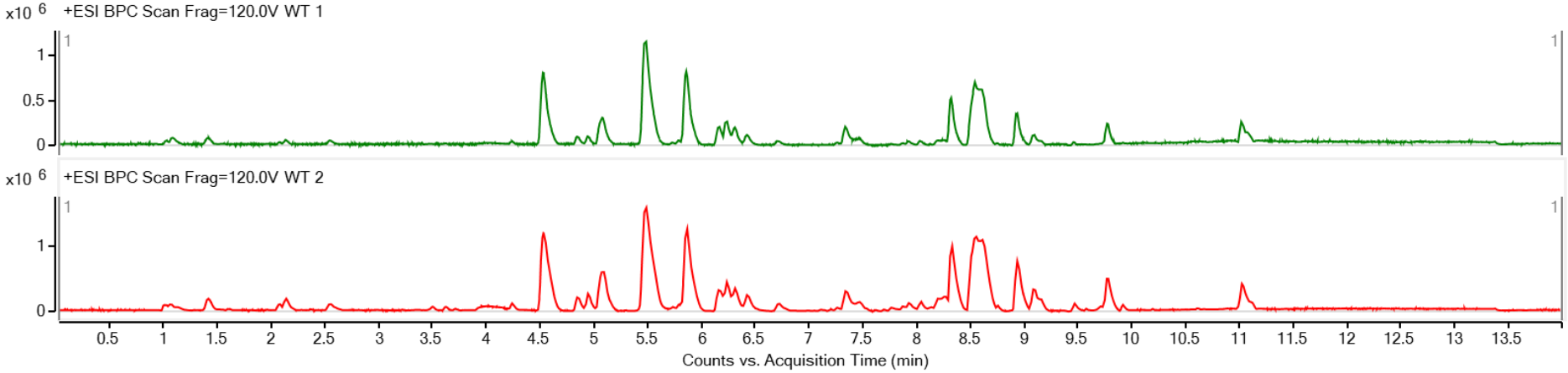

Figure 8.4. Base peak chromatogram – Results of LC-MS analysis to WT intracellular extracts.

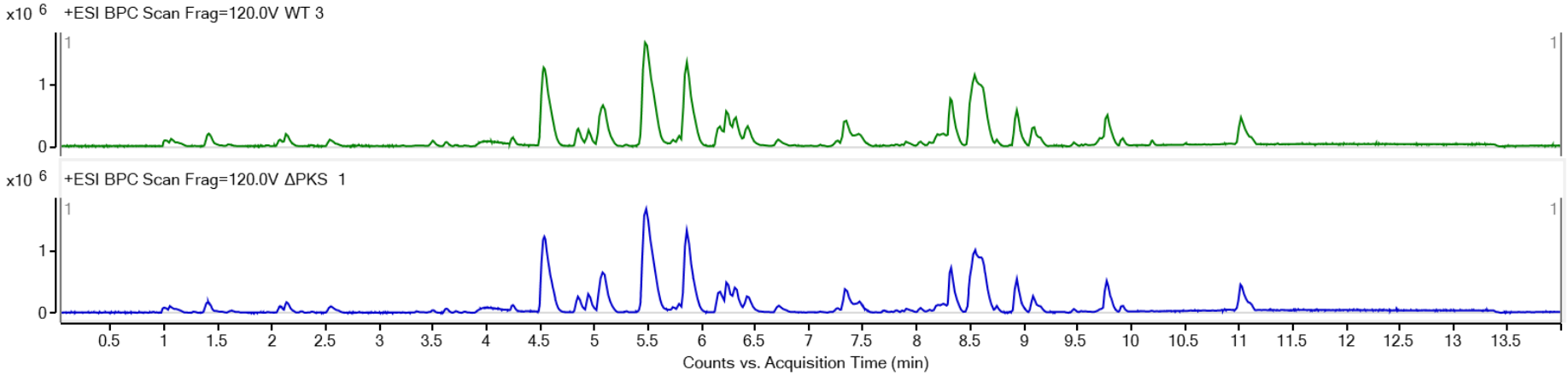

Figure 8.5. Base peak chromatogram – Results of LC-MS analysis to WT and ΔPKS intracellular extracts.

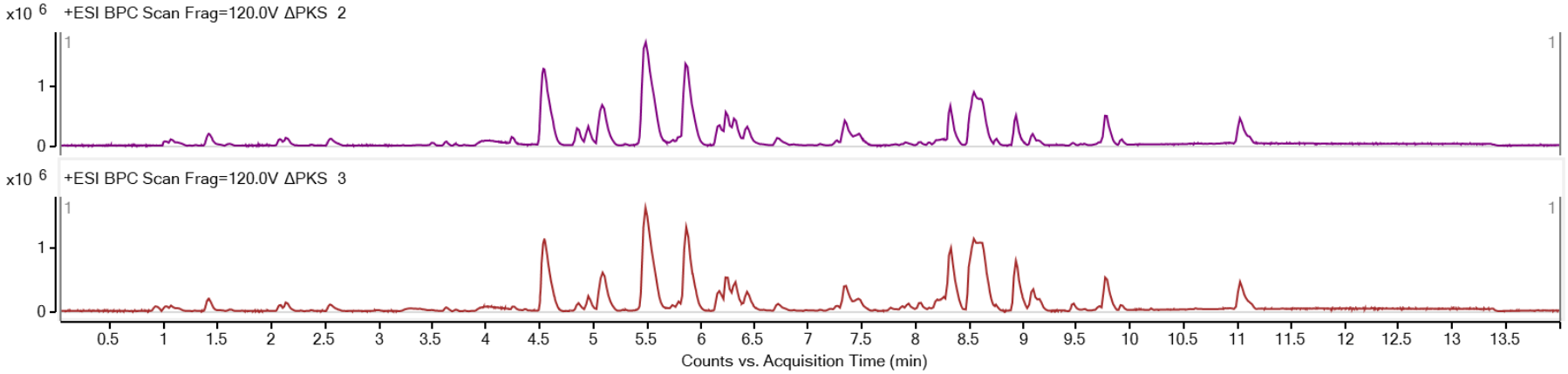

Figure 8.6. Base peak chromatogram – Results of LC-MS analysis to ΔPKS intracellular extracts.

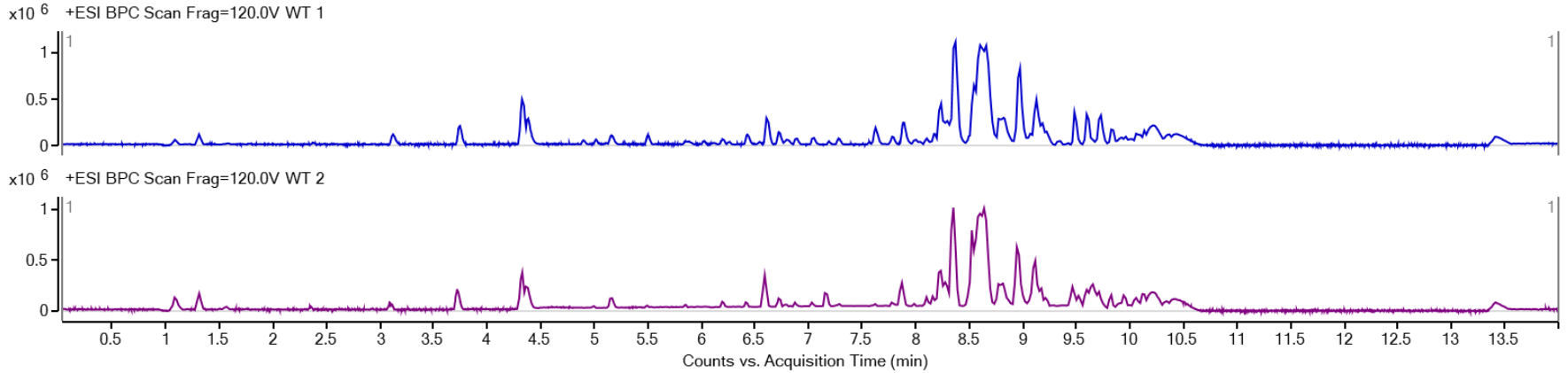

Figure 8.7. Base peak chromatogram – Results of LC-MS analysis to WT extracellular extracts.

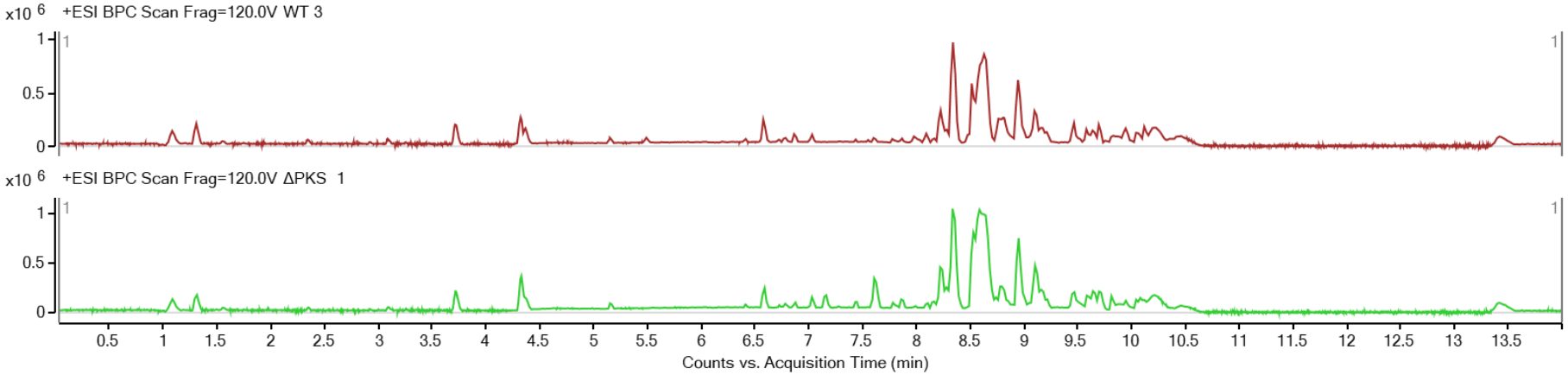

Figure 8.8. Base peak chromatogram – Results of LC-MS analysis to WT and ΔPKS extracellular extracts.

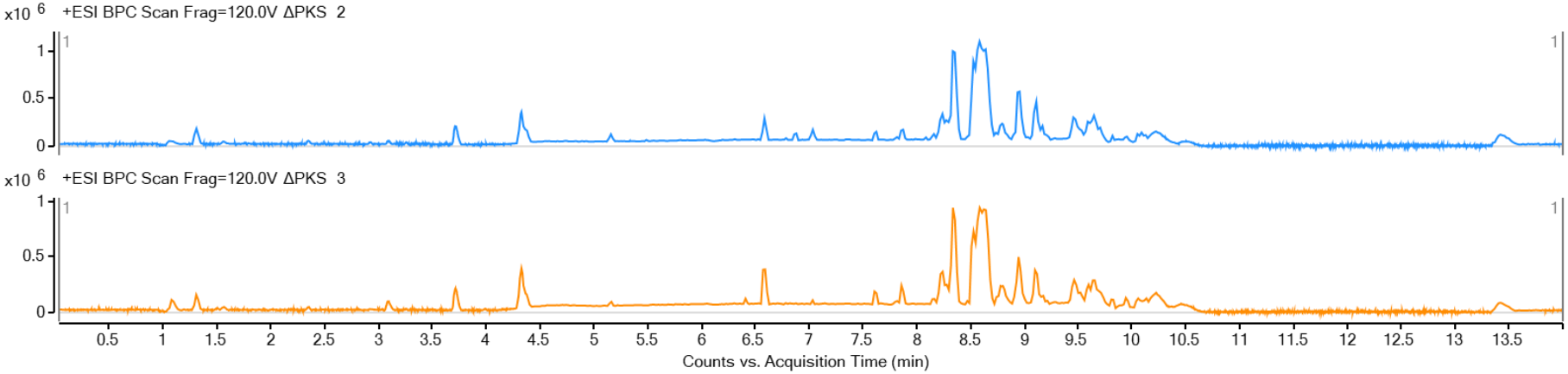

Figure 8.9. Base peak chromatogram – Results of LC-MS analysis to ΔPKS extracellular extracts.

8.5. Annex E

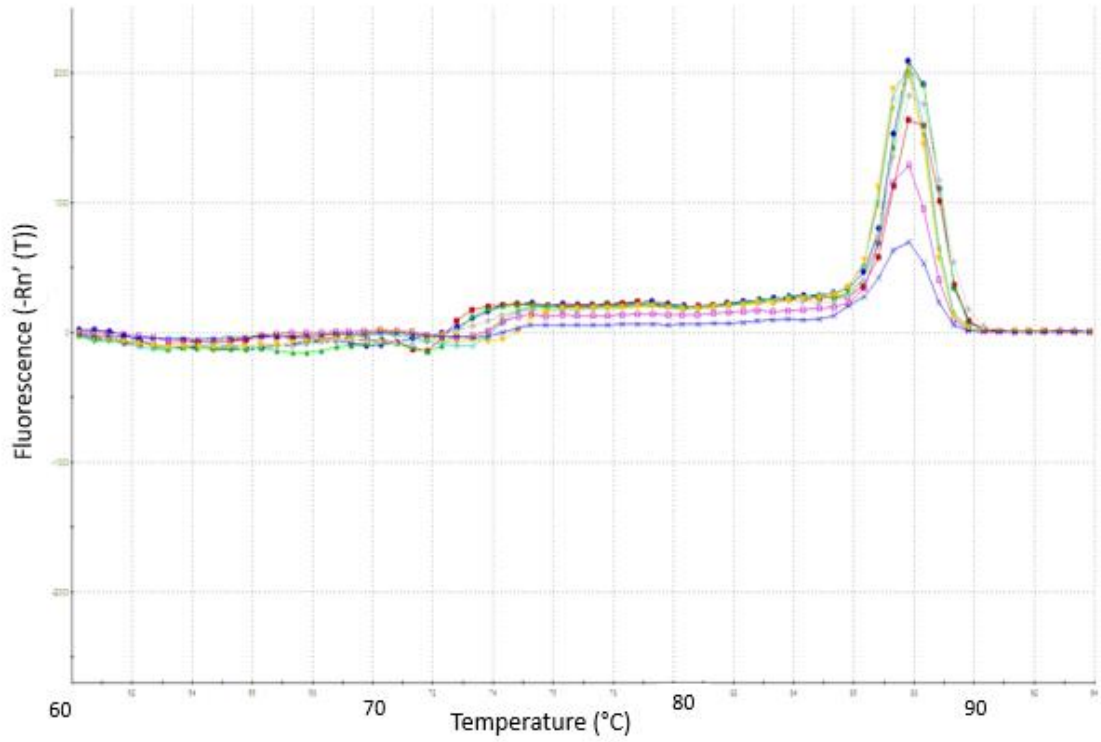

Figure 8.10. Melting curves – Analysis of reference gene gyrB amplicons for the 14h samples.

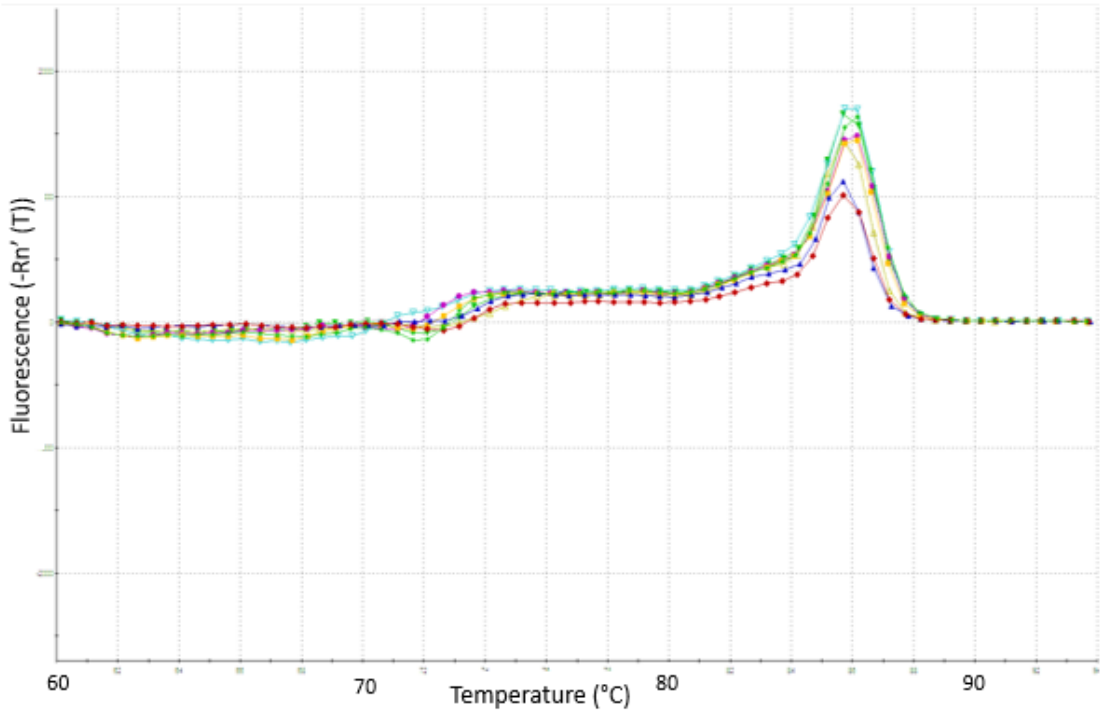

Figure 8.11. Melting curves – Analysis of unknown BGC amplicons for the 14h samples.

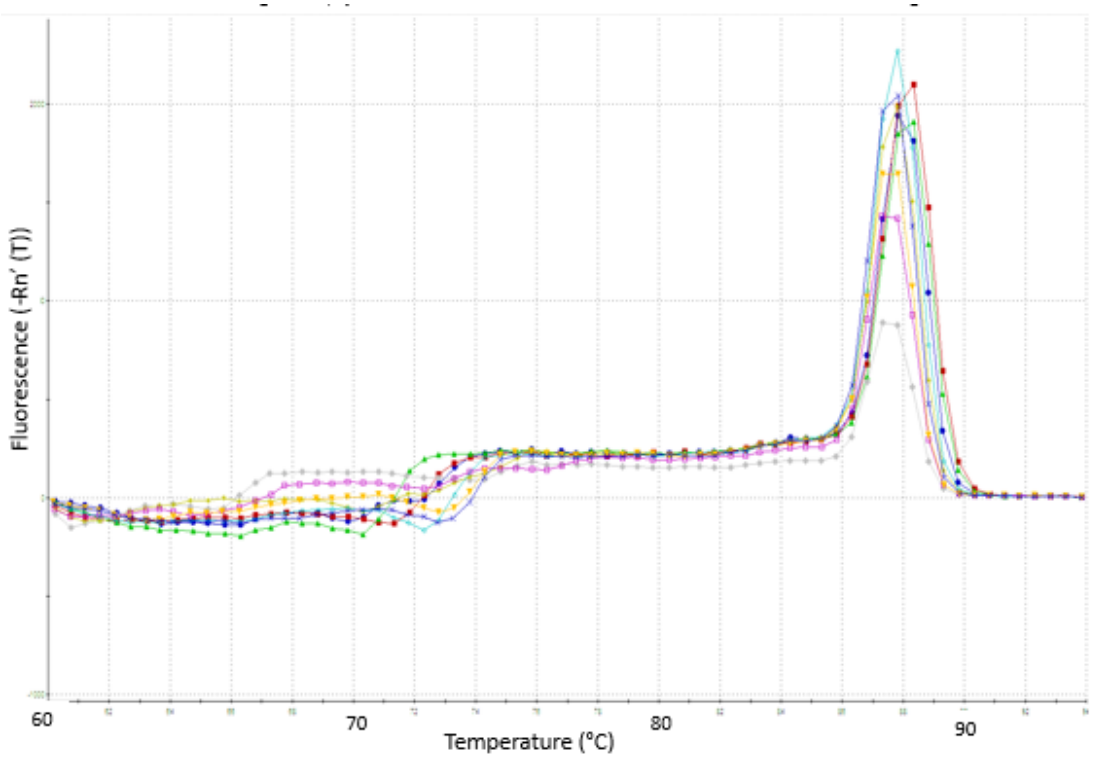

Figure 8.12. Melting curves – Analysis of reference gene rpoD amplicons for the 24h samples.

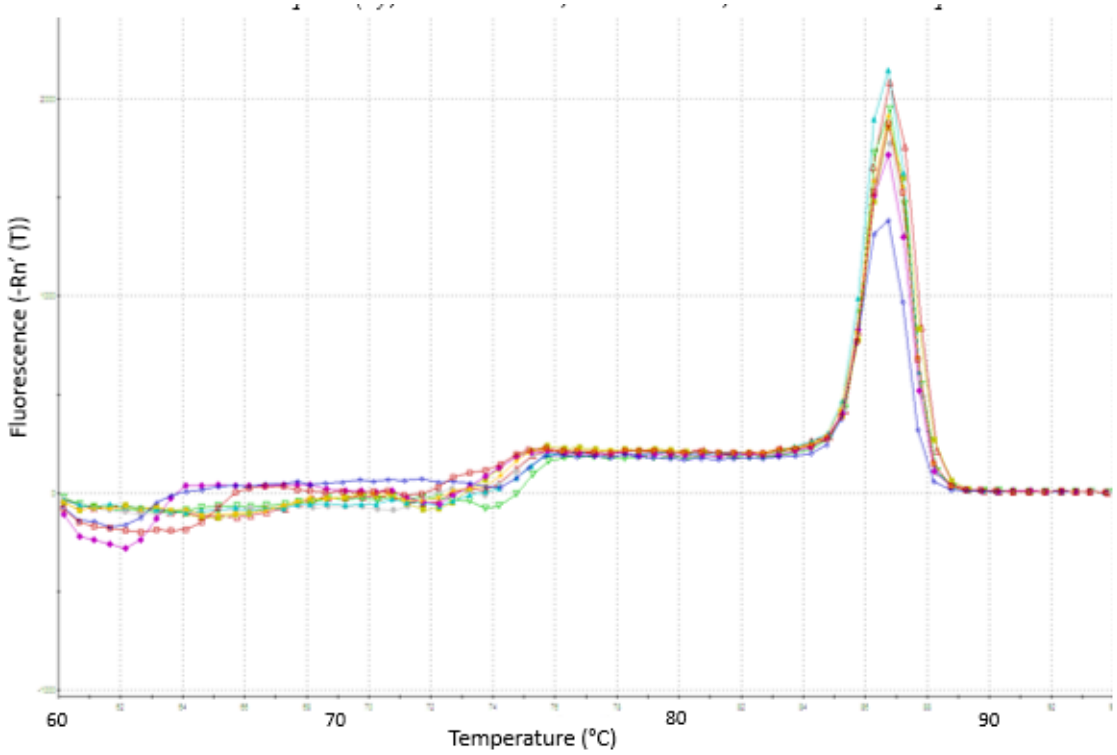

Figure 8.13. Melting curves – Analysis of reference gene gyrB amplicons for the 24h samples.

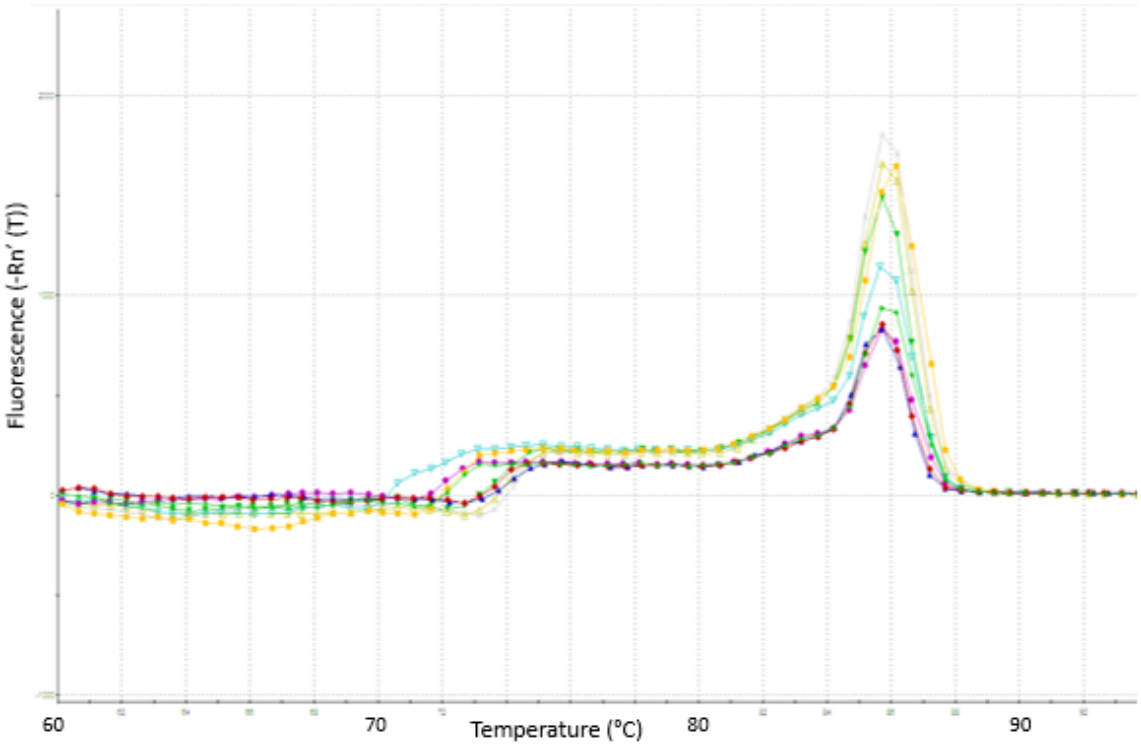

Figure 8.14. Melting curves – Analysis of unknown BGC amplicons for the 24h samples.

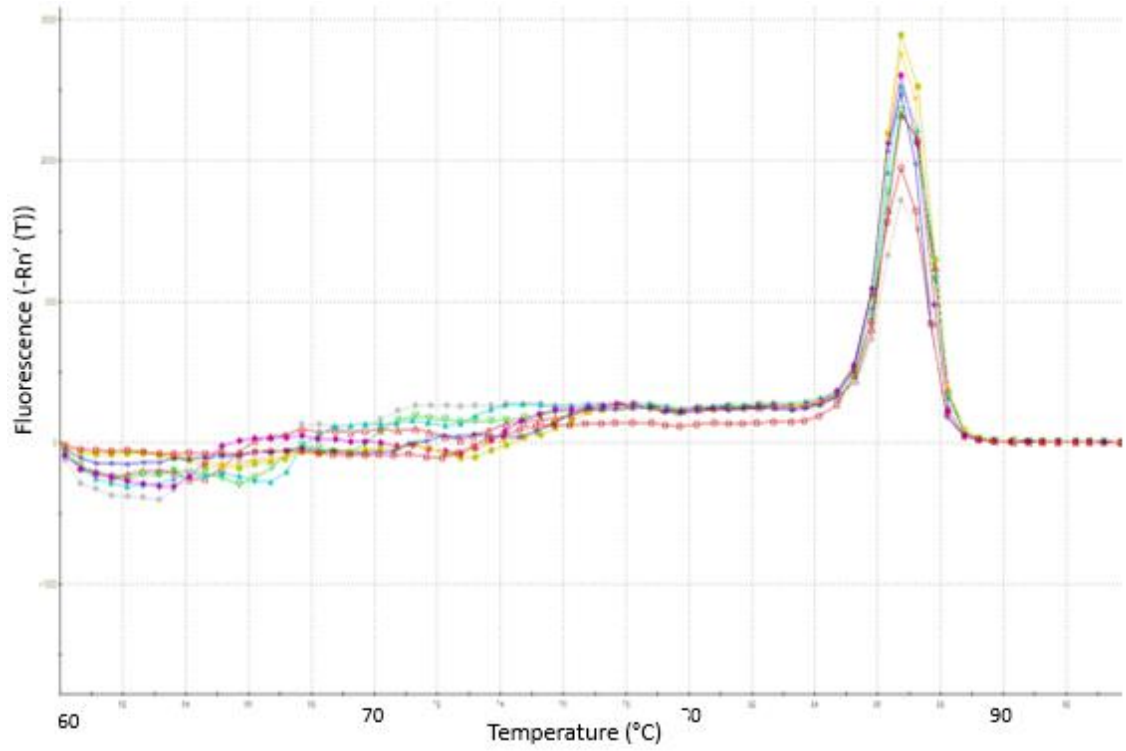

Figure 8.15. Melting curves – Analysis of reference gene rpoD amplicons for the 30h samples.

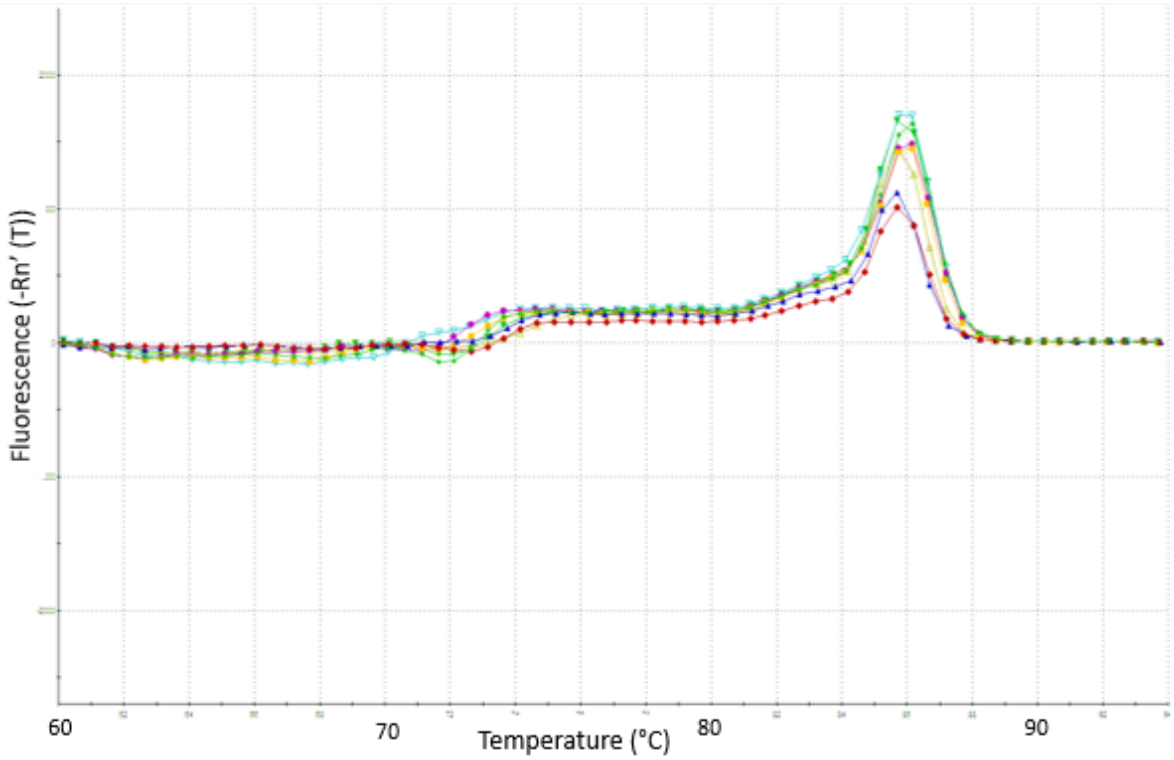

Figure 8.16. Melting curves – Analysis of unknown BGC amplicons for the 30h samples.